

INFORMATION TO USERS

This material was produced from a microfilm copy of the original document. While the most advanced technological means to photograph and reproduce this document have been used, the quality is heavily dependent upon the quality of the original submitted.

The following explanation of techniques is provided to help you understand markings or patterns which may appear on this reproduction.

1. The sign or "target" for pages apparently lacking from the document photographed is "Missing Page(s)". If it was possible to obtain the missing page(s) or section, they are spliced into the film along with adjacent pages. This may have necessitated cutting thru an image and duplicating adjacent pages to insure you complete continuity.
2. When an image on the film is obliterated with a large round black mark, it is an indication that the photographer suspected that the copy may have moved during exposure and thus cause a blurred image. You will find a good image of the page in the adjacent frame.
3. When a map, drawing or chart, etc., was part of the material being photographed the photographer followed a definite method in "sectioning" the material. It is customary to begin photoing at the upper left hand corner of a large sheet and to continue photoing from left to right in equal sections with a small overlap. If necessary, sectioning is continued again — beginning below the first row and continuing on until complete.
4. The majority of users indicate that the textual content is of greatest value, however, a somewhat higher quality reproduction could be made from "photographs" if essential to the understanding of the dissertation. Silver prints of "photographs" may be ordered at additional charge by writing the Order Department, giving the catalog number, title, author and specific pages you wish reproduced.
5. PLEASE NOTE: Some pages may have indistinct print. Filmed as received.

University Microfilms International

300 North Zeeb Road
Ann Arbor, Michigan 48106 USA
St. John's Road, Tyler's Green
High Wycombe, Bucks, England HP10 8HR

78-8703

WICHACHEEWA, Pichai Peter, 1946-
THE KINETICS OF THE EXPOXIDATION OF POLY
(TRANS-1,4-BUTADIENE) CRYSTALS IN SUSPENSION
AND RELATED STUDIES.

City University of New York,
Ph.D., 1978
Chemistry, polymer

University Microfilms International, Ann Arbor, Michigan 48106

THE KINETICS OF THE EPOXIDATION OF POLY (TRANS-1,4-BUTADIENE)
CRYSTALS IN SUSPENSION AND RELATED STUDIES

BY

PICHAI WICHACHEEWA

A dissertation submitted to the Graduate
Faculty in Chemistry in partial fulfillment
of the requirements for the degree of Doctor
of Philosophy, The City University of New York

1977

This manuscript has been read and accepted for the Graduate Faculty in Chemistry in satisfaction of the dissertation requirement for degree of Doctor of Philosophy.

January 4, 1978
date

Arthur E. Woodward
Chairman of Examining Committee

JANUARY 4, 1978
date

Leonard H. Schwartz
Executive Officer

Meier I. Rosau.
Sam Sh. Yang

Supervisory committee

Abstract

THE KINETICS OF EPOXIDATION OF POLY (TRANS-1,4-BUTADIENE)
CRYSTALS IN SUSPENSION AND RELATED STUDIES

BY
PICHAI WICHACHEEWA

Adviser : Professor Arthur E. Woodward

The kinetics of the epoxidation of poly (trans 1,4-butadiene), (PTBD), crystals in toluene suspension using m-chloro perbenzoic acid (MCPBA) was investigated in the 6° to 21° C range by means of infrared spectroscopy. Crystals of PTBD with $M_n = 36,000$ grown from heptane and from toluene solutions and crystals with $M_n = 5510$ grown from heptane were studied. For toluene grown crystals using the higher molecular weight sample, the total number of double bonds available from reaction increases with reaction temperature. This is not true for heptane grown crystals from the same sample. For crystals grown from the lower molecular weight sample, the total number of available double bonds increases within the range 6° to 12° C only. For all preparations investigated the epoxidation reaction is initially second order, first order with respect to the concentration of MCPBA and first order with respect to the concentration of the available double bonds. The second order rate constant is found to be dependent on molecular weight, on temperature and also on the crystal preparation conditions. The bromination of crystals grown from the higher molecular

weight sample was studied in CCl_4 suspension at 0°C using an ultra violet spectrometer Cary 8 to follow the change in bromine concentration. The reaction was found to be complete within one hour and the % double bonds brominated being consistent with the epoxidation results. The infrared spectra for dried mats of epoxidized and brominated PTBD crystals were obtained. It was apparent that there are some changes in the amorphous band at 1350 cm^{-1} due to reaction of double bonds in the fold region. The results of this investigation are discussed in terms of the amorphous component in the fold region of PTBD crystals.

ACKNOWLEDGEMENT

It is the author's sincere pleasure to thank his research mentor, Professor Arthur E. Woodward for his valuable time and excellent guidance and unfailing dedication to the progress of the research project. The author would like to extend his gratitude to both, Professor Henry L. Rosano and Professor Nan Loh Yang, for their most helpful suggestions and discussions.

He is also very grateful to his wife, Oranuch, for her help, understanding and encouragement.

TABLE OF CONTENTS

	Page
ABSTRACT	iii
List of Figures	vii
List of Tables	xi
INTRODUCTION	1
EXPERIMENTAL	20
1) Samples	20
2) Crystal Growth Techniques	21
3) Epoxidation Experiments	22
4) Bromination Experiments	23
5) Infrared Spectroscopy	24
6) Electron Microscope Study	24
RESULTS	26
1) Electron Microscopy	26
2) Epoxidation Results	30
3) Bromination Results	66
4) Infrared Results	71
DISCUSSION	94
CONCLUSIONS	109
REFERENCES	110

LIST OF FIGURES

Figures No.	Caption	Page
1	A drawing of an idealized polymer crystal	1
2	Models of chain folding in single crystal lamellae	
	a) regular adjacent re-entry (tight fold)	4
	b) switchboard (random non-adjacent re-entry) ..	4
	c) irregular adjacent re-entry (loose fold)	4
3	Electron micrograph of PTBD-K toluene grown crystals	27
4	Electron micrograph of PTBD-K heptane grown crystals	28
5	Electron micrograph of PTBD-U heptane grown crystals	29
6	IR absorbance ratios at 1700 to 1735 cm^{-1} vs. mole ratios of MCBA / MCPBA	31
7	% double bonds reacted vs. time for the epoxidation of PTBD-K toluene grown crystals at 6 $^{\circ}$ C	34
8	% double bonds reacted vs. time for the epoxidation of PTBD-K toluene grown crystals at 12 $^{\circ}$ C	35
9	% double bonds reacted vs. time for the epoxidation of PTBD-K toluene grown crystals at 21 $^{\circ}$ C	36
10	% double bonds reacted vs. time for the epoxidation of PTBD-K heptane grown crystals at 21 $^{\circ}$ C	37
11	% double bonds reacted vs. time for the epoxidation of PTBD-U heptane grown crystals at 6 $^{\circ}$ C	38
12	% double bonds reacted vs. time for the epoxidation of PTBD-U heptane grown crystals at 12 $^{\circ}$ C	39
13	% double bonds reacted vs. time for the epoxidation of PTBD-U heptane grown crystals at 16 $^{\circ}$ C	40
14	% double bonds reacted vs. time for the epoxidation of PTBD-U heptane grown crystals at 21 $^{\circ}$ C	41

Figure No.	Caption	Page
15	Second order plot for PTBD-K heptane grown crystals epoxidized at 21 ^o C	44
16	Second order plot for PTBD-K toluene grown crystals epoxidized at 6 ^o and 12 ^o C	45
17	Second order plot for PTBD-K toluene grown crystals epoxidized at 21 ^o C	46
18	Second order plot for PTBD-U heptane grown crystals epoxidized at 6 ^o C	47
19	Second order plot for PTBD-U heptane grown crystals epoxidized at 12 ^o C	48
20	Second order plot for PTBD-U heptane grown crystals epoxidized at 16 ^o C	49
21	Second order plot for PTBD-U heptane grown crystals epoxidized at 21 ^o C	50
22	The Arrhenius plots of PTBD crystals	55
23	Electron micrograph of PTBD-K toluene grown crystals after epoxidation by MCPBA at 6 ^o C	58
24	Electron micrograph of PTBD-K toluene grown crystals after epoxidation by MCPBA at 12 ^o C	59
25	Electron micrograph of PTBD-K toluene grown crystals after epoxidation by MCPBA at 21 ^o C	60
26	Electron micrograph of PTBD-U heptane grown crystals after epoxidation by MCPBA at 6 ^o C	61
27	Electron micrograph of PTBD-U heptane grown crystals after epoxidation by MCPBA at 12 ^o C	62
28	Electron micrograph of PTBD-U heptane grown crystals after epoxidation by MCPBA at 16 ^o C	63

Figure No.	Caption	Page
29	Electron micrograph of PTBD-U heptane grown crystals after epoxidation by MCPBA at 21 ^o C	64
30	Electron micrograph of PTBD-K heptane grown crystals after epoxidation by MCPBA at 21 ^o C	65
31	Absorbance at 416 nm vs. concentrations of Br ₂ in CCl ₄	67
32	Electron micrograph of PTBD-K heptane grown crystals after bromination at 0 ^o C	68
33	Electron micrograph of PTBD-K toluene grown crystals after bromination at 0 ^o C	69
34	IR spectrum of as-grown PTBD-K toluene grown crystals	72
35	IR spectrum of PTBD-K toluene grown crystals annealed at 68 ^o C	73
36	IR spectrum of PTBD-K toluene grown crystals annealed at 80 ^o C	74
37	IR spectrum of PTBD-K toluene grown crystals annealed at 138 ^o C	75
38	IR spectrum of PTBD-K toluene grown crystals epoxidized at 6 ^o C	76
39	IR spectrum of PTBD-K toluene grown crystals epoxidized at 6 ^o C and annealed at 90 ^o C	77
40	IR spectrum of PTBD-K toluene grown crystals epoxidized at 12 ^o C	78
41	IR spectrum of PTBD-K toluene grown crystals epoxidized at 12 ^o C and annealed at 90 ^o C	79
42	IR spectrum of PTBD-K toluene grown crystals epoxidized at 21 ^o C	80

Figure No.	Caption	Page
43	IR spectrum of PTBD-K toluene grown crystals brominated at 0°C	81
44	IR spectrum of PTBD-K toluene grown crystals brominated at 0°C and annealed at 90°C	82
45	IR spectrum of PTBD-K heptane grown crystals.....	83
46	IR spectrum of PTBD-K heptane grown crystals annealed at 68°C	84
47	IR spectrum of PTBD-K heptane grown crystals annealed at 80°C	85
48	IR spectrum of PTBD-K heptane grown crystals annealed at 138°C	86
49	IR spectrum of PTBD-K heptane grown crystals epoxidized at 21°C.....	87
50	IR spectrum of PTBD-K heptane grown crystals brominated at 0°C	88
51	Two component microcrystalline model of PTBD	98
52	Crystal defects due to fold buried deep inside the crystals	99
53	Different kinds of defects in the crystalline region	102
54	Different models of fold region for PTBD crystals from various preparations	104

LIST OF TABLES

Table No.	Caption	Page
I	I_{1350}/I_{1335} for PTBD crystal mats at 25°C	11
II	Comparison of crystallinities for PTBD crystals	13
III	IR Absorbance ratios of various mixtures of MCPBA and MCBA at different mole ratios	30
IV	Initial amount of reactants for epoxidation of PTBD-K crystals at various temperatures	32
V	Initial amount of reactants for epoxidation of PTBD-U crystals grown from heptane at various temperatures .	33
VI	Results for epoxidation of PTBD-K crystals by MCPBA at various temperatures	53
VII	Results for epoxidation at various temperatures of PTBD-U crystals grown from heptane	54
VIII	Calculation of energy of activation for the epoxidation of PTBD-K crystals grown from toluene....	56
IX	Calculation of energy of activation for the epoxidation of PTBD-U crystals grown from heptane....	56
X	Comparison of the thermodynamic parameters of activation for the epoxidation of various olefins....	57
XI	Bromination of heptane and toluene grown PTBD-K crystals in CCl_4 at 0°C	66
XII	Comparison of amorphous content for PTBD crystals....	70
XIII	IR spectra of PTBD-K toluene grown crystals	89
XIV	IR spectra of PTBD-K heptane grown crystals	91
XV	The amorphous content of PTBD-K crystals from the infrared measurements	92

INTRODUCTION

In 1957¹⁻⁵, it was discovered that polyethylene when precipitated from dilute solution crystallized in the form of platlets or lamella-like single crystals. Since this discovery, single crystals from many polymers have been grown and studied⁶ in an attempt to elucidate their morphology and to understand the details of their formation. The understanding of single crystal structure is considered to be a necessary background for the study of polymers crystallized from the melt.

When polymers crystallize from dilute solution, they usually do so in the form of individual microscopic crystals that exhibit varying degrees of morphological complexity depending on the particular polymer and conditions of crystallization. The simplest entity obtained is a monolayer crystal. An idealized representation of a monolayer polymer crystal is depicted in Fig. 1.

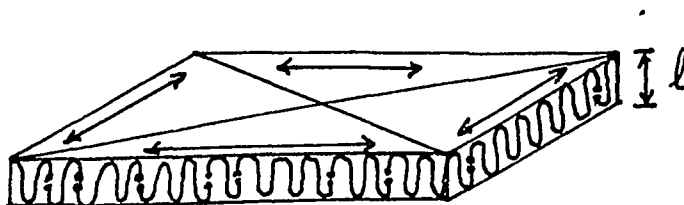


Fig. 1 A drawing of an idealized polymer crystal.

The lateral dimensions of polymer crystals grown from solution fall in the range 1-50 μm . The habit of the crystals is characteristically lamellar. These lamellae are about 100 \AA thick but the thickness is very sensitive to the crystallization conditions, particularly the crystallization temperature. The uniformity of the thickness can be deduced from detailed examination of electron micrographs or from the low angle x-ray diffraction maxima of a collection of such crystals. In many cases four orders of diffraction are observed and there is very good agreement between the dimensions obtained from the electron micrographs and the x-ray diffraction measurements. The orientation of the chain molecules within the platelets has been determined from selected area electron diffraction studies^{4-5,7-10}. The patterns are usually sharp and detailed analysis indicates that the chain axis is preferentially oriented perpendicular to the wide face of the crystal; moreover, the direction of the a and b crystallographic axes are preserved throughout the platelet structure so that the designation "single crystal" has been commonly given to such structures.

The platelet thicknesses are usually no more than the order of a few hundred angstroms thick and this crystal habit is observed for very high molecular weight chains. It becomes clear that a given molecule must traverse a crystallite many times to satisfy the molecular weight requirements, the crystallite thickness requirements and the requirements of orientation. Therefore, the chains should fold back on themselves at the two lateral surfaces. The nature of the fold region has been the subject of intensive study and controversy.

Two different theories have been developed describing the formation of polymer single crystals grown from dilute solution. One theory, as developed by Peterlin, Fischer and Reinhold¹¹⁻¹⁴, suggests that the fold period is determined thermodynamically. The other theory, which is based upon a kinetic approach, was given independently by Lin, Price, Lauritzen and Hoffmann¹⁵⁻¹⁸.

Some workers¹⁹⁻²² reported that polymer single crystals were perfectly regular crystalline entities and the polymer chains are regularly re-entrant meaning the chains enter the crystal at adjacent sites (see Fig. 2a). The fold periods vary slightly about some mean values²³. However, it is clear that morphological studies are inherently limited with respect to providing information at the molecular level. Fischer and Lorenz²⁴⁻²⁵, Jackson et. al.²⁶, and Flory²⁷ measured the density of single crystal mats of polyethylene and arrived at a conclusion in favor of random irregular polymer chain re-entry (non-adjacent re-entry or switchboard model, see Fig. 2b). Several recent studies by Peterlin, Roe, Baer, Keller and others²⁸⁻³⁰ support models in which there is a distribution of fold sizes, ranging from very short to very long (see Fig. 2c). The models proposed are difficult to test because the experiments carried out by these workers involve physico-chemical techniques. The analysis of such quantities as mechanical loss data, infrared spectra and heat measurements in term of the fold region is uncertain because it is not easy to separate the effect due to fold disorder from that due to defects in the interior of the crystals.

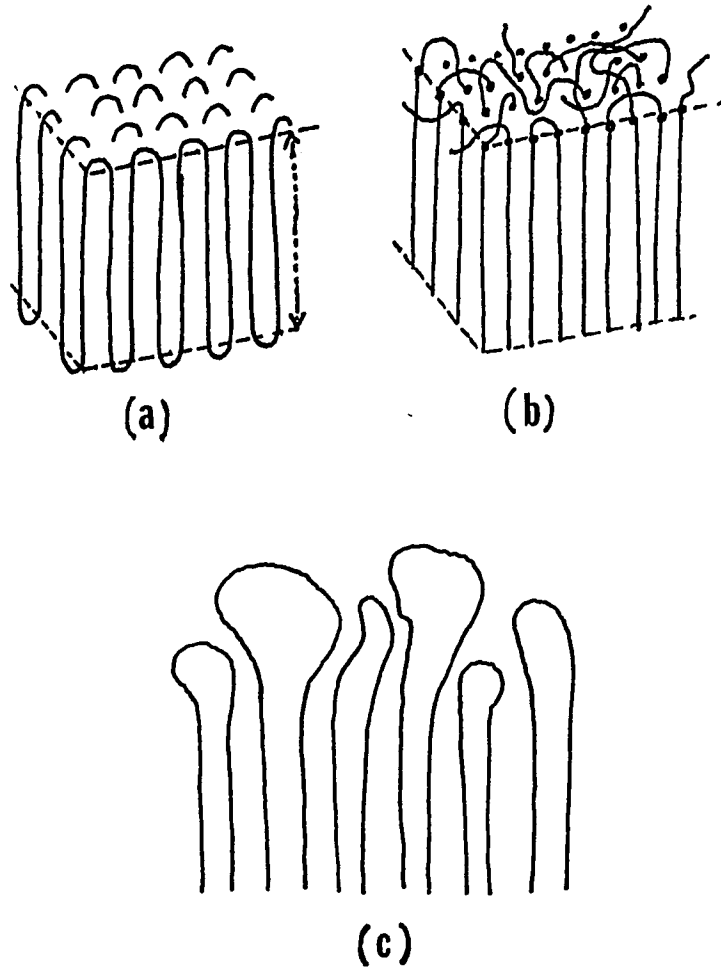


Fig. 2 Models of chain folding packing in single crystal lamellae a) regular adjacent re-entry (tight fold), b) switchboard (random non-adjacent re-entry), c) irregular adjacent re-entry (loose fold).

Several workers³¹⁻³³ have studied the infrared absorption spectra of polymer single crystals and tried to correlate specific absorption bands with the fold region conformation. Krimm and Bank³⁴⁻³⁵ carried out an infrared study of the 71 cm^{-1} absorption for polyethylene single crystals consisting of a mixture of normal and deuterated hydrocarbon; they concluded that adjacent re-entry folding is predominant. Kawai et. al.³⁶ studied the dependence of crystallinity and fold region structure of polyethylene on molecular weight and their results support adjacent re-entry chain folding. Koenig and Agboatwalla³⁷ have given various polymer crystals different physical treatments and then searched the infrared spectra for changes in absorption bands which correspond to changes in the fold region morphology. Udagawa and Keller³⁸ have found from the study of the change of x-ray long spacing by swelling polyethylene single crystals with a liquid that there is a disordered amorphous layer in the fold region which expands by swelling.

Attempts have been made to study the fold region of polyethylene crystals directly by chemical assay but the degradative chemical reactions employed have resulted in destruction of the crystals themselves, and the results are difficult to interpret. Peterlin and Keller and their coworkers³⁹⁻⁴¹ studied polyethylene single crystals by degrading the amorphous portion with fuming nitric acid at high temperature (85°C). The initial rate of weight loss, NMR intensity ratio, NMR second moment, heat of fusion, density of the crystals, molecular weight distribution by gel permeation chromatography

and x-ray diffraction were measured as functions of the time of acid treatment. It was found that at first the reaction was a rapid one, followed by a markedly decreased rate. It was assumed that during the fast part, the easily accessible amorphous region at the crystal fold region are destroyed and during the slow part of the reaction, the rate of nitric acid penetration into the crystal interior diminishes because of steric hindrance. The extent of degradation seemed to indicate that the crystals were more than 50% amorphous and that this component was almost all located in the disordered fold region. More recent work by Keller and coworkers⁴²⁻⁴³ indicated that the diminished rate is actually due to the accumulation of degradation products blocking the remaining reaction sites. It is clear that there is no reaction rate difference between amorphous and crystalline portions in the polyethylene single crystals reacted with a reagent as powerful as fuming nitric acid. They concluded that a milder degradative reagent should be used.

Another study by Winslow et. al.⁴⁴ using gel permeation chromatograph to analyze molecular weight distribution of single crystals showed that there are two peaks in a 2 : 1 ratio dominating the chromatograms. These two peaks were related to molecular weight fractions corresponding to single and double chain traverse lengths that were cut by nitric acid. In 1971 Keller²⁹ reinvestigated the data again and concluded that the fold region of the crystals consists of folds of various lengths, some folds buried at different

depths in the crystals. As the chains are cut at various locations, the peaks corresponding to longer chains decrease in intensity while those of shorter length increase. The same results⁴⁵ were obtained when annealed polyethylene single crystals were used in the investigation.

More recently⁴⁶⁻⁴⁸ ozone gas has been used to oxidized polyethylene single crystals; the reaction was investigated the same way as mentioned above but in addition quantitative analysis of carboxyl groups by dilute sodium hydroxide and infrared spectroscopy was carried out. These experiments have been interpreted as confirming the model of adjacently re-entrant folds of various lengths, terminating at different depths within the crystals.

As the molecule is not of indefinite length, there will be chain ends (cilia). It was found by infrared studies⁴⁹ that the chain ends are outside the crystal lattice, and the length of the chain outside the lattice is less than a single traverse of the lamella. It was assumed that on the average the length of a cilia is one-half the length of a traverse. The fold region is therefore defined as the region which contains chain ends and chain folds.

Based on the discussion above, it is clear that in spite of the large number of investigations that have been carried out on polyethylene, the need for a nondegradative quantitative method of assaying the fold region morphology of polymer single crystals is apparent. For this reason, a series of investigations was started by Woodward and coworkers⁵⁰⁻⁵⁶ on poly (trans-1,4-butadiene), PTBD. In the following section earlier pertinent work is reviewed.

Single crystals of PTBD can be readily grown from a variety of solvents⁵⁷. The crystals were prepared using a growth technique similar to that developed by Blundell and Keller⁸². The procedure involves a minimum temperature of dissolution and self nucleation.

Two crystalline forms are known to exist for PTBD, one is stable at room temperature and transforms to the other at 76°C⁵⁸ by a reversible first order solid-solid phase transition. The low temperature form is designated as form I, and the high temperature form is form II.

The crystal structure of the low temperature form of PTBD was given by Iwayanagi et.al.⁵⁹; it is revealed by x-ray structure analysis that the crystal belongs to the monoclinic system with the space group $P2_1/a$. The unit cell with the lattice constant $a = 8.63 \text{ \AA}$, $b = 9.11 \text{ \AA}$, $c = 4.83 \text{ \AA}$ and $\beta = 114^\circ$ includes four separate repeat units. Although the crystal symmetry is monoclinic, the molecular packing (arrangement of the center of mass of each chain projected on the ab plane) is hexagonal. The monoclinic symmetry comes from a slight asymmetry of the molecule viewed along the c-axis. The staggered succession of the plane repeating units makes the overall molecular shape nearly cylindrical.

The chain conformation of the high temperature form is similar to that of the low temperature form. A rotational motion occurs quite readily, causing the phase transition from the low temperature form to the high temperature form to take place without appreciable relative translation of

the molecules. Takayanaki et. al.⁸³ concluded from the three discrete reflections in the x-ray diffraction pattern that the high temperature form of the crystal belongs to the hexagonal lattice. The assignment of the lattice is still uncertain because the x-ray diffraction pattern consists of a diffuse spot. The dimension of the unit cell are $a = 4.95 \text{ \AA}$, $c = 4.66 \text{ \AA}$, the $\text{CH}_2\text{-CH}_2$ bond remains trans, but the internal rotation angles around the two $\text{CH}_2\text{-CH}_2$ bonds are decreased to 80° and -80° from 109° and -109° respectively. The molecular chains are considered to be in a considerably distorted state due to torsional oscillation about the C-C bonds. Stellman et. al.⁶⁰ found that the high temperature form of PTBD crystals has almost constant heat capacity, indicating that many of the available conformation states are accessible.

The double bond in the repeat unit of PTBD reacts quantitatively with many reactants; peroxidation of the double bonds in polybutadiene has been shown to be a quantitative reaction⁶¹⁻⁶². It can be used to disclose the number of double bonds that are available for reaction at the crystal fold region, and thus serves as a "chemical handle" on the chain folding phenomenon. Moreover, with this technique, an apparent non-destructive one, it is possible to assay the effects of different growth conditions, solvents and polymer molecular weights on the number of double bonds available for the reaction. The knowledge of the number of double bonds available for the reaction can lead to a good estimate of the tightness of the folds in the

fold region of various PTBD single crystal preparations if accurate data concerning the crystal structure and the thickness of the crystals are known. Quantitative chemical assay on PTBD crystals was carried out by Stellman and Woodward⁵²⁻⁵³ by epoxidation of the double bonds in crystals suspended in benzene at 6°C. The crystals were grown from a number of solvents. It was found that depending on the crystal growth conditions from 14-27 % of the double bonds are available for reaction with m-chloroperbenzoic acid (MCPBA) for crystals of approximately the same thickness. This leads to an average value of 2.5 monomer units per fold for heptane grown crystals to 5 monomer units per fold for benzene grown crystals. The number of double bonds necessary for the tightest re-entrant fold calculated from the crystal structure given by Iwayanagi⁵⁹ is between 1.5 - 2 double bonds. Comparison of the value of double bonds per fold from the experiments of Stellman and Woodward⁵²⁻⁵³ led to the conclusion that re-entrant folding is highly probable, although some fold looseness occurs.

High resolution infrared spectra have been obtained in the 1000-1400 cm^{-1} region for crystal mats of PTBD grown from six different solvents⁵⁰. It was found that the ratio of the intensity of the infrared band at 1350 cm^{-1} , an amorphous band, to that at 1335 cm^{-1} , a regularity band varies from 1.3 to 0.1 with the solvent used for crystal preparation, the PTBD used and with the thermal history. The ratio is larger for crystals grown at temperatures well below the transition temperature than those grown near to it. When the crystals were heated to 80°C and cooled down to room temperature, it

was found that the infrared intensity ratio I_{1350}/I_{1335} decreased. The values of I_{1350}/I_{1335} for PTBD crystals grown from different solvents and for the crystals after 80°C annealing are listed in Table I.

TABLE I

I_{1350}/I_{1335} for PTBD Crystal Mats at 25°C⁵⁰

Sample	Mn	Solvent	I_{1350}/I_{1335}	
			As prepared	After 80°C annealed
PTBD-K	3.6×10^4	MIBK	0.2	0.2
		Heptane	0.2	0.1
		Toluene-ethanol	1.0	0.4
		Toluene	1.2	0.6
		Benzene	0.9	0.3
		Benzene cast film	0.3	-
		melt form	0.5	-
PTBD-U	5510	MIBK	0.2	0.3
		Heptane	0.3	0.2
		Toluene-ethanol	1.3	0.2
		Benzene-ethanol	1.2	0.3
		Melt form	1.0	-

Ng, Stellman and Woodward⁵¹ also studied PTBD crystals by using differential scanning calorimetry. Assuming that ΔH_t , the heat of transition from form I to form II, is proportion to the crystallinity, the crystallinity was obtained for toluene and benzene grown crystals by taking that for heptane grown crystals as 0.8 as given by the infrared measurements.

It was found that toluene and benzene grown crystals have a greater amorphous content than heptane grown crystals, in agreement with the infrared results.

Another method which can be used to estimate the total amount of amorphous material in a solid is broadline nuclear magnetic resonance. If conditions are such that some reorientation motion is taking place in the amorphous component and the crystalline regions are effectively rigid, then a two component NMR absorption will be found, the narrow part being associated with the mobile regions. Ng and Woodward⁵¹ reported the measurements of NMR intensity ratios for PTBD crystals grown from heptane and toluene. The crystals were wetted with a non-protonated solvent (CS₂) which served as a surface penetrant. The NMR determinations were carried out at low temperature (-24° to -90°C range). If it is assumed that the narrow line accounts for all or most of the amorphous regions, toluene grown crystals have a greater amorphous content than heptane grown crystals.

The crystallinities of PTBD crystals as obtained by various methods are given in Table II. It was concluded that for some preparations the total amorphous content exceeded that present at the crystal surface region alone. That implied that amorphous regions do exist in the interior of the crystals.

TABLE II
Comparison of Crystallinities for PTBD Crystals

Growth Condition	Crystalline Fraction			
	ΔH_t ⁵¹	NMR ⁵⁴	IR ⁵⁰	Epox ⁿ ⁵¹
Heptane 76 / 63 C	(0.8)	0.87	0.8	0.86
Toluene 50 / 23 C	0.6	0.77	0.5	0.81
Benzene 52 / 8 C	0.5	-	0.5	0.73

The effect of heat treatment of PTBD single crystals prepared from dilute benzene solution was studied by dilatometry, x-ray diffraction and dynamic viscoelastic measurement⁶³. The crystal transition temperature of the single crystals grown from that solvent was found to be 55.5°C, 20°C lower than that of the bulk crystallized sample⁶⁴⁻⁶⁵. The dynamic viscoelastic measurement showed that the single crystals of PTBD have two viscoelastic absorption peaks at -10°C and 35°C respectively. The -10°C peak has been attributed to the primary absorption (α_a). The appearance of the primary absorption indicates that a considerable amount of the amorphous polymer exists in the single crystal mats. A primary absorption is caused by initiation of micro-brownian motion of the molecular chains. After heat treatment of the single crystals above 55.5°C, the transition temperature increased to 69.5°C. At the same time, thickening of the lamellae occurred and the viscoelastic primary absorption observed in the single crystal mats disappeared. These results

suggested that the amorphous regions rapidly crystallized above a temperature of 55.5°C , and therefore the loose folds attached to the end surface of the crystal are dragged into the crystalline phase to form tight folds as a result of the sliding diffusion of the molecules along their axes. This is accompanied by the sudden thickening of the lamellae at the crystal transition temperature. It is claimed that a likely possibility for the formation of loose folds was due to the hindering effect of 1,2 (side chain vinyl) impurities which can not be easily accommodated in the crystal component.

White and coworkers⁶⁶ reported that the influence of the first order crystalline transformation at about 60°C on the infrared bands of PTBD crystals yields microscopic information that supports the two component microcrystalline model of a folded chain having loose and tight folds at the lamellar surfaces. Loose and tight fold surface regions are illustrated in Fig. 2 above. The temperature dependence of the band parameters of the 908 cm^{-1} vinyl band indicates that 1,2 (side vinyl) units are not easily taken into the crystalline component, thus forming loose folds at the crystal fold region that account for the micro-brownian motion detected in the low temperature form. It was shown that the infrared band parameters such as integrated intensity and band width are excellent probes for the microscopic thermodynamic properties of polymers. Most significantly it was shown that the non-responsive behavior of the band width of the 908 cm^{-1} vinyl band of PTBD near the crystalline

phase transition is consistent with the loose fold property of the folded chain model.

In 1974 Oyama et.al.⁶⁷ reported the assignment and the method of resolving the infrared spectrum of PTBD in the region of 1450 cm^{-1} in order to analyze the conformation of butadiene units in the fold. Four conformation sensitive methylene scissoring bands were assigned by the rotational state of the $\text{CH}_2\text{-CH}_2$ rotational axes. Two bands at 1458 cm^{-1} and 1449 cm^{-1} were assigned to the amorphous conformation, and the other two bands at 1451 cm^{-1} and 1438 cm^{-1} to the crystalline conformation. From two parameters determined experimentally and the assumption of a Lorentzian representation for each band, the spectrum was resolved into four bands. The average conformation in the non-crystalline part of the as-grown crystals was considered to be nearly the same as that for the random coil. It was concluded that the average conformation in the non-crystalline part became Gauche-rich. Using reasonable assumptions, the number of trans mers, $N(T)$, and gauche mers, $N(G)$, per fold of the single crystals were estimated; $N(T) = 2-3$, $N(G) = 3-2$ for as-grown sample and $N(T) = 0-1$, $N(G) = 3-2$ for the 80°C annealed sample. The distance between adjacent chains in a fold is 4.60 \AA for PTBD, and three rotational axes are included in a mer of PTBD; therefore it was assumed that three mer folds in PTBD single crystals may be the shortest. This fold was expected to be tight and rigid and therefore would not show the α_a dispersion in dynamic viscoelastic measurements as mentioned before by Takayanaki et. al.⁶³.

Evans and Woodward⁵⁶ studied the Raman spectra of mats of PTBD crystals grown from dilute solution. The effect of crystal growth temperature, of solvent and of various thermal and mechanical treatments on the spectrum at 25°C were explored. The changes accompanying the form I to form II crystal-crystal transition were observed by obtaining Raman spectra at various temperatures in the 25-78°C range.

The spin-probe technique has been employed by Nagamura and Woodward⁵⁵ to study the nature of the surface regions of PTBD crystals grown from dilute heptane and toluene solution. The spin probe method is based on the response of the line shape of the ESR spectrum of a paramagnetic probe, usually a nitroxide radical, embedded in a polymer matrix to molecular motion of the matrix. The probes are not chemically bound but only weakly held by the polymer chains. The narrowing of the ESR spectrum of the nitroxide radical probe added to the PTBD crystals and the activation energy for the rotational motion of the probes were found to vary with crystallization solvent and annealing temperature; in every case heptane grown crystals showed a higher line narrowing temperature and activation energy than toluene grown crystals. Annealing at 80°C raised the narrowing temperature and activation energy for crystals prepared from both solvents, but annealing at higher temperature near to but below the melting point, lowered both parameters again. This confirmed earlier work concerning the dependence of the amount of amorphous material at the crystal surface region on the solvent (and temperature) of crystal growth.

In 1976 Martucelli et.al.⁶⁸ reported that the bromination of a suspension of single crystals of PTBD is selective at the surface region from studies by differential scanning calorimetry, infrared spectroscopy and small angle x-ray diffraction. They interpreted their results in such a way as to conclude that as the thickness of the crystals was increased a larger number of double bonds per fold were brominated. This is consistent with an increase in the thickness of the disordered surface region with an increase in the crystallization temperature. The thermal behavior of the bulk material obtained by recrystallization of melted brominated single crystals of PTBD shows that $\text{CH}_2\text{-CHBr-CHBr-CH}_2$ units are incorporated into the crystal lattice and lower its degree of order and act as chain defects.

Martucelli et. al.⁶⁹ also investigated the morphology and thermal behavior of PTBD single crystals grown from heptane using the electron microscope, wide angle x-ray diffraction and differential scanning calorimetry. The thickness of the crystals reported by them was much greater than those reported earlier by Woodward et. al.⁵²⁻⁵³ and Takayanagi et. al.⁶³. From the calorimetric study, convincing evidence of the presence of two different thermodynamic stabilities of crystalline blocks of form I was obtained and the relative amounts of each were calculated. It was found that the equilibrium transition temperature of form I and form II is at 75°C and the melting temperature of form II is 139°C .

In the earlier epoxidation studies of PTBD crystals by Woodward and coworkers, the principal interest was in

establishing the maximum number of double bonds reacted for crystals grown from different solvents; little attention was paid to 1) any differences in the reaction rate prior to the levelling off period for different crystal preparations or to 2) reaction temperature effects. For this reason, this project was originated to study the rate of epoxidation in more detail, and the effect of temperature on the maximum number of double bonds available for reaction in order to obtain more information concerning the amorphous component at the fold region of PTBD crystals. The effect of temperature and molecular weight on the rate of epoxidation was to be investigated. It was expected that the differences in rate of epoxidation at the same temperature should be related to the different types of fold region in the crystals.

STATEMENT OF THE PROBLEM

The major purposes for this investigation were the following :

- 1) to obtain more information about the fold surfaces of different PTBD crystal preparations,
- 2) to investigate in more detail the interior amorphous content of PTBD crystals,
- 3) to study the kinetics and the order of the epoxidation reaction at the surface regions of PTBD crystals suspended in toluene,
- 4) to determine the effect of temperature on the number of double bonds available for reaction and on the rate of reaction, and
- 5) to determine the effect of molecular weight on the rate of epoxidation reaction.

EXPERIMENTAL

SAMPLES

The samples of PTBD used in this investigation as supplied by Ube Kosan Co., Ltd. of Japan and by Uniroyal Inc. were found from infrared analysis, using a Perkin Elmer 621 spectrometer, to have more than 95% trans content⁵³. These sample were designated as PTBD-K and PTBD-U respectively by Woodward and coworkers. For the PTBD-K sample, as received, a number average molecular weight, M_n of 8670 ($\pm 10\%$) was reported by Debell and Richardson Co. Inc. using a Hitachi Perkin Elmer vapor pressure osmometer. After crystallization the molecular weight was found to increase to 36,000 ($\pm 10\%$).

The viscosity average molecular weight M_v was obtained for PTBD-K using the following relationship derived by R. Endo⁸⁴

$$[\eta] = 2.9 \times 10^{-4} M_v^{0.75} \dots\dots\dots (1)$$

where $[\eta]$ is the intrinsic viscosity determined by using a Ubbelohde dilution viscometer at 30°C in a chloroform solution. The intrinsic viscosity and the M_v for PTBD-K were 1.53 dl/g and 92,000 respectively.

The viscosity average molecular weight (M_v) for the PTBD-U bulk polymer was given as 11,000 ($\pm 10\%$). After crystallization the number average molecular weight, M_n , was found to be 5510 ($\pm 10\%$) using a Hewlett Packard 302B vapor pressure osmometer.

CRYSTAL GROWTH TECHNIQUES

Toluene grown crystals of PTBD-K were prepared by a method which is similar to that used by Stellman and Woodward⁵³. A weight of 0.02 gm. of polymer was dissolved at 50°C in a test tube which contained 50 ml. of toluene. The solution was then filtered through a sintered glass funnel and cooled in an ice bath for nucleation, a procedure which differs from that of Stellman. The solution was reheated to 50°C and then placed in a 23°C bath. Crystallization appeared complete within 10-12 hours. The suspension was filtered and washed with fresh toluene.

Heptane grown crystals of PTBD-K were prepared in the following manner. A weight of 0.01 gm. of polymer was dissolved at 78°C in a test tube which contained 50 ml. of heptane. This solution is less concentrated than those prepared by Stellman (0.01% by weight as compared to 0.02% by weight). It was found in preliminary experiments that using 0.01% solution tends to give more uniform sized single crystals. The solution was then filtered and left to cool to room temperature for nucleation of crystals. The solution was reheated to 78°C and then placed in a 63.5°C bath. Crystallization appeared complete within 4-5 hours. The suspension was filtered hot and then washed with fresh solvent.

Crystals of PTBD-U in heptane solvent were grown from 0.02% solution by the same method as PTBD-K crystals. The polymer (0.01 gm.) was dissolved in 400 ml. of heptane at 69°C and then filtered and left to cool to room temperature

for nucleation of crystals. The solution was reheated to 55°C and then was placed in a 45°C bath. It took about 10-12 hours for the crystallization to be complete.

EPOXIDATION EXPERIMENTS

In the epoxidation of PTBD crystals by m-chloro perbenzoic acid (MCPBA), one of the two principal products is m-chloro benzoic acid (MCBA). MCPBA has a carbonyl stretching band at 1735 cm⁻¹ and MCBA has one at 1700 cm⁻¹. The comparison of the values of log I₀ / I for the two different absorption peaks can be written.

$$\frac{A}{A'} = \frac{\log I_0 / I}{\log I_0 / I'} = \frac{\epsilon c l}{\epsilon' c' l} = \frac{\epsilon c}{\epsilon' c'} \dots\dots(2)$$

$$\frac{A}{A'} = k B \dots\dots(3)$$

B is the mole ratio of the two components, k is a constant which can be evaluated by means of a calibration curve in which the left hand term, calculated directly from the relative height of the absorption peaks, is plotted as ordinate and the mole ratio as abscissa.

Mixture of MCPBA and MCBA were prepared at different mole ratios and the infrared spectrum were run using a Perkin Elmer 621 spectrometer.

In the epoxidation runs, a known weight of crystals (50-100 mg.) suspended in 50 ml. toluene at constant temperature was mixed with enough MCPBA to react with 20-40% of the double bonds present in a particular sample. Aliquots of the reaction mixture were taken out at various times up

to at least 75 hours and the infrared spectrum in the 1650-1800 cm^{-1} region were obtained at room temperature. A blank solution containing the same amount of MCPBA in toluene with no crystals present was kept at the same temperature in order to monitor the amount of decomposed MCPBA. The mole ratio of MCPBA and MCBA in the reaction mixture was calculated from the measured absorbance ratio at 1700 and 1735 cm^{-1} using the calibration curve obtained from the known mixtures with a correction for thermal decomposition of MCPBA being made. The amount of double bonds reacted is equal to the decrease in concentration of MCPBA. Prior to epoxidation, PTBD-K and PTBD-U heptane grown crystals were resuspended in toluene.

BROMINATION EXPERIMENTS

Bromine in CCl_4 gives a very strong absorption peak at 416 nm. From the Beer Lambert equation

$$A = \epsilon c l \quad \dots\dots\dots(4)$$

A = Absorbance

c = concentration of the solution

l = path length of the cell

ϵ = extinction coefficient

The extinction coefficient can be calculated from the slope of plot of absorbance against the concentration of the solution. Different concentrations of bromine in CCl_4 were prepared and the spectrum run using a Cary 8 Ultraviolet spectrometer.

A known weight of crystal was suspended in CCl_4 , the flask was covered with aluminum foil and then cooled in the refrigerator. A known amount of bromine, enough to react with 30-40% of the double bonds in the polymer was added. The reaction seemed to be completed within one hour. The amount of bromine reacted with the double bonds was calculated from the change in the absorbance of the reaction mixture.

INFRARED SPECTRUM OF PTBD-K CRYSTAL MATS

Crystal mats were prepared by filtration of crystals using millipore filters. The crystals were washed several times using pure liquid (Toluene or CCl_4) to eliminate non-polymeric reactants and products. The mats were then mounted between two KBr pellets. Infrared spectrum were obtained using a Perkin Elmer 621 infrared grating double beam spectrometer in the high resolution mode for as prepared crystal mats, surface epoxidized crystal mats, surface brominated crystal mats, as grown crystal mats annealed at 68° , 80° , and 138°C , and epoxidized and brominated crystal mats annealed at 90°C . The annealed crystal mats were held at the specified temperature for 1.5 hours in vacuum, the oven was then turned off, and the sample allowed to cool to room temperature where the spectra were run.

ELECTRON MICROSCOPE OBSERVATIONS

Crystals were deposited from suspension onto a copper grid which was coated with carbon. The grid was then shadowed with gold for better contrast. The crystals were usually observed under the electron microscope at magnifications in the range of 6000 to 25,000 times, and

the pictures of crystals were taken directly with a plate camera attached to the electron microscope.

As grown, epoxidized and brominated PTBD-K crystals grown from heptane and toluene were observed under the electron microscope to monitor possible changes in surface morphology. It was necessary to wash the epoxidized or brominated crystals several times with pure liquid (Toluene or acetone) to get rid of non-polymeric reactants and products before depositing on the copper grid. As grown and epoxidized PTBD-U crystals grown from heptane were also studied under the electron microscope.

RESULTS

ELECTRON MICROSCOPY

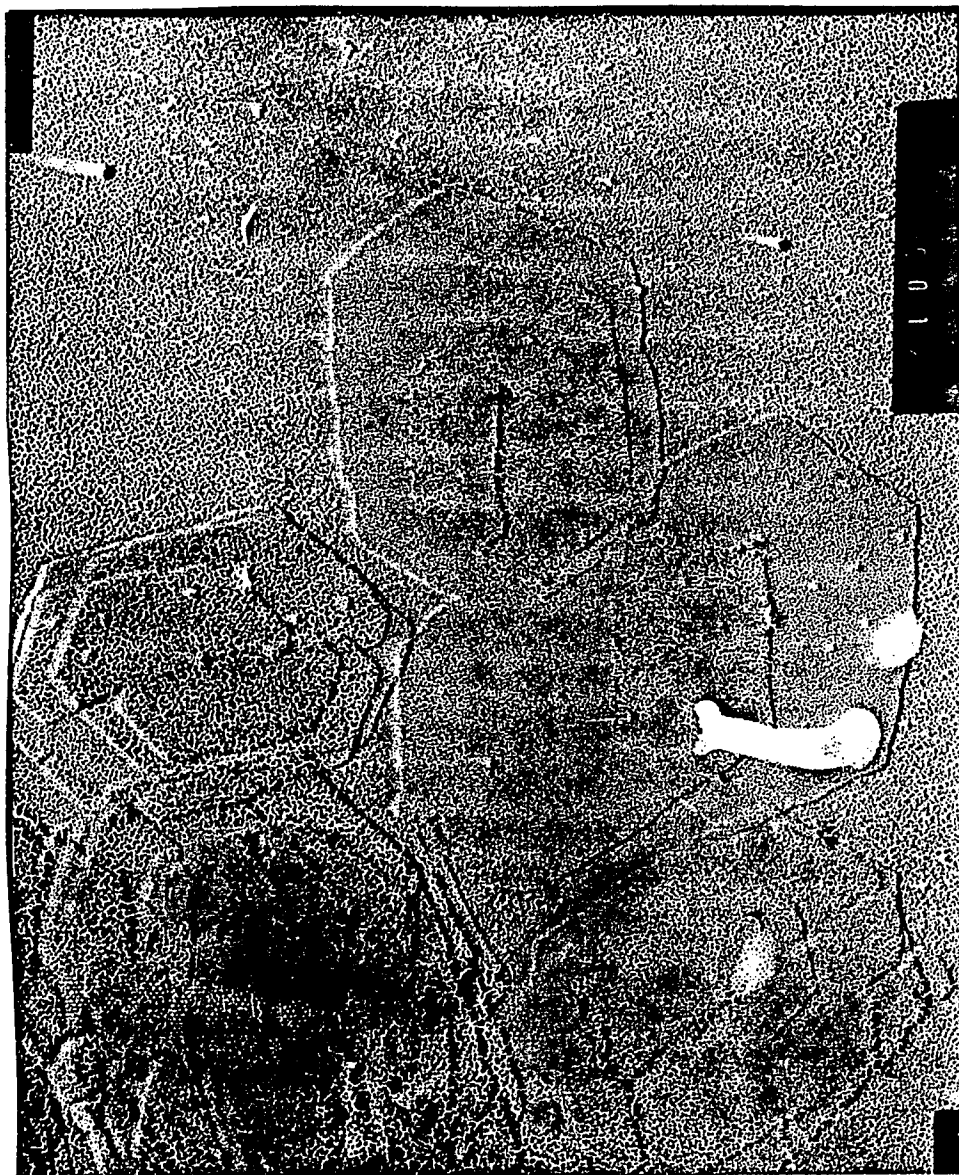
Electron micrographs of PTBD-K crystals grown from heptane and toluene and PTBD-U crystals grown from heptane are shown in Fig. 3,4 and 5 respectively. The PTBD-K heptane grown crystals are regular hexagons with a cross section diameter of about 5-6 microns. The PTBD-K toluene grown crystals are smaller by a factor of two than those grown from heptane, and the shape is an elongated hexagon with sharp regular edges. The crystal size is approximately uniform since the crystals start to grow simultaneously from nuclei already present and each individual crystal is approximately representative of the preparation as a whole. The thickness of the PTBD-K crystals grown from heptane was found to be 95 \AA by Professor Brian Newman of Rutgers university using low angle x-ray diffraction on a brominated crystal mat. The thickness of PTBD-K toluene grown crystals was reported earlier⁵³ as 94 \AA .

The PTBD-U heptane grown crystals were also elongated hexagonal crystals but consisted of several layers stacked on top of each other. The size was about 5 microns wide and 10 microns long with a thickness of $82 \pm 15 \text{ \AA}$. This value is obtained by measuring the shadow length of crystals from electron micrograph and then calculating the thickness by comparison with the shadow length of PTBD-K toluene grown crystals with approximately same shadowing angle.



Fig 3 Electron micrograph of PTBD-K heptane grown crystals
(Mag. 10,600)

2μ



1 μ

Fig. 4 Electron micrograph of PTBD-K toluene grown crystals
(Mag. 43,000).

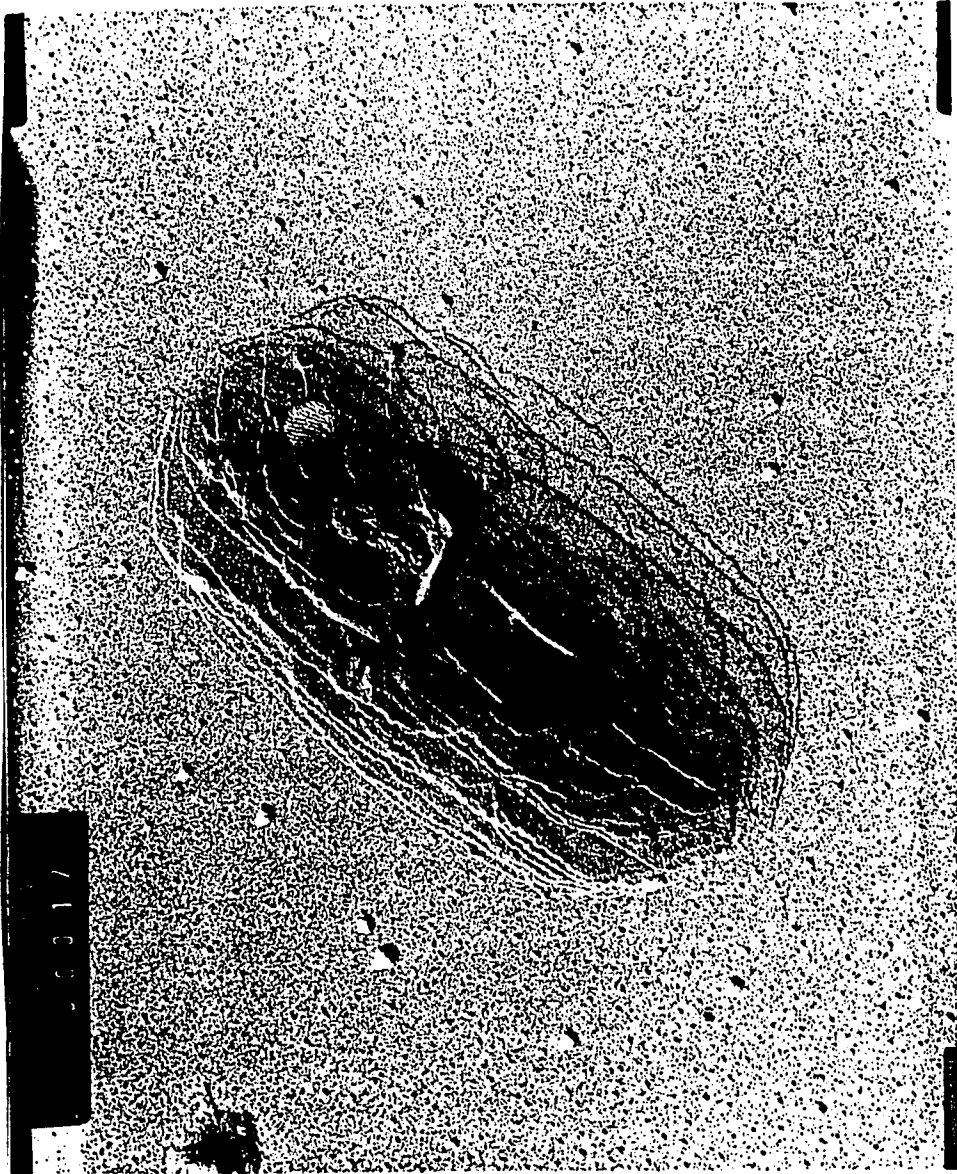


Fig. 5 Electron micrograph of PTBD-U heptane grown crystals
(Mag. 17,000)

2 μ

EPOXIDATION RESULTS

A) The calibration curve

The results of the absorbance ratios (A_{1700}/A_{1735}) of mixtures of MCPBA and MCBA at different mole ratios are reported in Table III. The graph of the ratio of absorbance of MCPBA and MCBA is plotted against mole ratio in Fig. 6.

TABLE III

Absorbance Ratios of Various Mixtures of MCPBA and MCBA at Different Mole Ratios.

Mole ratio MCBA / MCPBA	Absorbance ratio A_{1700} / A_{1735}	Mole ratio MCBA/MCPBA	Absorbance ratio A_{1700} / A_{1735}
0.05	0.034	0.80	1.343
0.10	0.052	0.90	2.183
0.15	0.121	1.00	1.865
0.20	0.150	1.10	2.200
0.25	0.239	1.20	2.365
0.30	0.320	1.30	2.433
0.35	0.369	1.40	2.965
0.40	0.476	1.50	3.141
0.45	0.586	2.00	3.883
0.50	0.603	3.00	7.170
0.60	0.883	4.00	9.069
0.70	1.068		

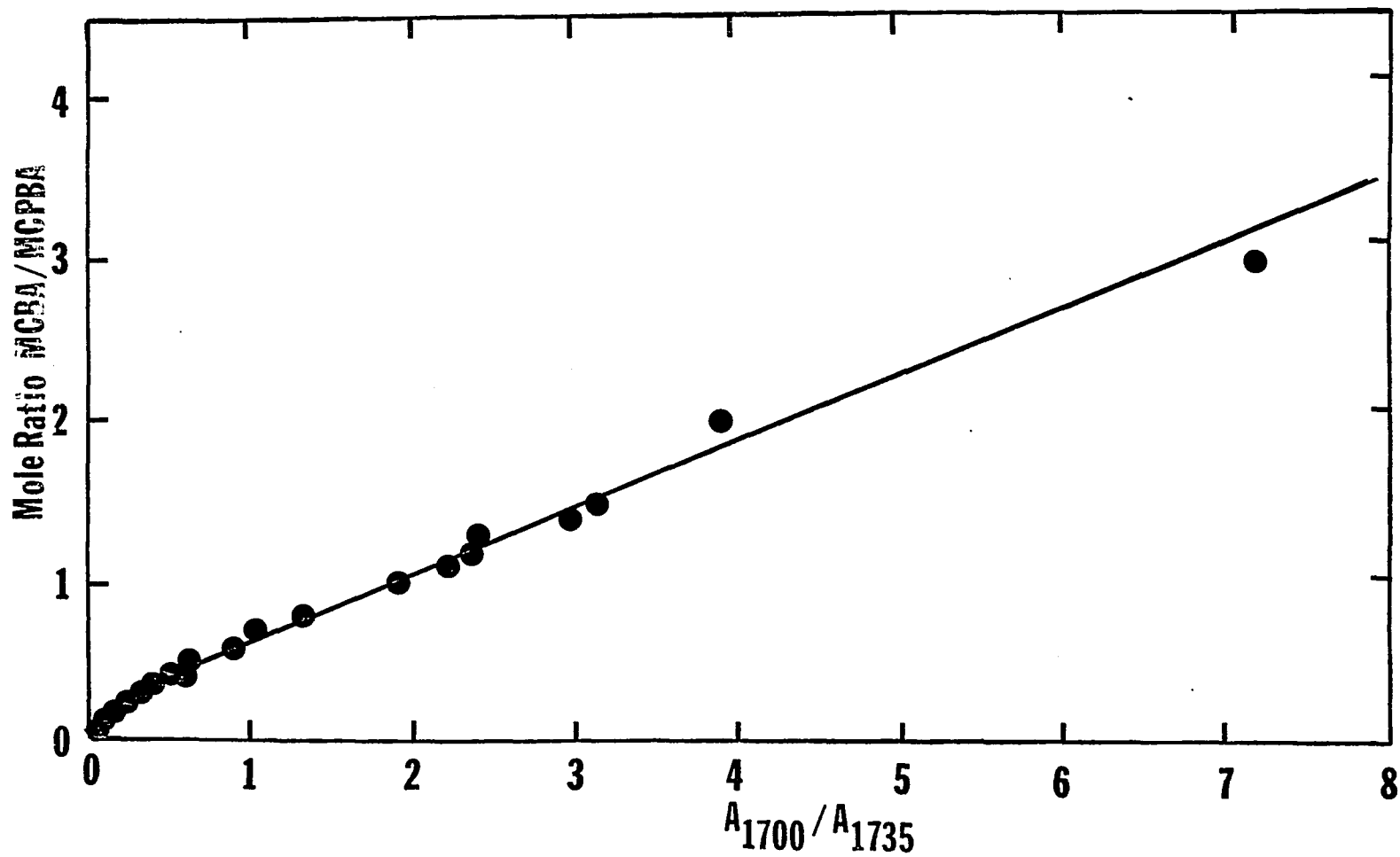


Fig. 6 IR absorbance ratios at 1700 to 1735 cm^{-1} vs. mole ratios of MCBA / MCPBA

B) Epoxidation Results of PTBD Crystals.

The epoxidation of PTBD crystals was investigated for three preparations. The results of various epoxidation reaction carried out are given in Fig. 7-14 in terms of % double bond reacted with time. The initial amount of reactants used in these experiments are given in Table IV and V.

TABLE IV

Initial Amount of Reactants for Epoxidation of PTBD-K Crystals at Various Temperatures.

Run #	Type of Crystals	Temp. °C	Wt. of Crystals mg.	Moles of Crystals $\times 10^3$	Wt. of MCPBA mg.	Mole of MCPBA $\times 10^4$	Mole ratio db / MCPBA
1	Toluene Grown Crystals	6	72.0	1.33	44.2	2.56	5.20
2	same	6	78.5	1.45	49.7	2.88	5.03
3	same	12	95.0	1.76	134.2	7.78	2.26
4	same	21	71.5	1.32	65.8	3.81	3.46
5	same	21	95.0	1.76	108.6	6.30	2.80
6	same	21	99.0	1.83	141.5	8.20	2.23
7	Heptane Grown Crystals	21	87.5	1.61	83.9	4.86	3.31
8	same	21	48.5	0.90	46.5	2.70	3.33

TABLE V

Initial Amount of Reactants for Epoxidation of PTBD-U Crystals
Grown from Heptane at Various Temperatures

Run #	Temp. °C	Wt. of Crystals mg.	Mole of Crystals $\times 10^3$	Wt. of MCPBA mg.	Mole of MCPBA $\times 10^4$	Mole ratio db / MCPBA
1	6	95.0	1.76	107.3	6.22	2.83
2	6	57.0	1.06	76.0	4.41	2.40
1	12	62.5	1.16	94.6	5.48	2.12
2	12	88.9	1.65	129.0	7.48	2.21
3	12	62.5	1.16	150.5	8.72	1.33
1	16	64.5	1.19	138.9	8.05	1.48
2	16	67.5	1.25	141.1	8.18	1.53
3	16	78.0	1.44	178.2	10.33	1.39
1	21	69.0	1.27	104.8	6.08	2.09
2	21	74.5	1.38	169.0	9.80	1.41
3	21	72.0	1.33	217.6	12.62	1.05
4	21	91.0	1.69	227.8	13.21	1.28

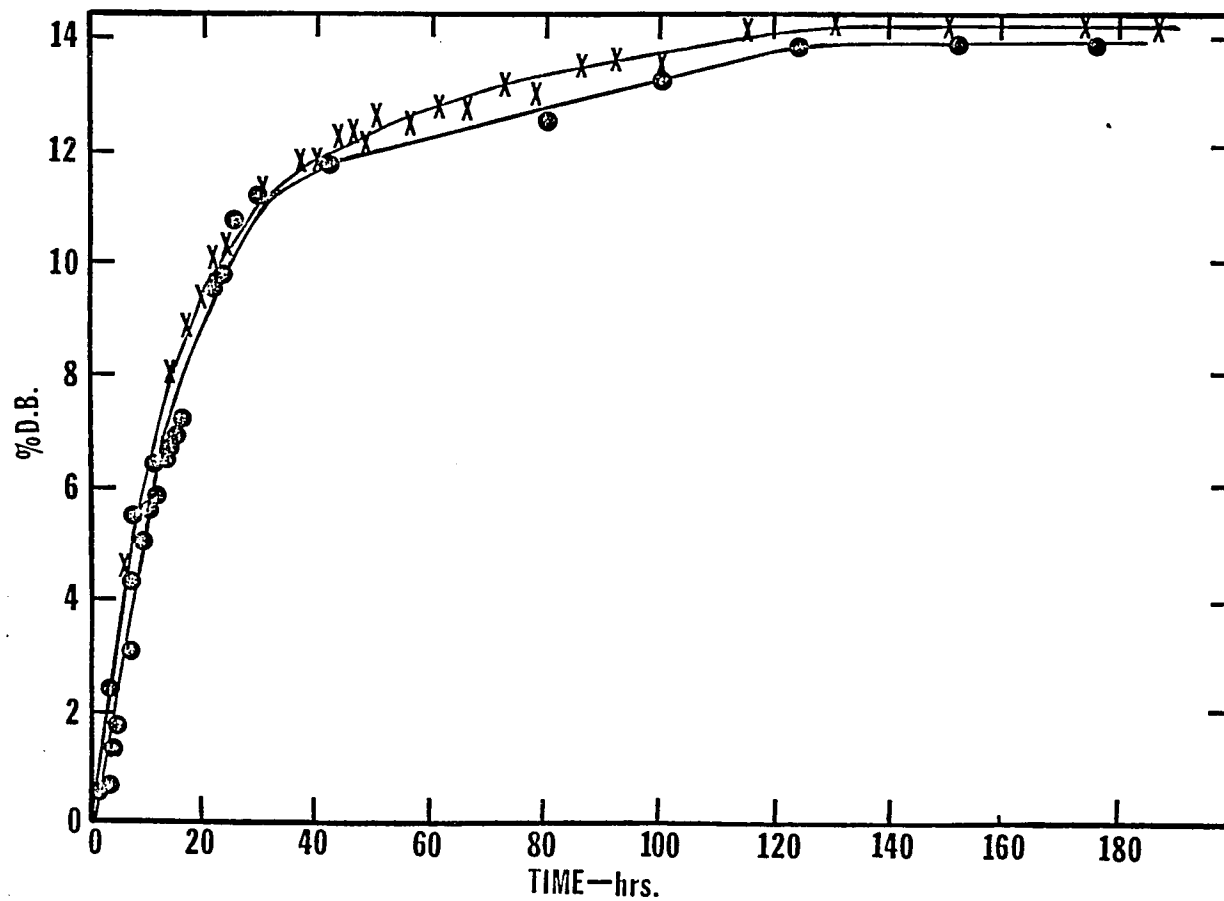


Fig. 7 % double bonds reacted vs. time for the epoxidation of PTBD-K toluene grown crystals at 6°C, ● 1 st run, X 2 nd run.

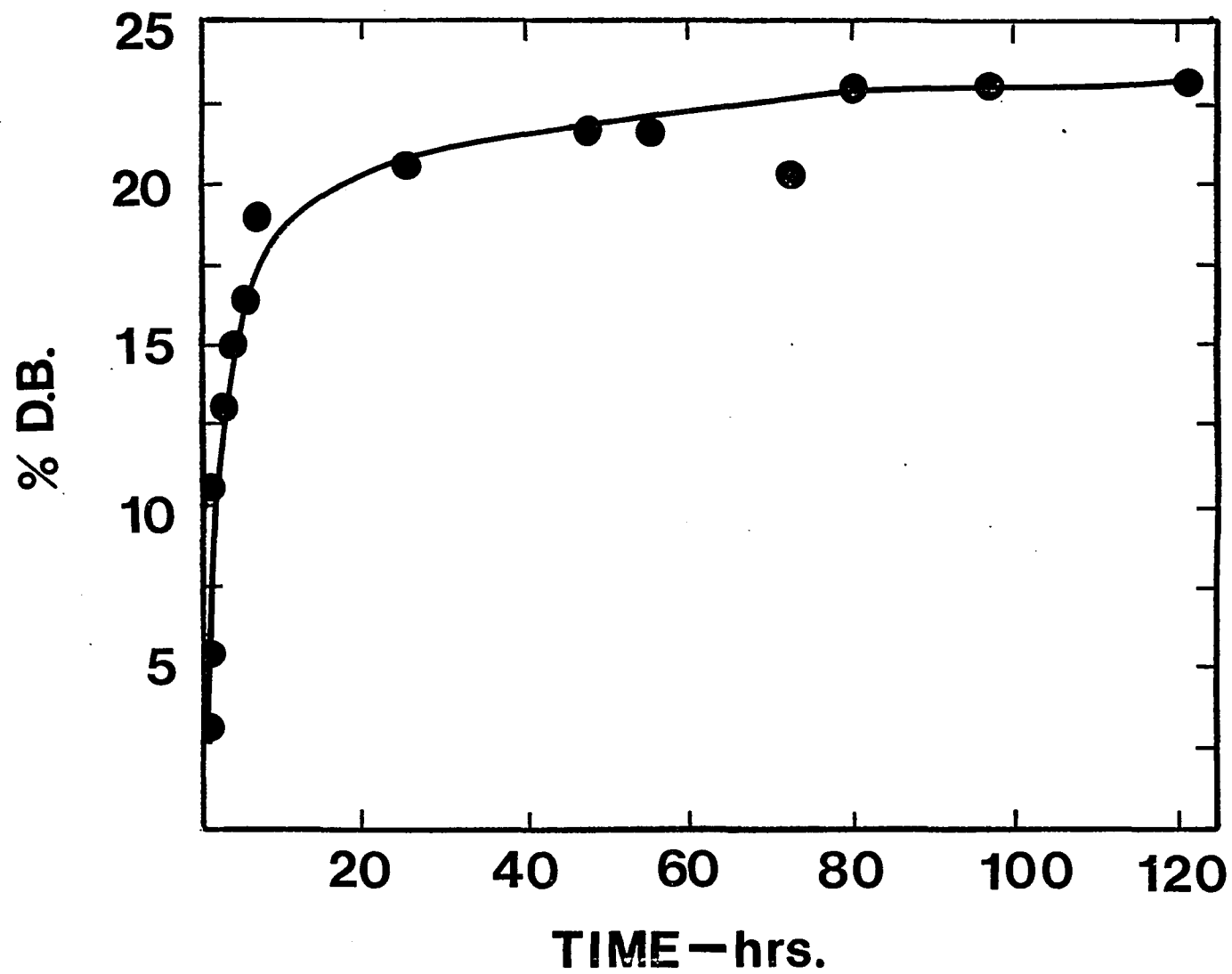


Fig. 8 % double bonds reacted vs. time for the epoxidation of PTBD-K toluene grown crystals at 12°C

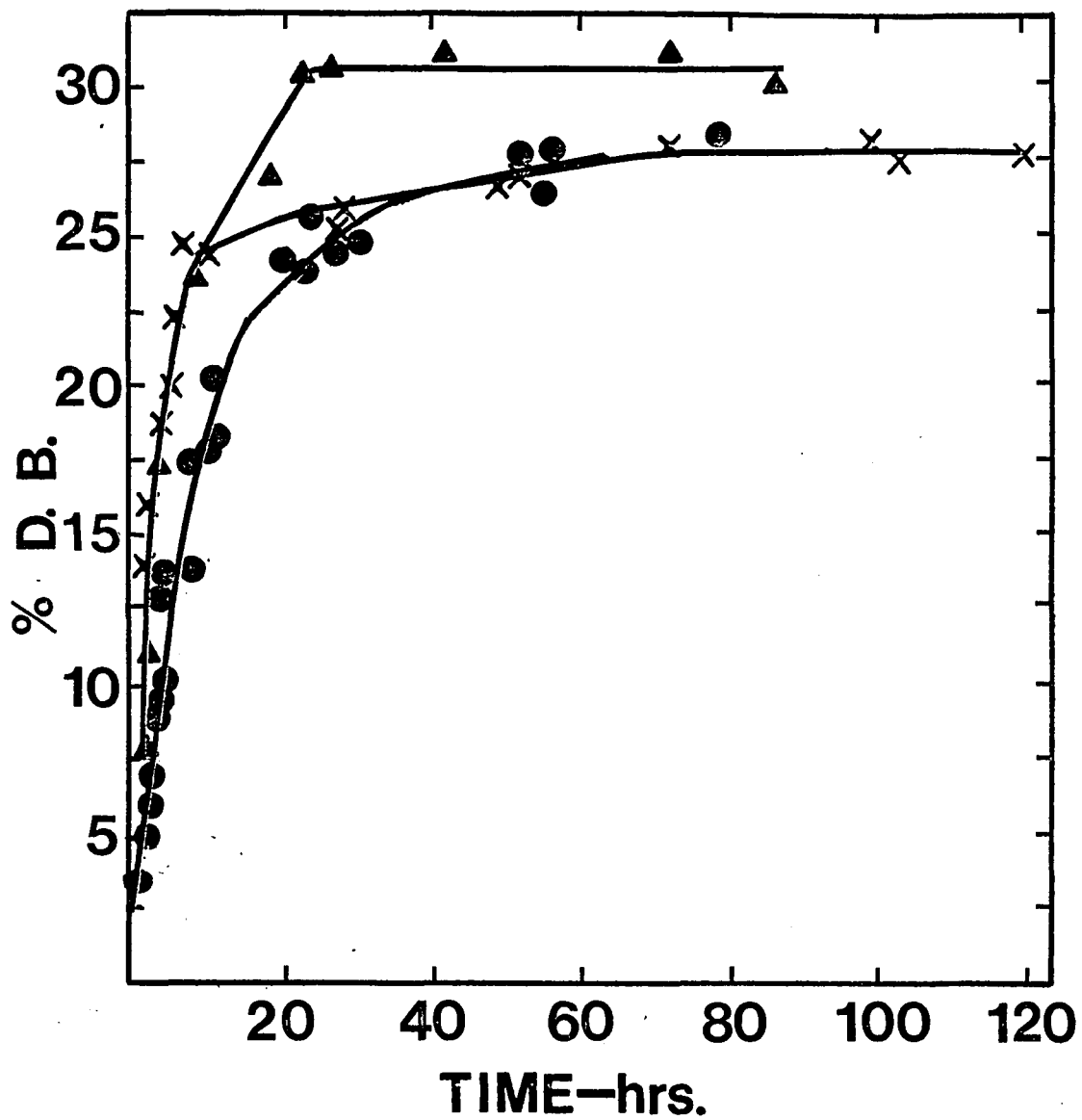


Fig. 9 % double bonds reacted vs. time for the epoxidation of PTBD-K toluene grown crystals at 21°C, ● 4th run, X 5th run, ▲ 6th run.

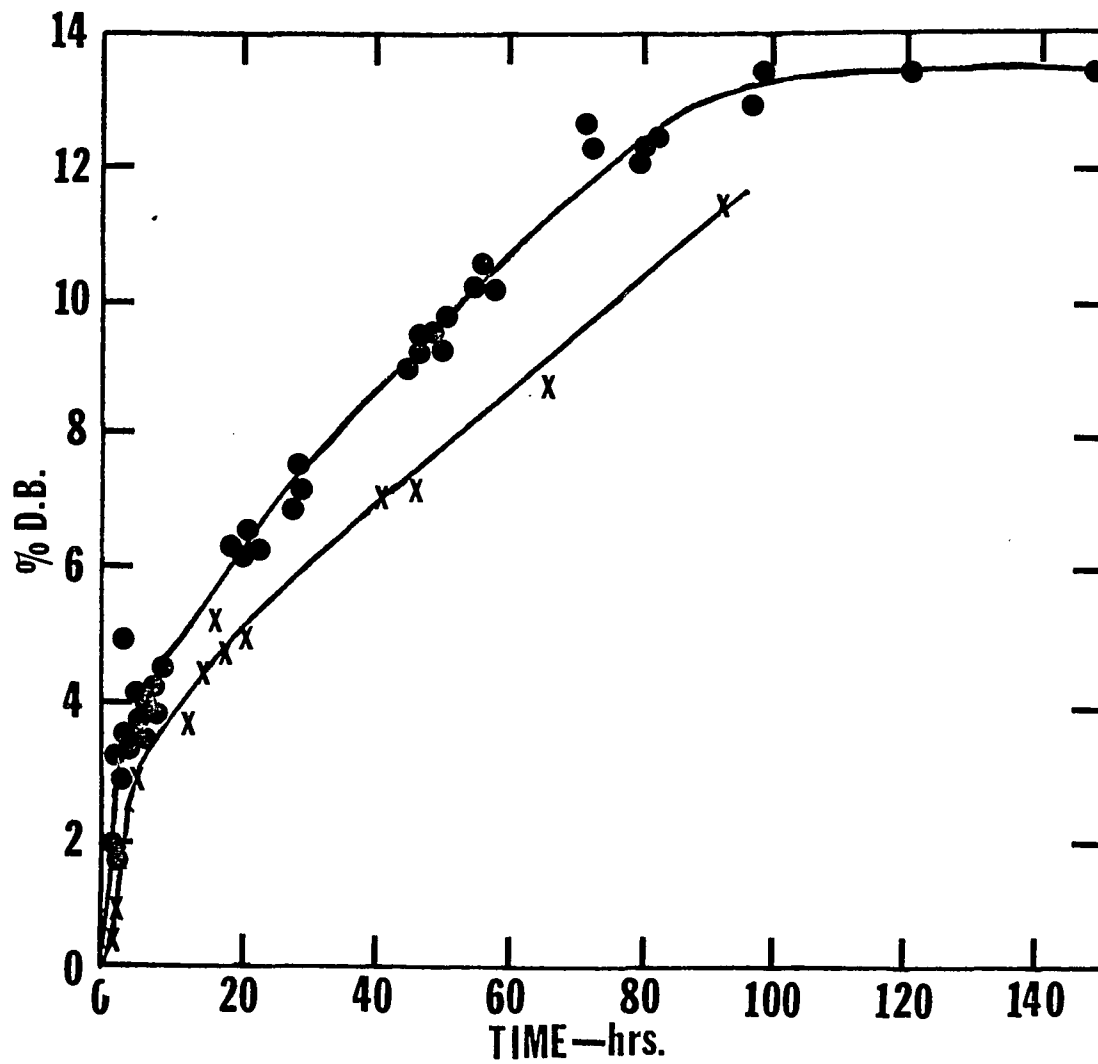


Fig. 10 % double bonds reacted vs. time for the epoxidation of PTBD-K heptane grown crystals at 21°C, 7th run (X), 8th run (●).

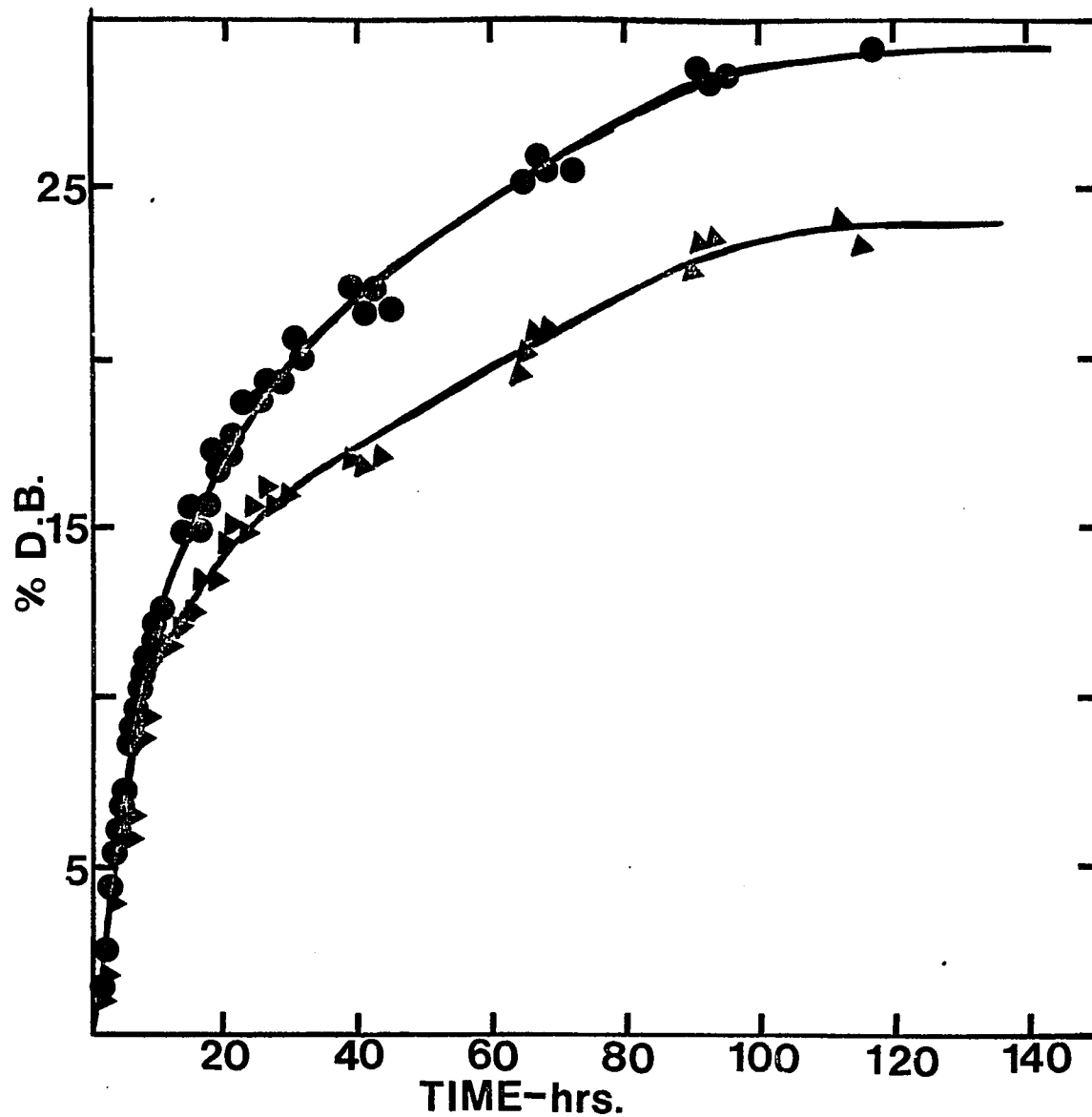


Fig. 11 % double bonds reacted vs. time for the epoxidation of PTBD-U heptane grown crystals, 1 st run (●), 2 nd run (▲). both runs at 6°C.

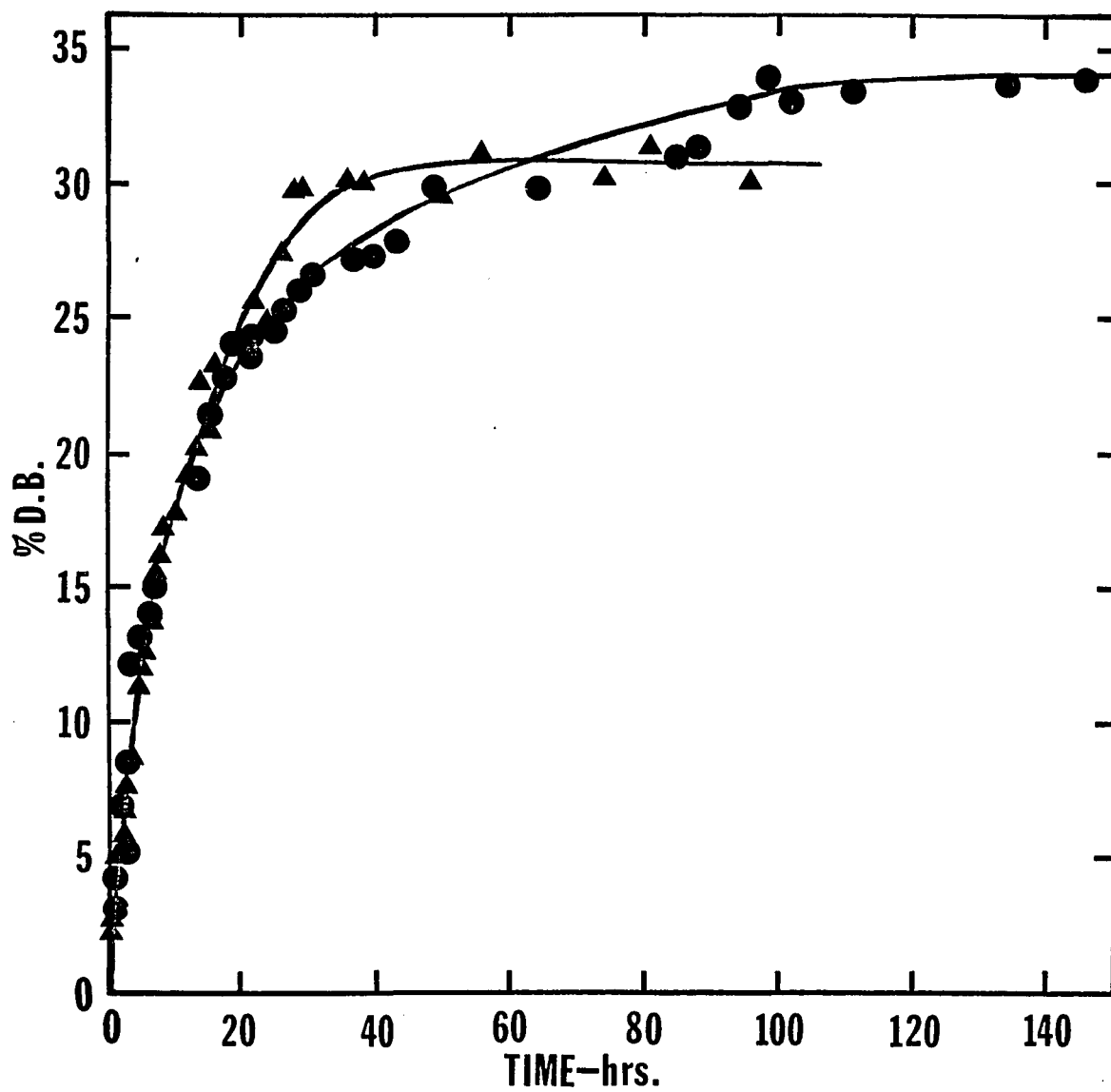


Fig. 12 % double bonds reacted vs. time for the epoxidation of PTBD-U heptane grown crystals, 1 st run(●), 2 nd run(▲). both runs at 12°C.

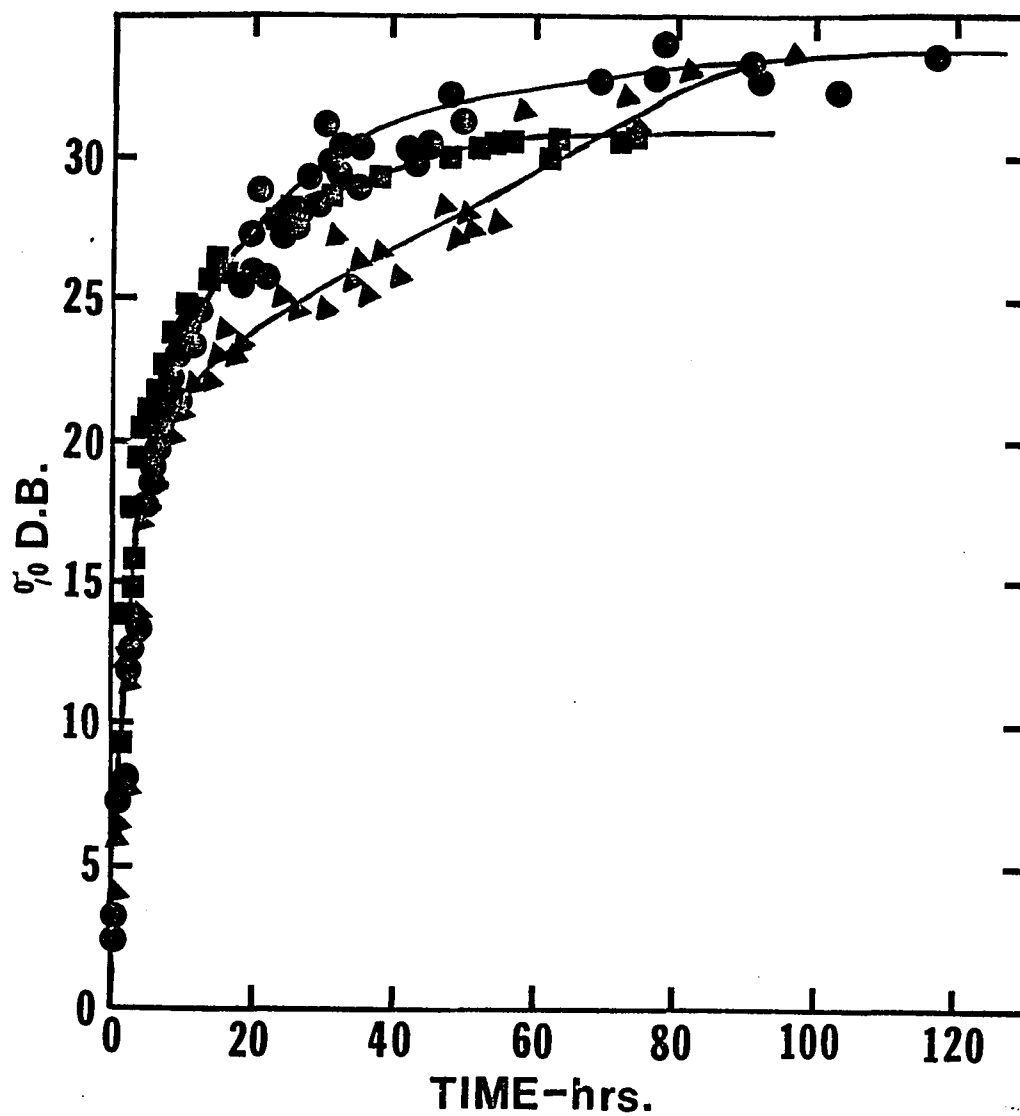


Fig. 13 % double bonds reacted vs. time for the epoxidation of PTBD-U heptane grown crystals at 16°C.
▲ 1 st run, ● 2 nd run, ■ 3 rd run.

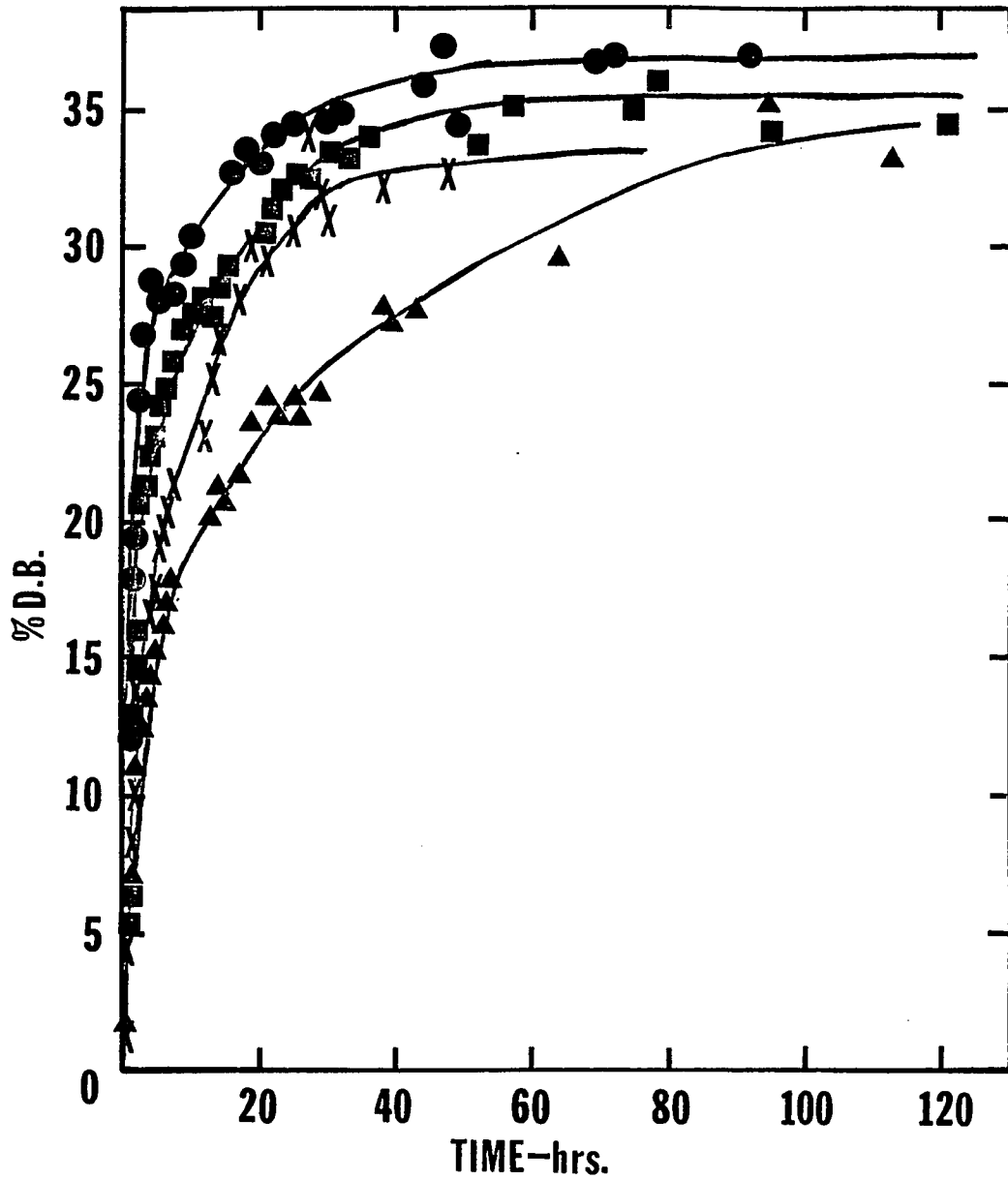


Fig. 14 % double bonds reacted vs. time for the epoxidation of PTBD-U heptane grown crystals at 21°C.

● 1 st run, ▲ 2 nd run, X 3 rd run, ■ 4 th run.

For toluene grown PTBD-K crystals it is seen that the data of the two runs at 6°C are in good agreement with each other. After about thirty hours, the rate decreases considerably and reaches zero at about 120 hours. The final percent of double bonds reacted is 14.0%. In the second run an additional amount of MCPBA was added at about 20 hours of reaction; as can be seen in Fig. 7, this did not effect the percent of double bonds reacted as compared to the other run.

Increasing the reaction temperature for toluene grown PTBD-K crystals is seen to have two effects. First, the initial rate at comparable concentrations increases and secondly, the final percentage of double bonds reacted increases (compare Fig. 2,3 and 4).

For the epoxidation of heptane grown PTBD-K crystals at 21°C, the initial rate is slower than that for toluene grown PTBD-K crystals at 6°C; also the percent of double bonds reacted levels off at 13.4 % after 100 hours of reaction time. This is about the same value as that found by Stellman⁵³ when the reaction was performed at a temperature of 0-5°C. This value is about 40 % of that found for toluene grown PTBD-K crystals epoxidized at 21°C. This indicates that the heptane grown PTBD-K crystals have a significantly lower amorphous content in the surface region than toluene grown PTBD-K crystals; also the maximum amount of double bonds reacted does not seem to be effected by the reaction temperature. Therefore the temperature effects found for toluene grown PTBD-K crystals are

probably not due to penetration of the crystalline portions but involves reaction of amorphous parts made available by expansion of these portions as the temperature is increased.

In the epoxidation of PTBD-U crystals grown from heptane, the final percentage of double bonds reacted increases in the temperature range 6° to 12°C, but stays approximately constant thereafter up to about 21°C. The results show that the initial rate is increasing with increasing temperature.

In separate blank runs it was found that the thermal decomposition rate of MCPBA was negligible at 6°, 12°, and 16°C but at 21°C it was constant at the rate of 0.27×10^{-4} moles-liters⁻¹ hours⁻¹ during the 0-120 hours time period.

A second order rate equation can be represented by the expression

$$\frac{dx}{dt} = k (a-x) (b-x) \dots\dots\dots (5)$$

By integration of eq. (5) we have

$$kt = \frac{1}{a-b} \ln \frac{b(a-x)}{a(b-x)} \dots\dots\dots (6)$$

When the epoxidation results of PTBD crystals are plotted against time, it is found that a considerable portion of each run (at least the first 50 % of reaction) can be satisfactorily represented by a second order plot, ie. first order with respect to concentration of each reactant. Second order rate plots for the various runs made are given in Fig. 15-21. In these plots, "a" represents the initial concentration of MCPBA, "b" represents the total available

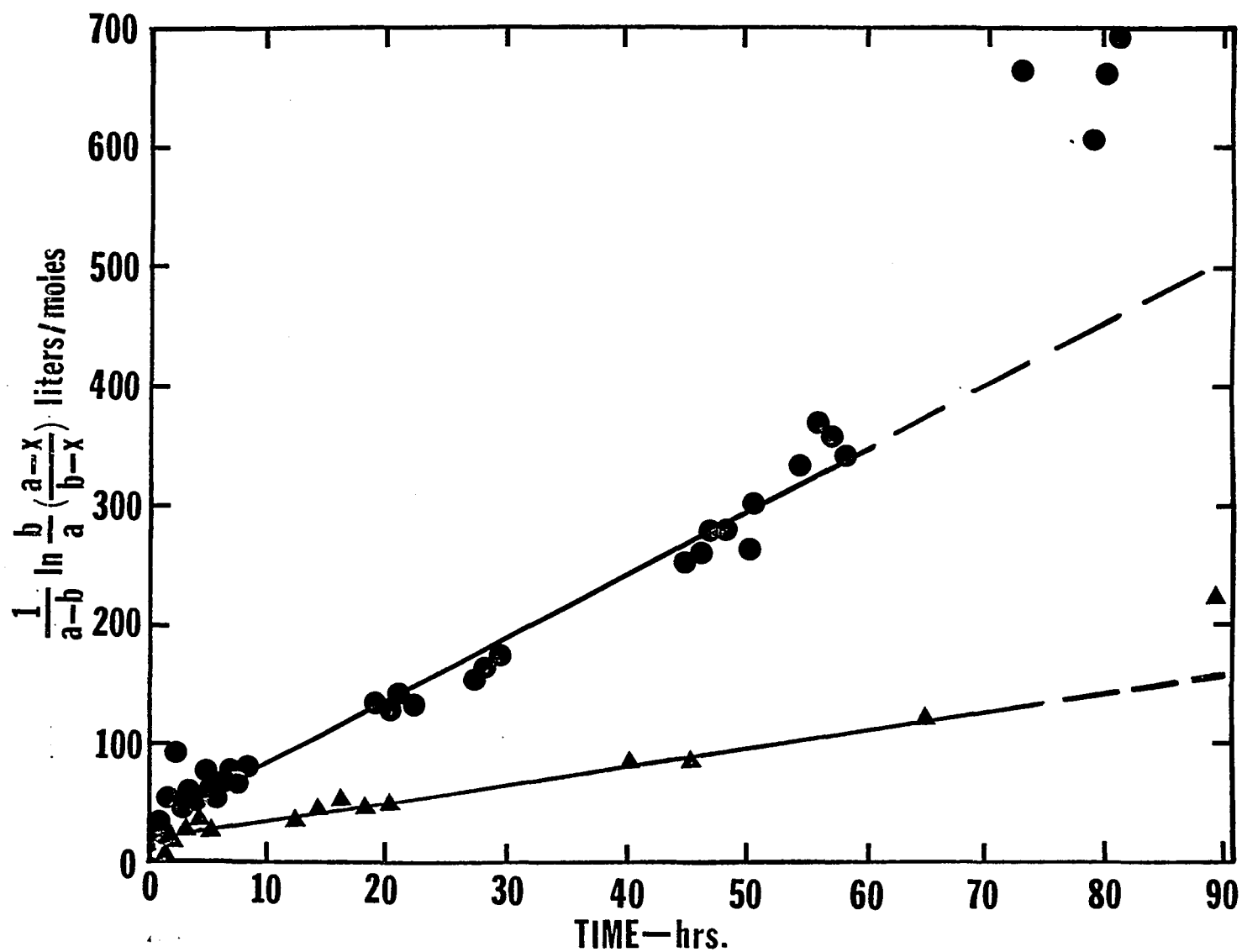


Fig. 15 Second order rate plot for PTBD-K heptane grown crystals epoxidized at 21°C
 7th run (●), 8th run (▲).

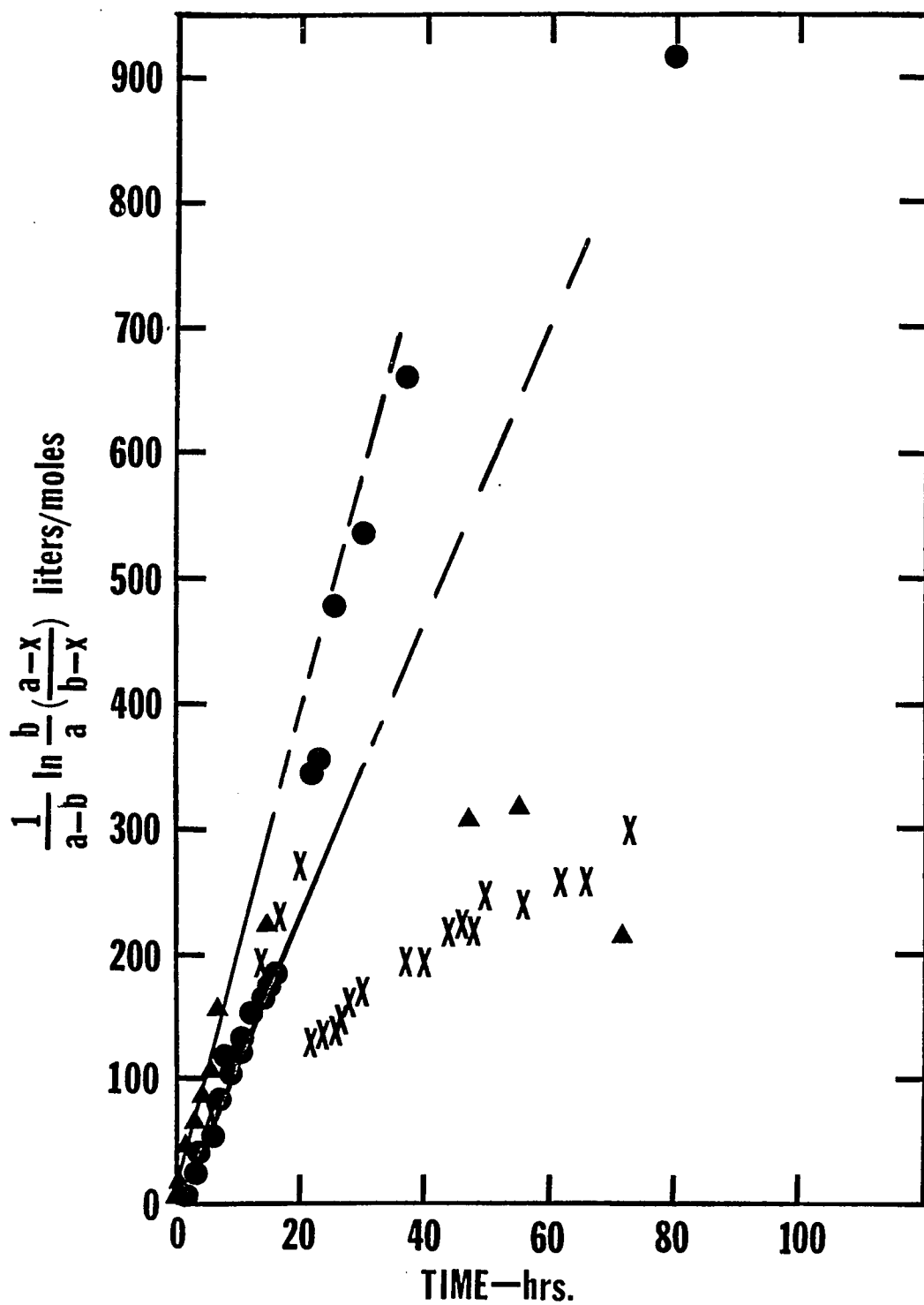


Fig. 16 Second order plot for PTBD-K toluene grown crystals epoxidized at 6°C (●, X), and at 12°C (▲).

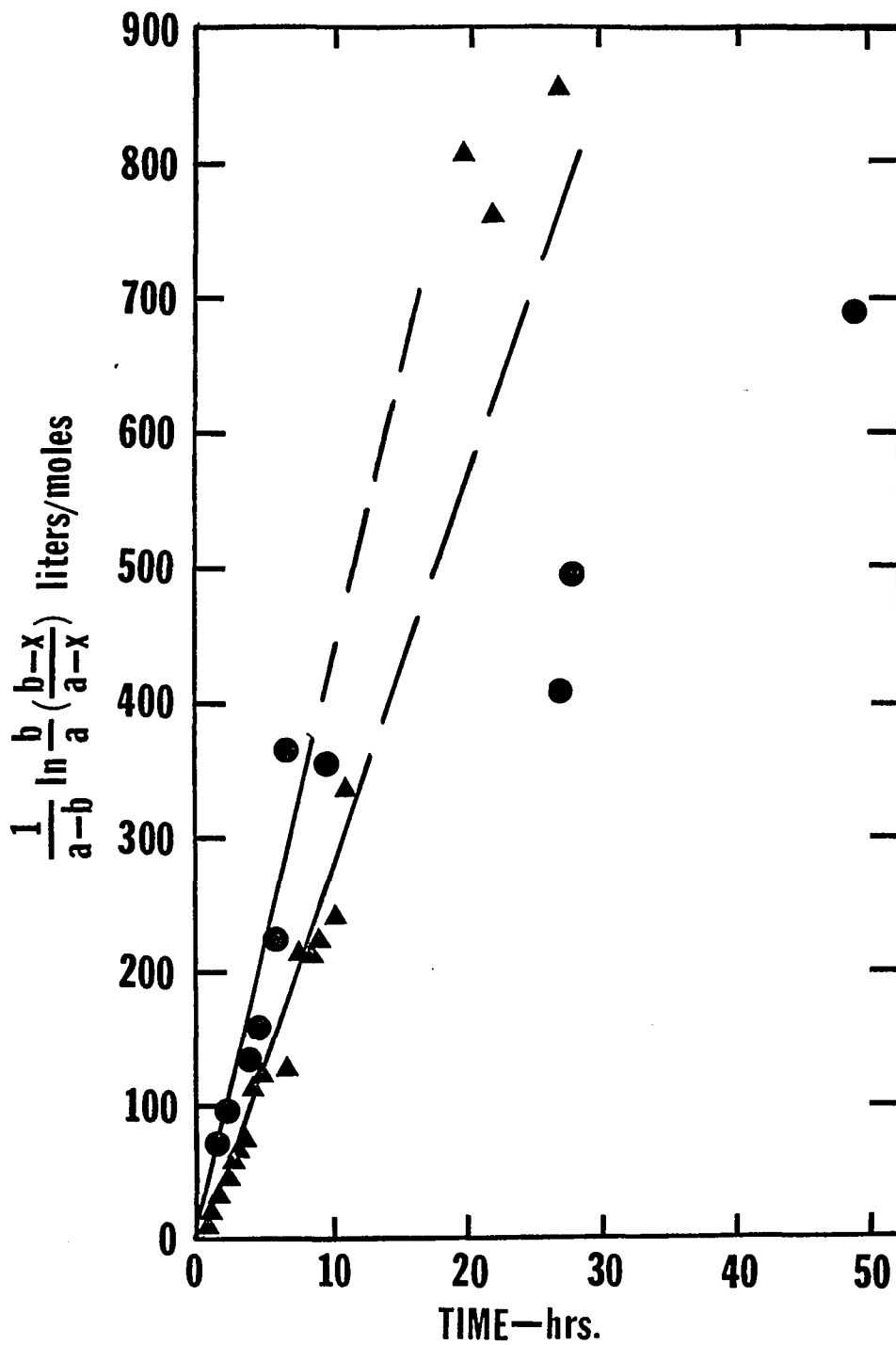


Fig. 17 Second order rate plot for the epoxidation of PTBD-K toluene grown crystals at 21°C.

▲ 1 st run, ● 2 nd run.

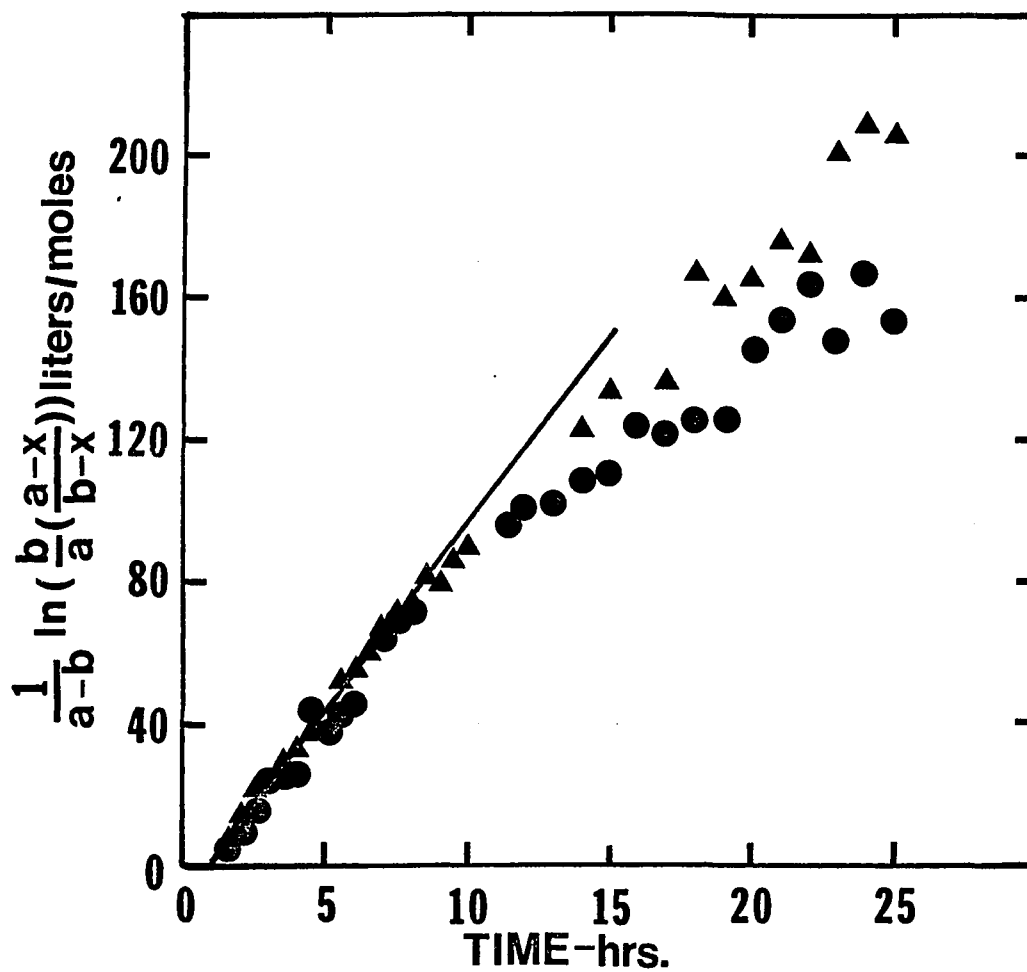


Fig. 18 Second order rate plot for the epoxidation of PTBD-U heptane grown crystals at 6°C.
▲ 1 st run, ● 2 nd run.

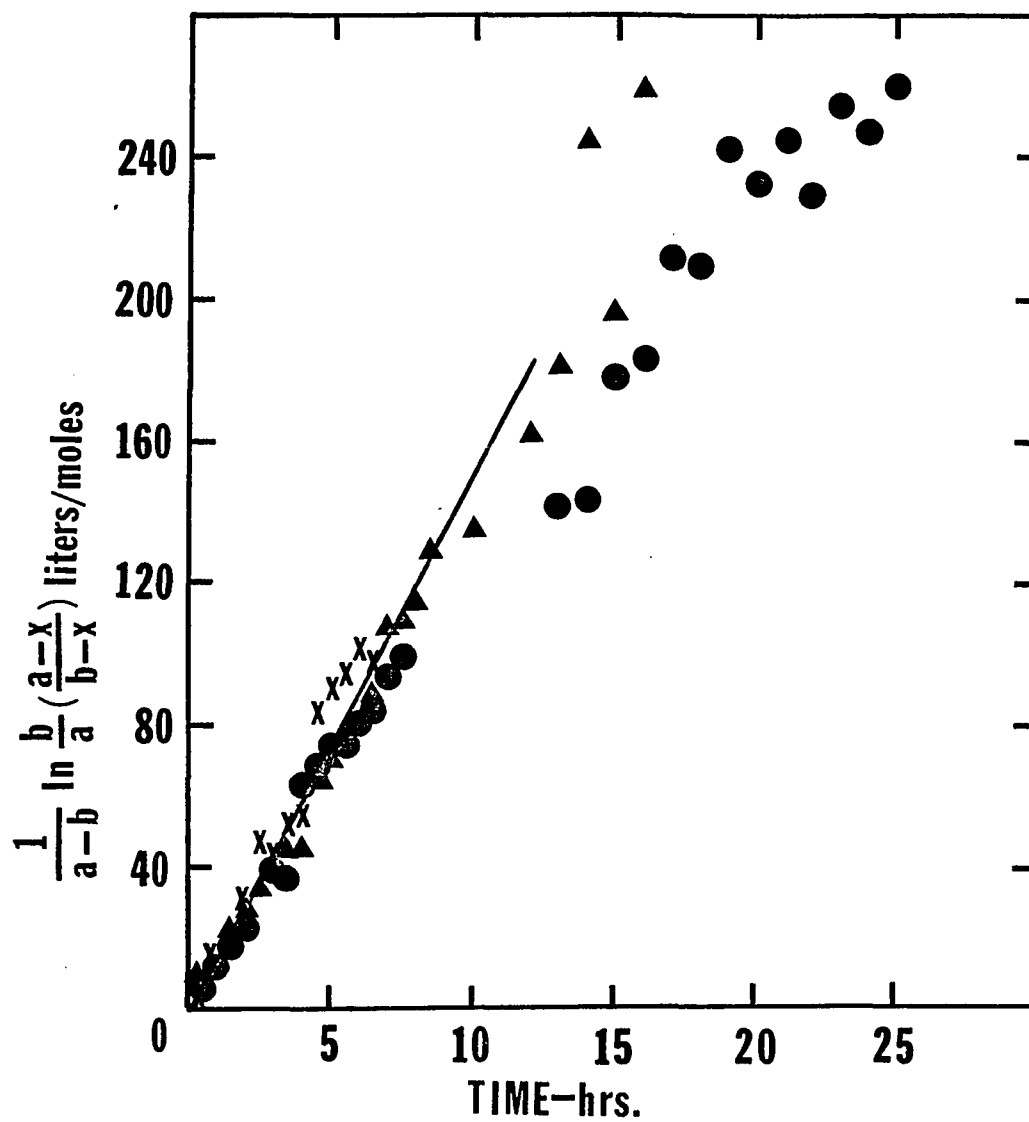


Fig. 19 Second order rate plot for the epoxidation of PTBD-U heptane grown crystals at 12°C.
 ● 1 st run, ▲ 2 nd run, X 3 rd run.

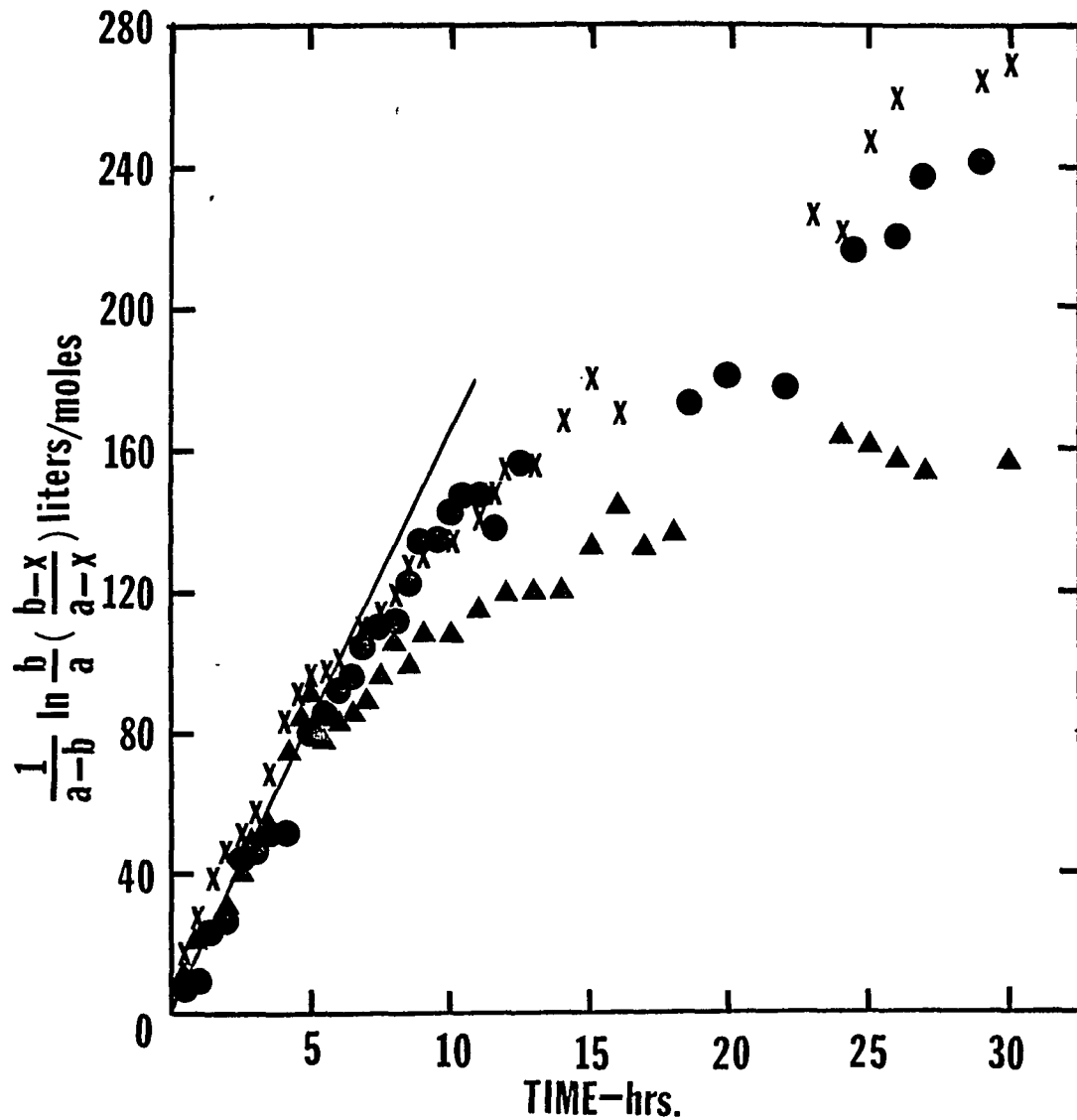


Fig. 20 Second order rate plot for the epoxidation of PTBD-U heptane grown crystals at 16°C.

● 1 st run, ▲ 2 nd run, X 3 rd run.

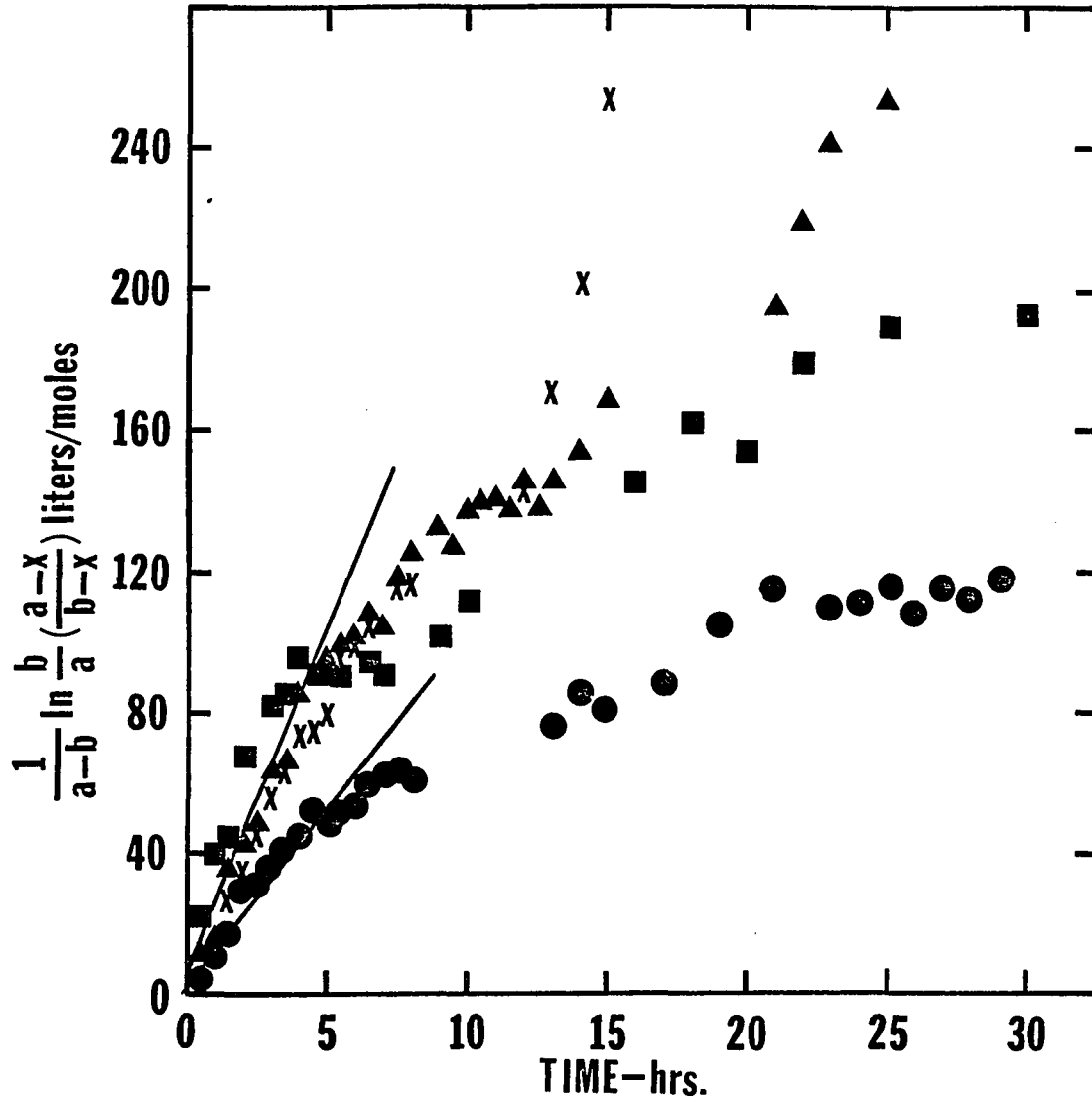


Fig. 21 Second order rate plot for the epoxidation of PTBD-U heptane grown crystals at 21°C.

■ 1 st run, ● 2 nd run, X 3 rd run, ▲ 4 th run.

double bond concentration which is taken as the concentration of double bonds times the total fraction of double bonds reacted, and "x" represents the amount of double bonds reacted at time (t). The extent of reaction, x, has been corrected for the thermal decomposition rate for the reaction at 21°C. It should be pointed out that the effect of the competing thermal reaction on the second order rate equation has not been taken into account in this analysis. It was found that up to about 40 hour of reaction, only 5% of the total amount of MCPBA was decomposed thermally; therefore at shorter times, the thermal decomposition is not considered to be significant. Deviations from a straight line plot is certainly expected at times above 40 hours for the 21°C runs.

For PTBD-K toluene frown crystals the reaction is second order up to about 60 % completion at 6°C and to 80 % completion at 12°C and 21°C. For PTBD-U heptane grown crystals it is second order up to 65 % completion at 6°C, 50-80 % completion at 12°C, 65 % completion at 16°C and 40-50% completion at 21°C.

In the second order rate plots, the deviations were usually found to be negative ones. In some runs it is apparent that there is a pseudo second order rate constant with a smaller value. However a number of these deviations seem to follow those seen in the plot of % double bonds VS. time, and are expected to be due to experimental uncertainties in obtaining the results.

The discontinuity in the plot for the epoxidation of PTBD-K toluene grown crystals at 6°C (Fig. 17) is due to an additional 2.8×10^{-4} mole of MCPBA that was added after 20 hours of reaction time.

The second order rate constant, k , obtained from the slope of the straight line portion of the plots in Figs. 15-21 are given in Table VI and VII. For PTBD-K toluene grown crystals, k increases with temperature. The mean rate constant for PTBD-K heptane grown crystals is about 6 times smaller than PTBD-U heptane grown crystals and about 9 times smaller than that for PTBD-K toluene grown crystals reacted at the same temperature. The deviation of the rate constant for various runs at a given temperature for a particular crystal preparation does not seem to be related to initial reactant concentrations.

The energy of activation calculated from the slope of the plot of the \ln of the rate constant vs $1/T$ for PTBD-K toluene grown crystals and PTBD-U heptane grown crystals given in Fig. 22 are reported in Table VIII and IX. The entropy, enthalpy and free energy of activation calculated from the energy of activation and the rate constant is given in Table X for this work along with values obtained from the epoxidation of various olefins of interest in solution.

TABLE VI

Results for Epoxidation of PTBD-K Crystals by m-chloro
perbenzoic acid at Various Temperatures.

Type	Run #	Temp. °C	db Molars $\times 10^2$	MCPBA Molars $\times 10^3$	% db reacted	k Molars hrs ⁻¹
T	1	6	2.677	5.125	13.7	12.4
T	2	6	2.907	5.762	14.0	13.7
				mean	13.8 ± 0.2	13.0 ± 0.7
T	3	12	3.519	1.556	23.1	20.7
T	4	21	2.648	7.629	27.5	25.4
T	5	21	3.520	1.259	27.7	35.5
T	6	21	3.677	1.641	30.6	26.0
				mean	29 ± 1	29 ± 4
H	7	21	3.241	9.728	*13.4	1.7
H	8	21	1.796	5.391	13.4	5.2
				mean	-	3.5 ± 1.7

T stands for toluene grown crystals, and H for heptane grown crystals.

* assumed % double bonds reacted = 13.4

TABLE VII

Results for Epoxidation at Various Temperatures of PTBD-U
Crystals Grown from Heptane.

Run #	Temp. °C	db x 10 ² Molars	MCPBA Molars x 10 ³	% db reacted	k 1/moles-hrs
1	6	2.199	7.775	29.1	9.7
2	6	1.804	7.531	25.3	10.5
			mean	27.2 ± 2	10.1 ± 0.4
1	12	1.653	7.830	33.5	13.8
2	12	1.829	8.309	30.6	13.7
3	12	1.653	1.246	*32.0	*16.8
			mean	32 ± 1.5	13.8 ± 0.5
1	16	1.706	1.150	33.0	14.5
2	16	1.785	1.168	33.0	12.8
3	16	2.064	1.476	30.6	18.5
			mean	32.2 ± 1.1	15.3 ± 2.2
1	21	1.905	1.905	37.0	23.9
2	21	1.971	1.399	34.2	11.4
3	21	2.130	1.070	35.6	15.7
4	21	1.872	1.467	34.8	21.2
			mean	35.4 ± 0.9	18.1 ± 4.5

* assumed % db reacted = 32.0, ** mean of the first two runs

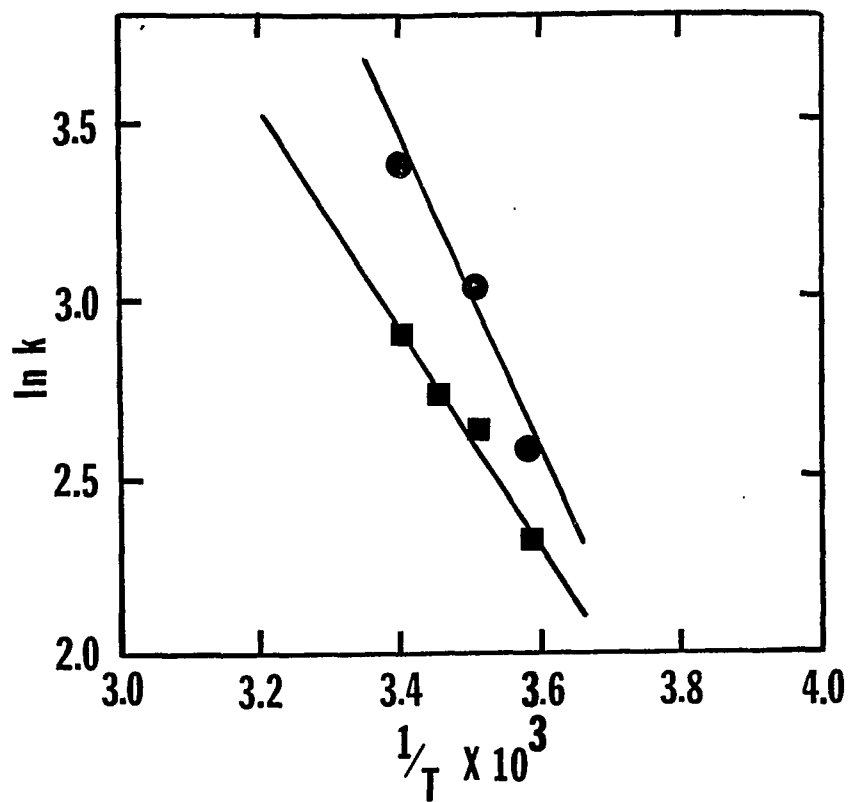


Fig. 22 The Arrhenius Plots of PTBD Crystals.

● PTBD-K Toluene Grown Crystals

■ PTBD-U Heptane Grown Crystals

TABLE VIII

Calculation of Energy of Activation for the Epoxidation of PTBD-K Crystals Grown from Toluene.

k	ln k	T°K	1/T x 10 ³	E _{act}
13.1	2.57	279	3.58	
20.7	3.03	285	3.51	9.01 kcal
29.0	3.37	294	3.40	

TABLE IX

Calculation of Energy of Activation of the Epoxidation of PTBD-U Crystals Grown from Heptane.

k	ln k	T°K	1/T x 10 ³	E _{act}
10.1	2.31	279	3.58	
13.8	2.63	285	3.51	6.13 kcal
15.3	2.73	290	3.45	
18.1	2.90	294	3.40	

TABLE X

Comparison of the Thermodynamic Parameters of Activation for the Epoxidation of Various Olefins.

Polymer	Epoxy Agent	$k \times 10^{-3}$ at $T^{\circ}\text{C}$			E_{act} kcal	$-\Delta S^{\ddagger}$ cal	ΔH^{\ddagger} kcal	ΔG^{\ddagger} kcal
		15°	20°	30°				
PTBD-K crystals	MCPBA	-	.0005	-	9.01	39.5	8.42	20.0
PTBD-U crystals	MCPBA	.00025	.0003	-	6.13	50.3	5.54	20.3
Poly-isoprene	PAA	8.53	13.15	22.70	15.7	23.0	15.1	21.8
Poly-piperylene	PAA	1.75	3.10	4.42	16.3	25.1	15.7	23.1
Poly-butadiene	PAA	0.65	0.93	1.50	17.2	25.6	16.6	24.1
Stilbene	MCPBA	-	.00006	.00009	15.1	22.9	14.5	21.4

MCPBA stands for m-chloro perbenzoic acid, and PAA for peracetic acid

The electron micrographs of epoxidized PTBD crystals are given in Figs. 23-30. For PTBD-K heptane grown crystals epoxidized at 21°C, there is no significant change as compared to the as grown crystals; this is also true for PTBD-K toluene grown crystals, and PTBD-U heptane crystals epoxidized at 6°C. Epoxidation at higher temperatures led to more noticeable effects for both PTBD-K toluene grown crystals and PTBD-U heptane grown crystals as seen in Figs. 25 and 29.

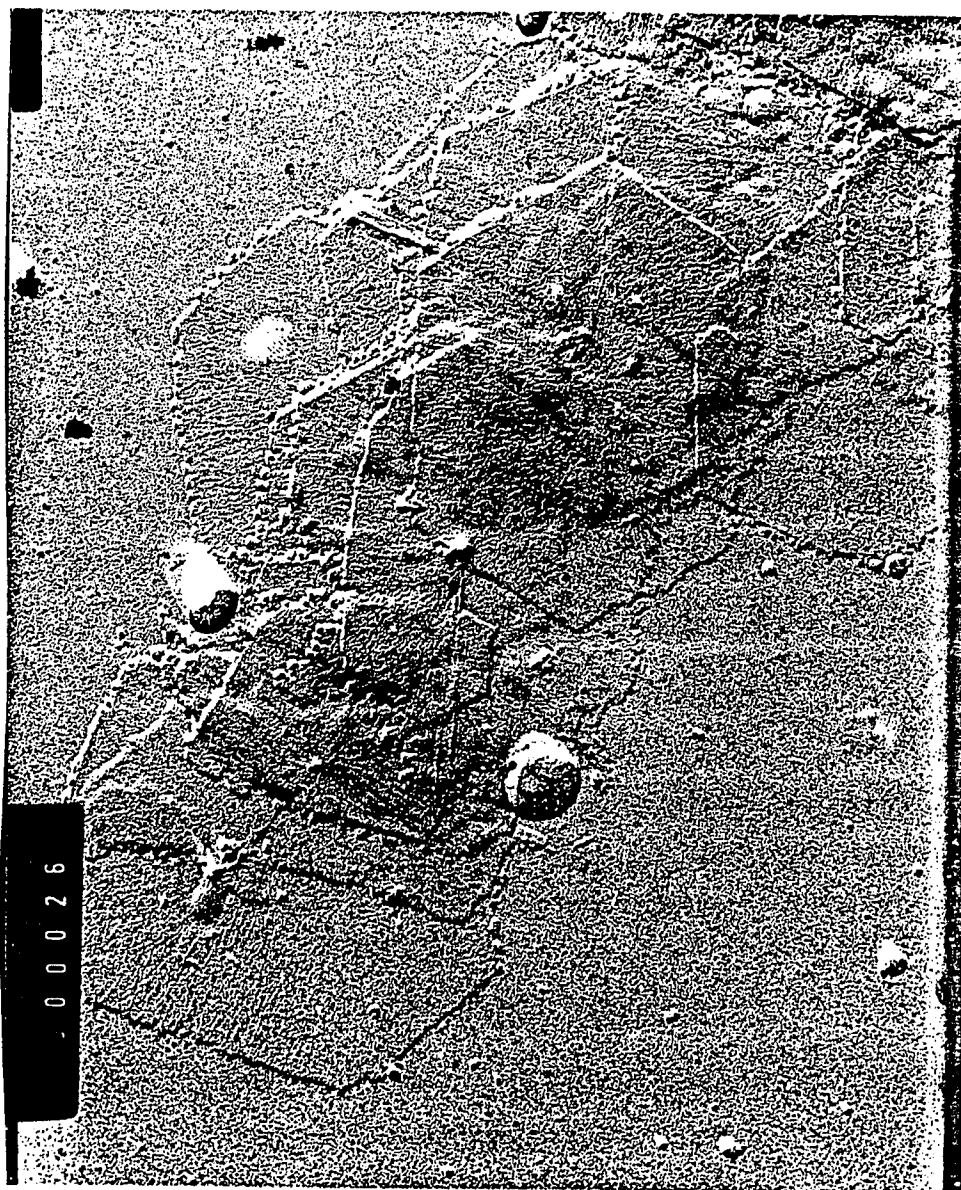


Fig. 23 Electron micrograph of PTBD-K toluene grown crystals after epoxidation at 6°C. (Mag. 27,000)



Fig. 24 Electron micrograph of PTBD-K toluene grown crystals
after epoxidation at 12°C (Mag. 17,000)

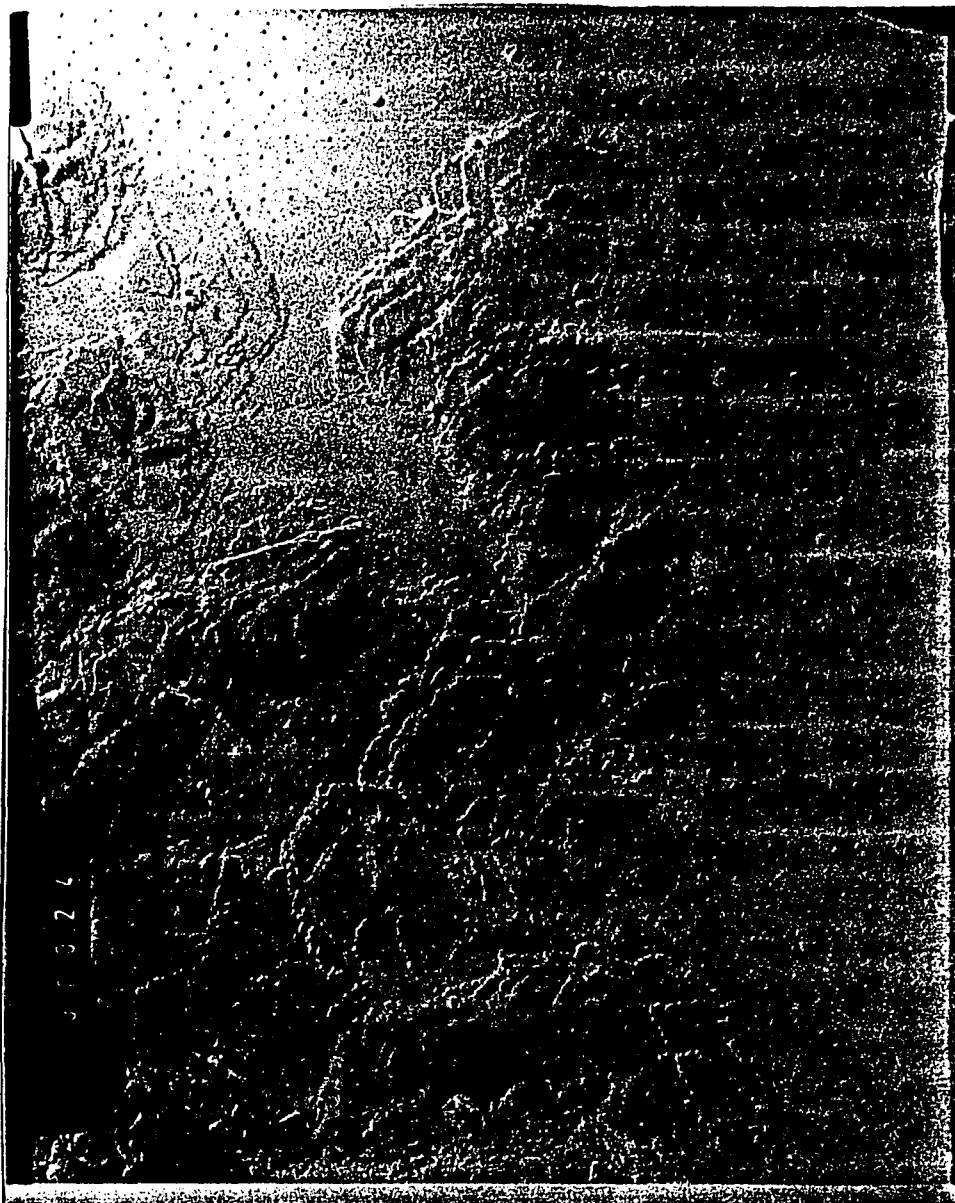
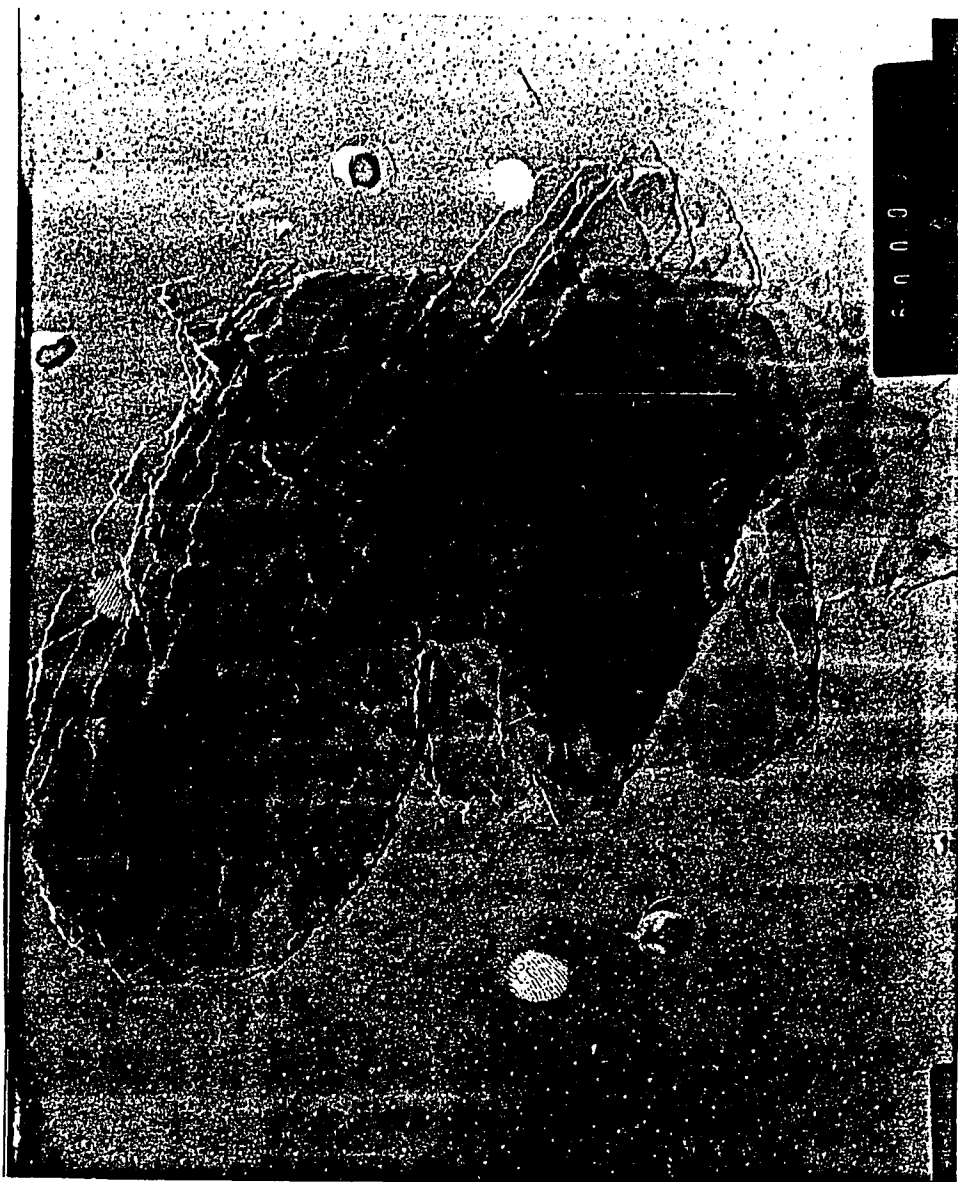


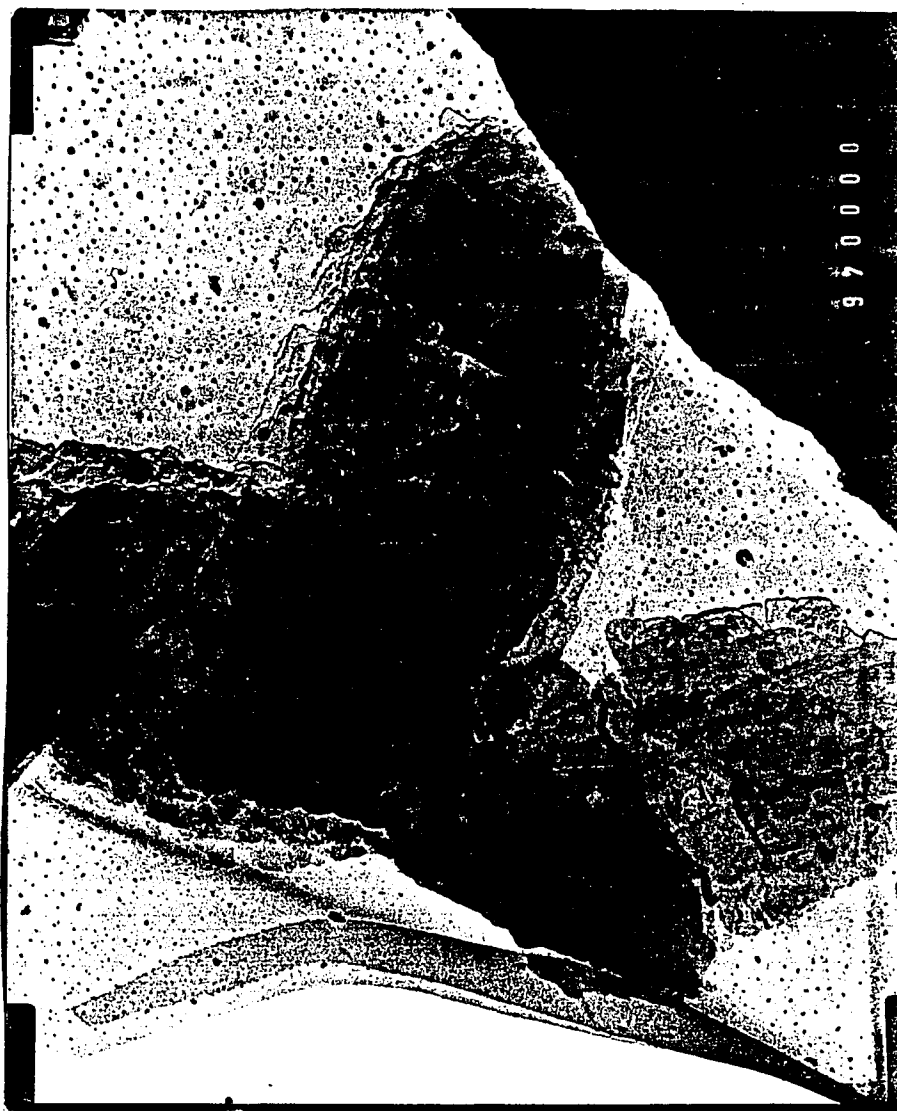
Fig. 25 Electron micrograph of PTBD-K toluene grown crystals after epoxidation at 21°C (mag.12,000).

2μ



2 μ

Fig. 26 Electron micrograph of PTBD-U heptane grown crystals after epoxidation by MCPBA at 6°C (Mag. 17,000).



2 μ

Fig. 27 Electron micrograph of PTBD-U heptane grown crystals after epoxidation by MCPBA at 12°C (Mag. 10,600).



Fig. 28 Electron micrograph of PTBD-U heptane grown crystals after epoxidation by MCPBA at 16°C (Mag. 19,400).



Fig. 29 Electron micrograph of PTBD-U heptane grown crystals after epoxidation by MCPBA at 21°C (Mag. 21,000).

1 μ



2μ

Fig. 30 Electron micrograph of PTBD-K heptane grown crystals after epoxidation by MCPBA at 21°C (Mag. 9500).

BROMINATION RESULTS

The calibration plot for the absorbance of bromine in carbon tetrachloride vs. the concentration of bromine in carbon tetrachloride is given in Fig. 31. The extinction coefficient which is calculated from the slope of the plot is $197 \text{ l mole}^{-1} \text{ sec}^{-1}$. The results of the bromination of heptane and toluene grown PTBD-K crystals in CCl_4 at 0°C are given in Table XI.

TABLE XI

Bromination of Heptane and Toluene Grown PTBD-K Crystals in CCl_4 at 0°C

Growth condition	% db reacted <u>1st</u> run	% db reacted <u>2nd</u> run
Heptane ($76^\circ / 63^\circ$)	13 ± 1	13 ± 1
Toluene ($50^\circ / 23^\circ$)	21 ± 1	21 ± 1

The bromination value for PTBD -K heptane grown crystals is in agreement with that from epoxidation results. The bromination value for PTBD-K toluene grown crystals falls between those obtained by epoxidation at 6° and 12°C respectively. Electron micrographs as given in Figs. 32 and 33 show that bromination of PTBD-K heptane and toluene grown crystals leads to no noticeable change in the surface appearance.

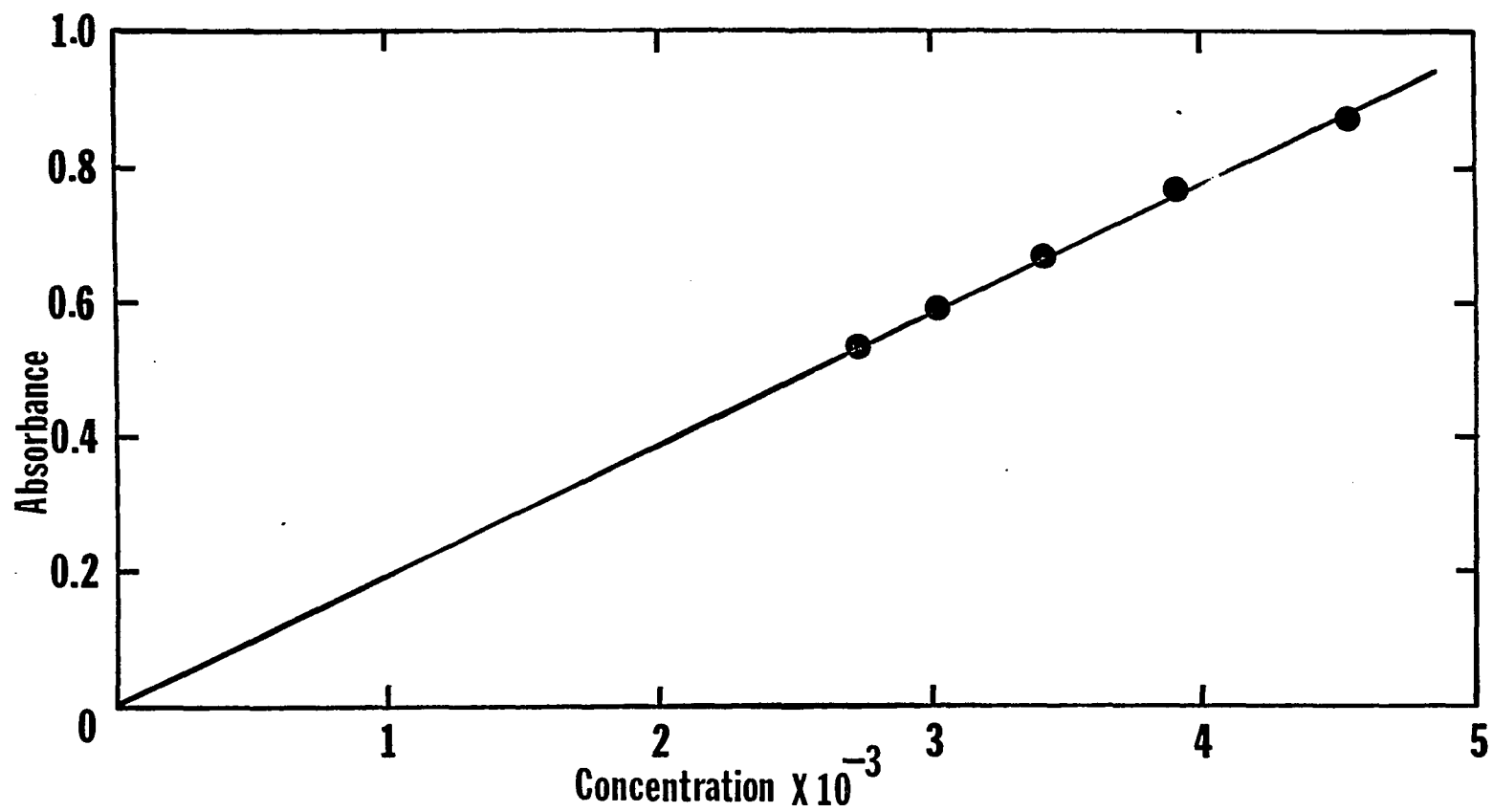
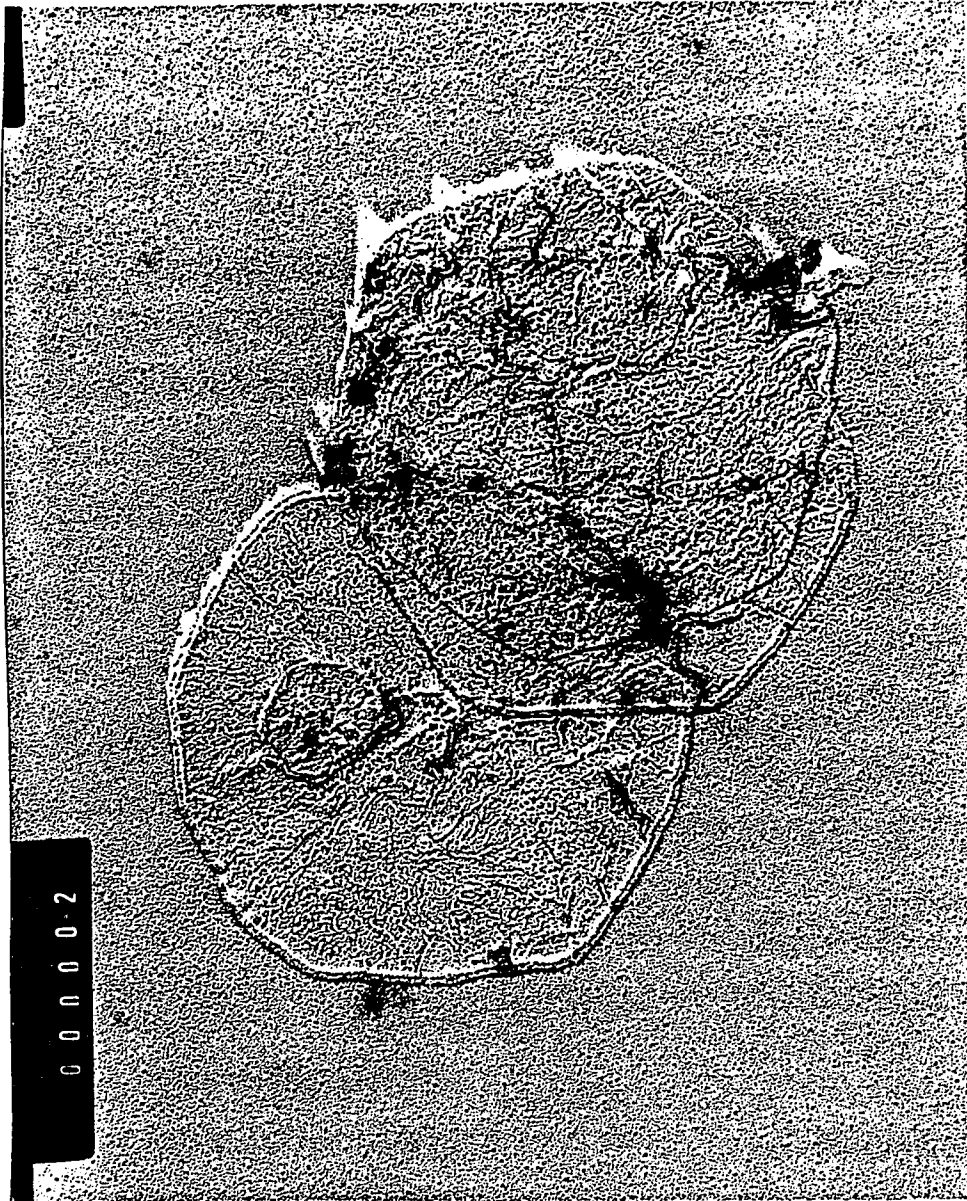
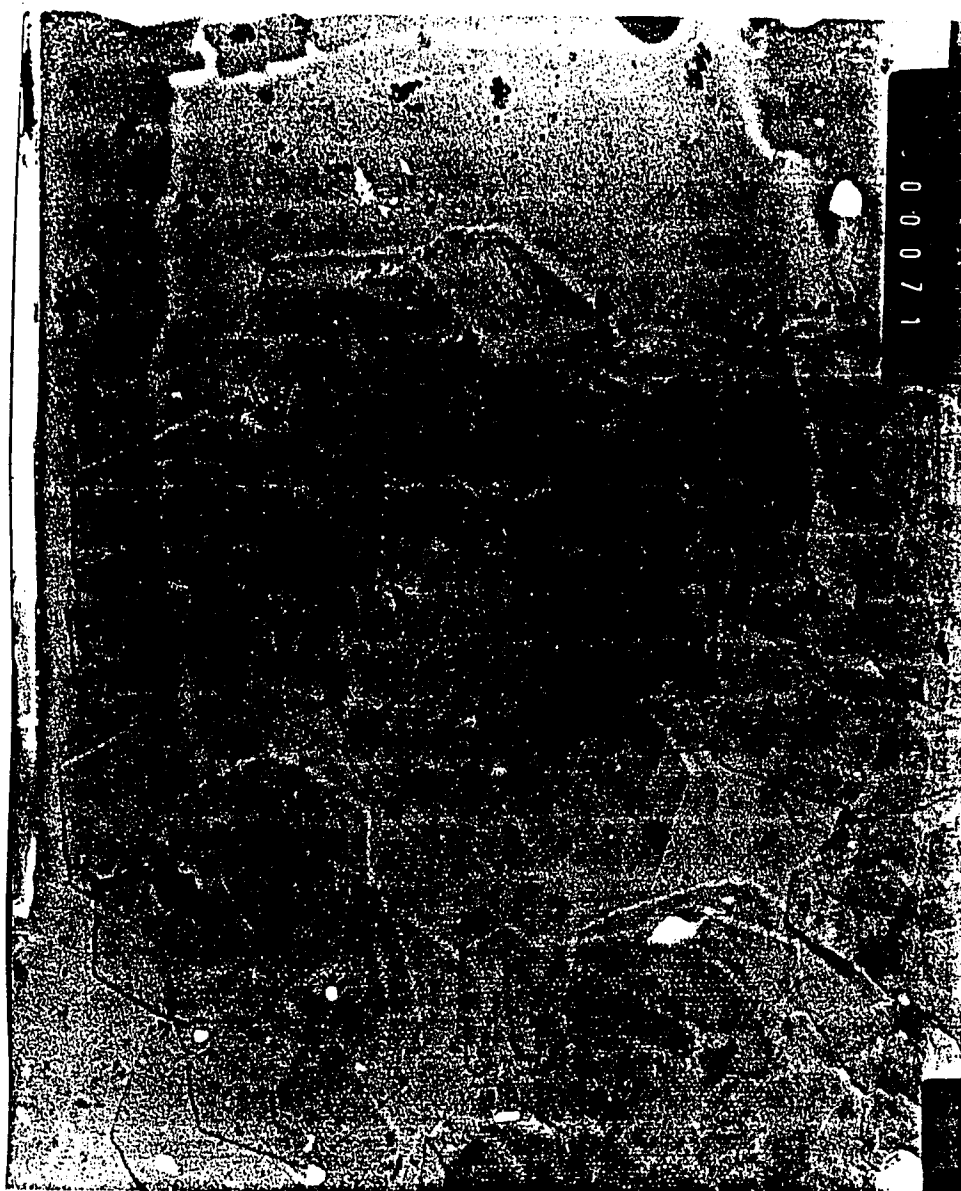


Fig. 31 Absorbance at 416 nm vs. concentrations of Bromine in CCl₄



1μ

Fig. 32 Electron micrograph of PTBD-K heptane grown crystals after bromination at 0°C (Mag. 17,000).



2μ

Fig. 33 Electron micrograph of PTBD-K toluene grown crystals after bromination at 0°C (Mag. 14,000).

Martuccelli et. al.⁶⁹ reported a bromination study at 0°C for PTBD crystals grown from heptane solution at various temperatures; the results showed that the amount of double bond reacted is 16 % for the three preparations studied.

The amorphous content for PTBD crystals found by different methods are given in Table XII.

TABLE XII

Comparison of Amorphous Contents for PTBD Crystals.

Growth condition	DSC ⁵³	NMR ⁵¹	IR ⁵⁰	Epoxidation		Bromination
				Stellman	This work	
PTBD-K Heptane (76°/ 63°C)	(0.2)	0.13	0.2	0.14(0°C)	0.14(21°C)	0.13
PTBD-K Toluene (50°/ 23°C)	0.4	0.23	0.5	0.19(0°C)	0.14(6°C) 0.23(12°C) 0.29(21°C)	0.21
PTBD-U Heptane (69°/ 45°C)	-	-	0.23	0.34(0°C)	0.27(6°C) 0.31(12°C) 0.32(16°C) 0.35(21°C)	-

It is seen that for PTBD-K heptane grown crystals the surface penetration methods give values which agree closely with one another independent of temperature and also agree with the results from the IR spectroscopy. For the PTBD-K toluene grown crystals the surface penetration methods give values

varying by a factor of two depending on the temperature and method used, however the largest of these values is lower than that given by the DSC and IR methods.

INFRARED RESULTS

Infrared spectra for PTBD-K crystals after epoxidation and bromination are given in Figs. 34-50. The absorption peak frequencies and absorption intensities are given in Table XIII and XIV.

Recently Krimm⁸¹ has reported an IR spectrum of PTBD single crystals, but he did not observe any bands below 330 cm^{-1} . From this study it is obvious that there are peaks at 310 cm^{-1} , 280 cm^{-1} , and 255 cm^{-1} ; all of these peaks are expected from the calculation of Krimm using crystal vibration analysis.

For brominated PTBD-K toluene and heptane grown crystals, the IR spectrum shows additional peaks at 500, 585, 690, 720, 1140 and 1220 cm^{-1} . For PTBD-K brominated toluene grown crystals the intensity of the peak at 1350 cm^{-1} is noticeably smaller.

For epoxidized PTBD-K crystals from heptane and toluene, additional peaks at 690, 726, 885, 1193, 1255, and 1365 cm^{-1} are found. For these crystals the intensity of the 1350 cm^{-1} decreases when the temperature is raised. Unfortunately, the new peak at 1365 cm^{-1} peak interferes and is apparently merged with the 1350 cm^{-1} peak. The peaks in the $800\text{-}1200\text{ cm}^{-1}$ region seem to broaden with a very high background absorption.

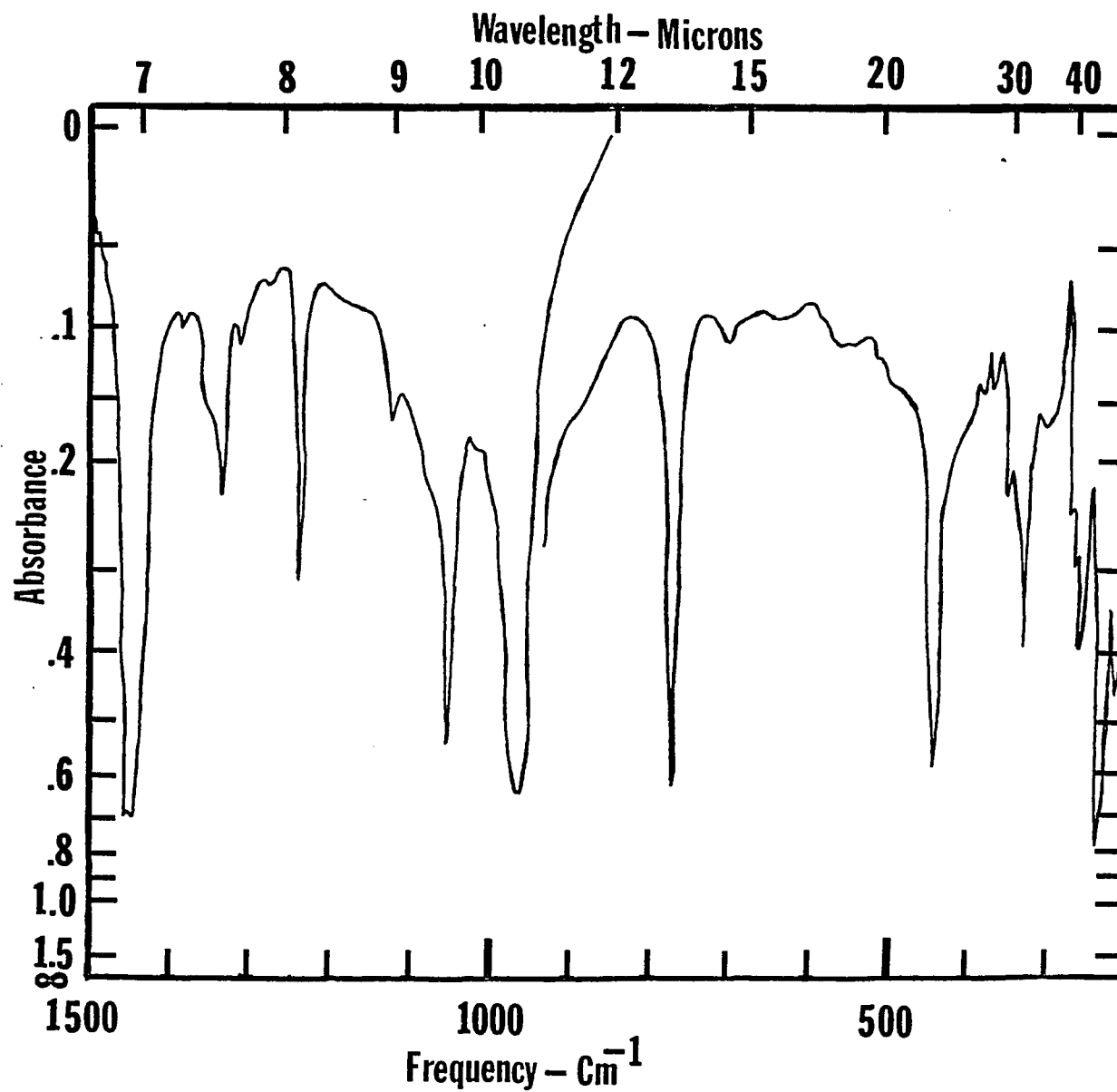


Fig. 34 IR spectrum of as-grown PTBD-K toluene grown crystals.

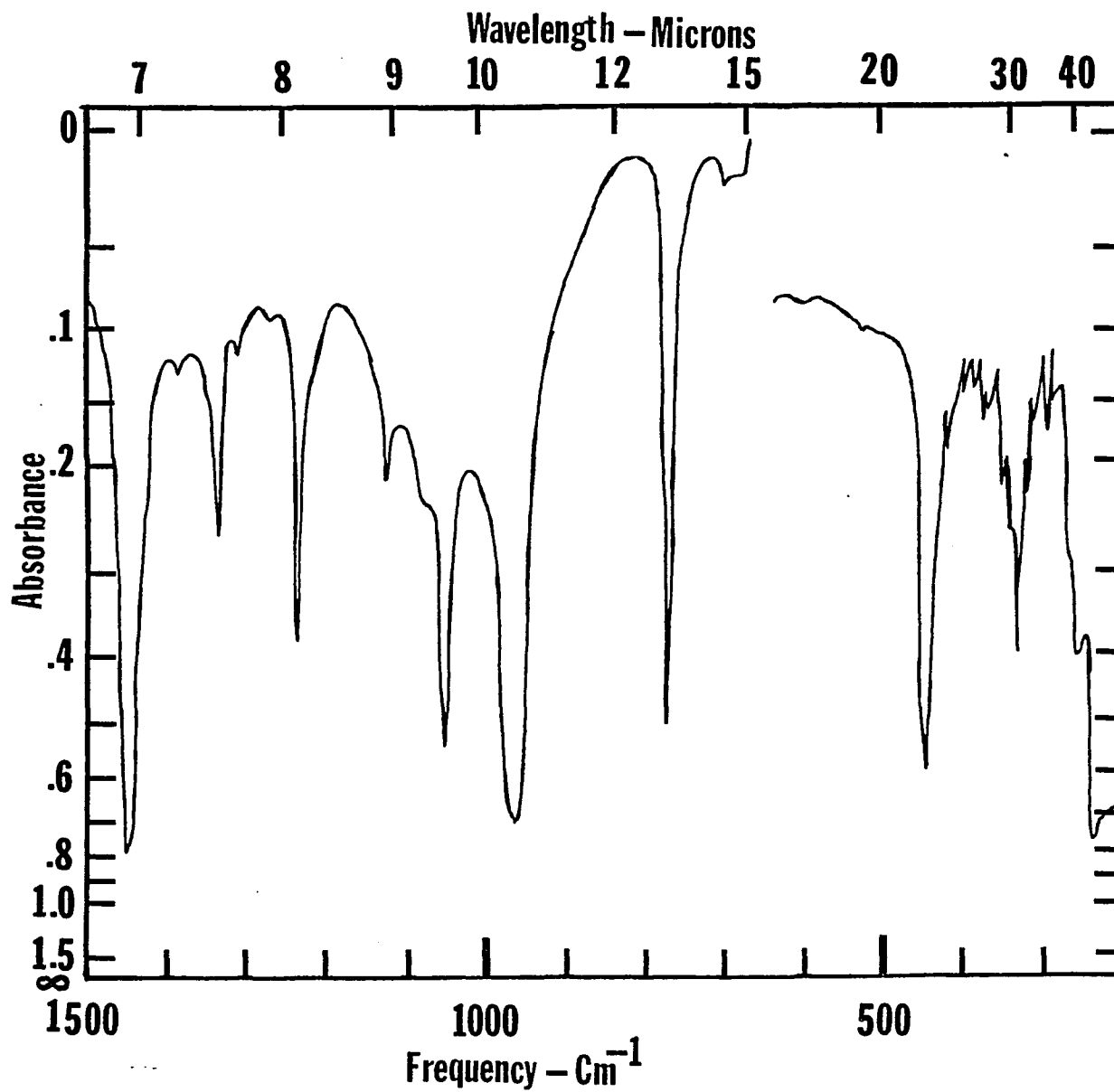


Fig. 35 IR spectrum of PTBD-K toluene grown crystals annealed at 68°C

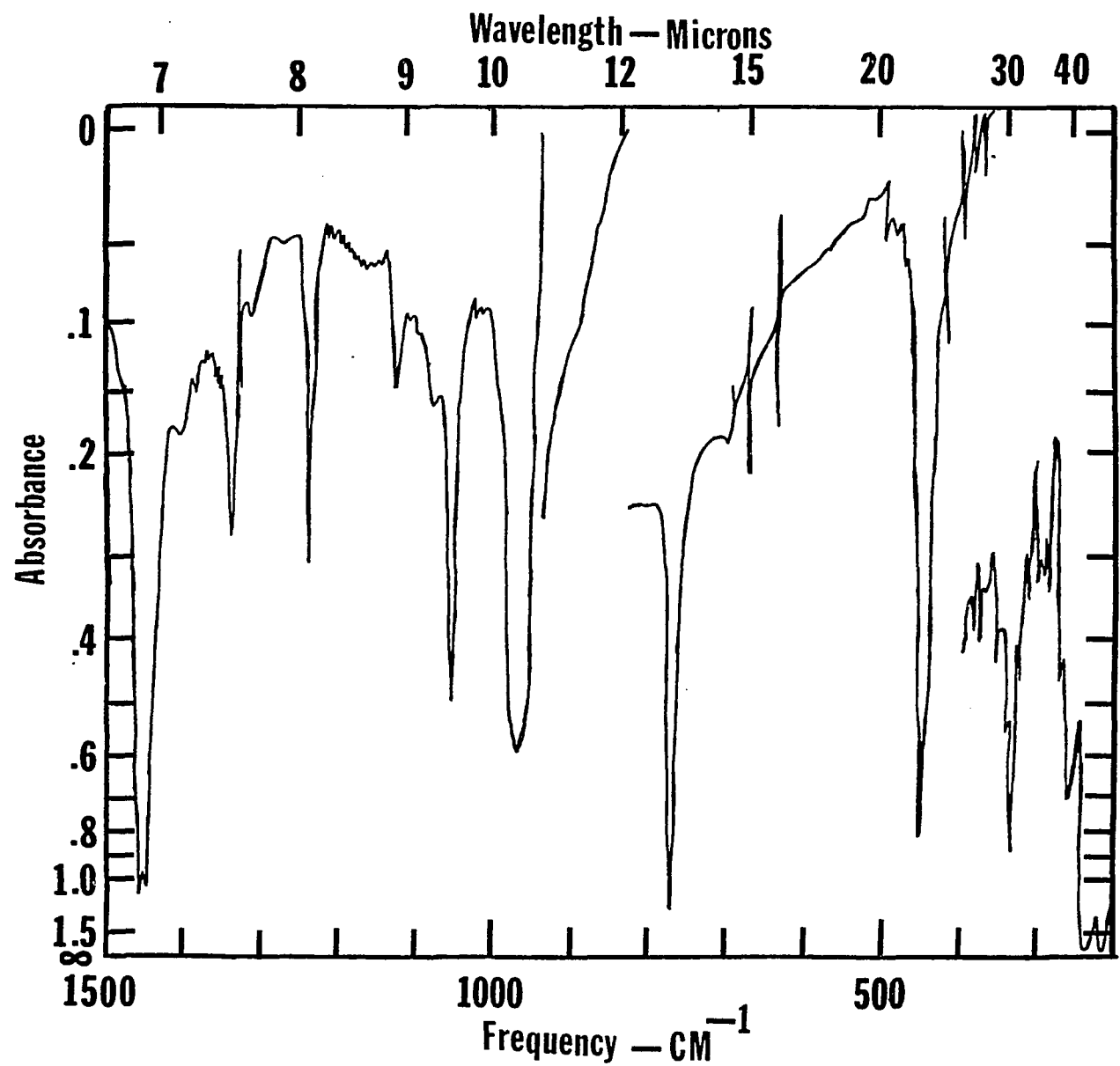


Fig. 36 IR spectrum of PTBD-K toluene grown crystals annealed 80°C.

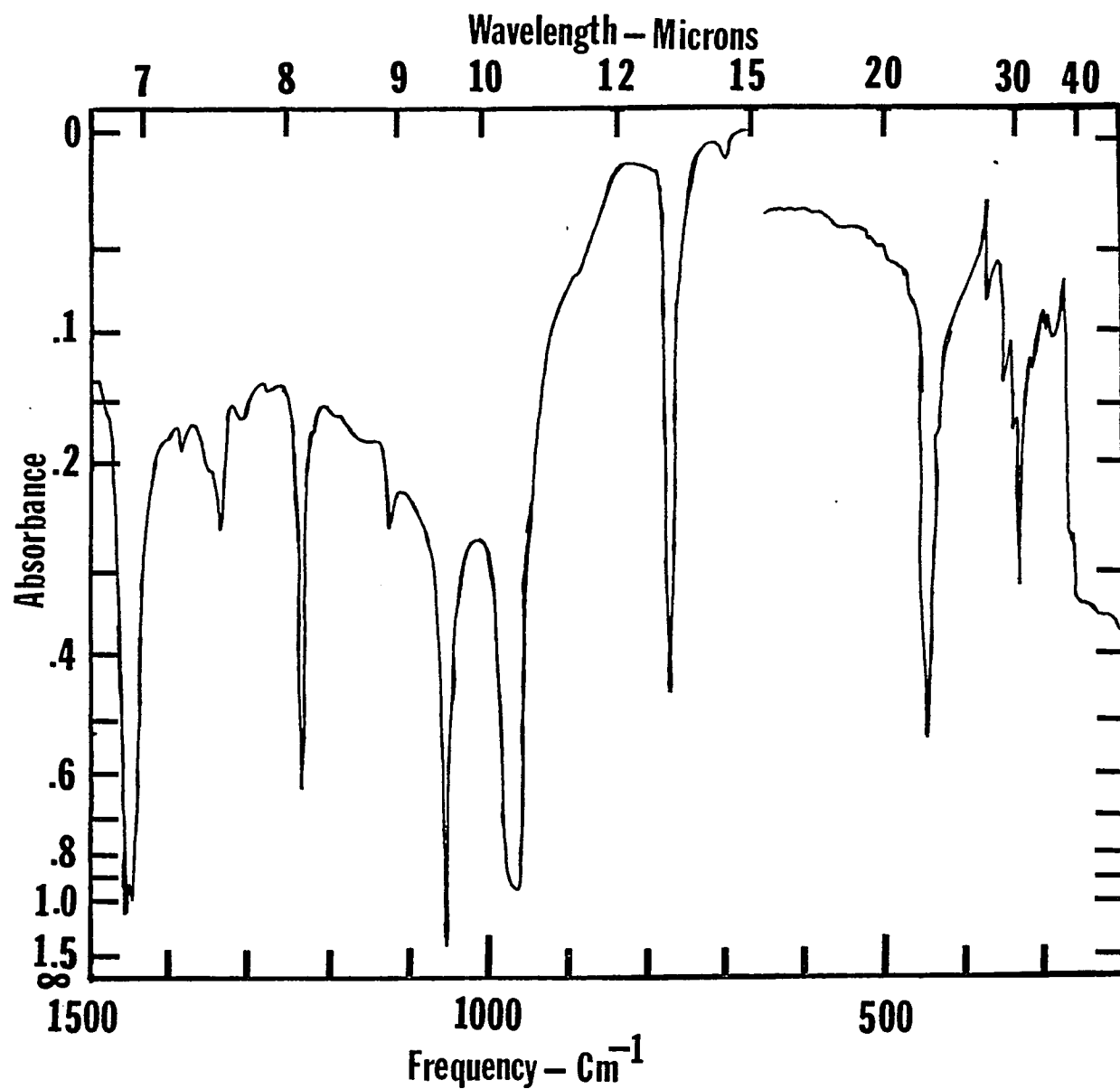


Fig. 37 IR spectrum of PTBD-K toluene grown crystals annealed at 138°C

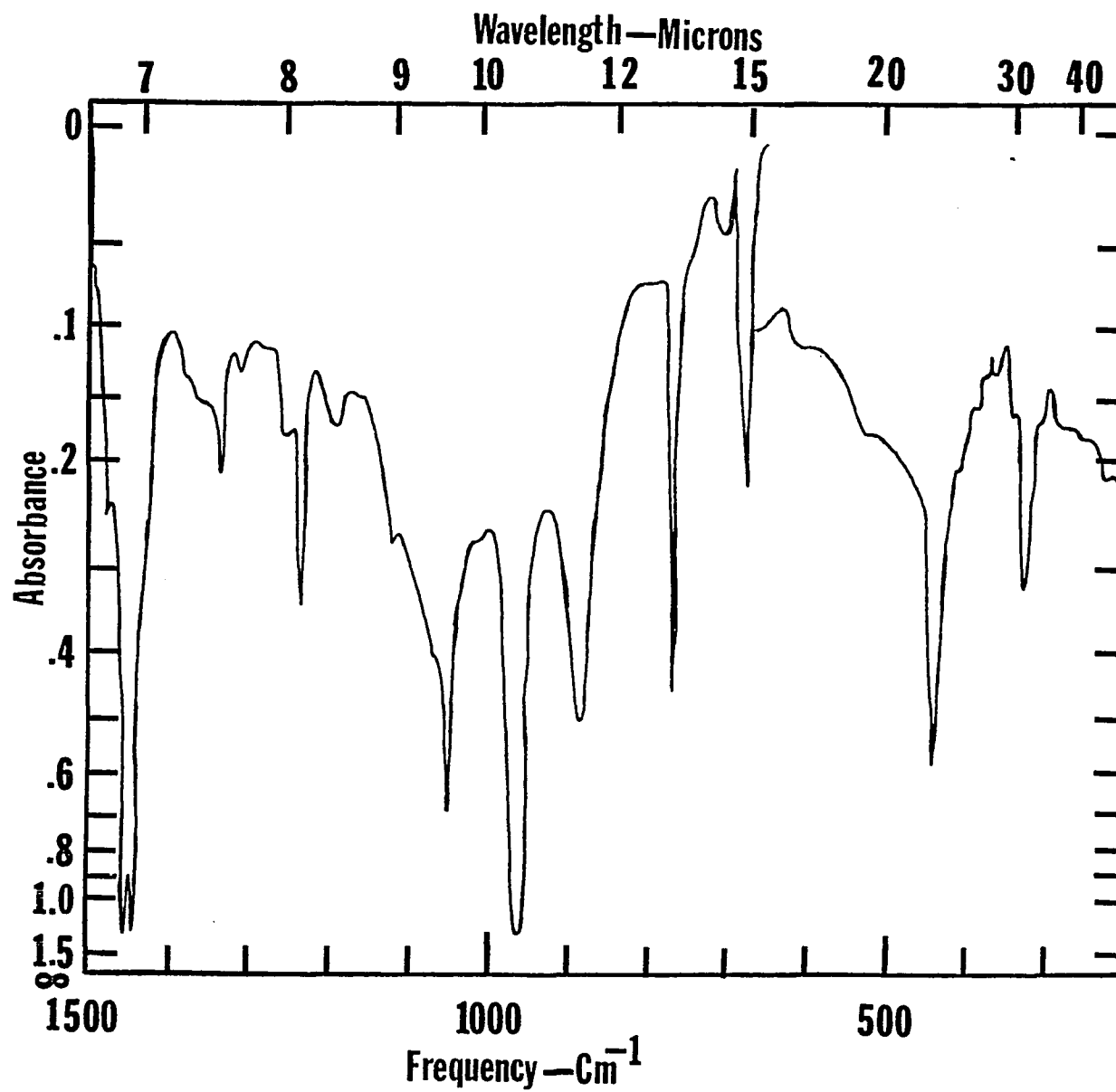
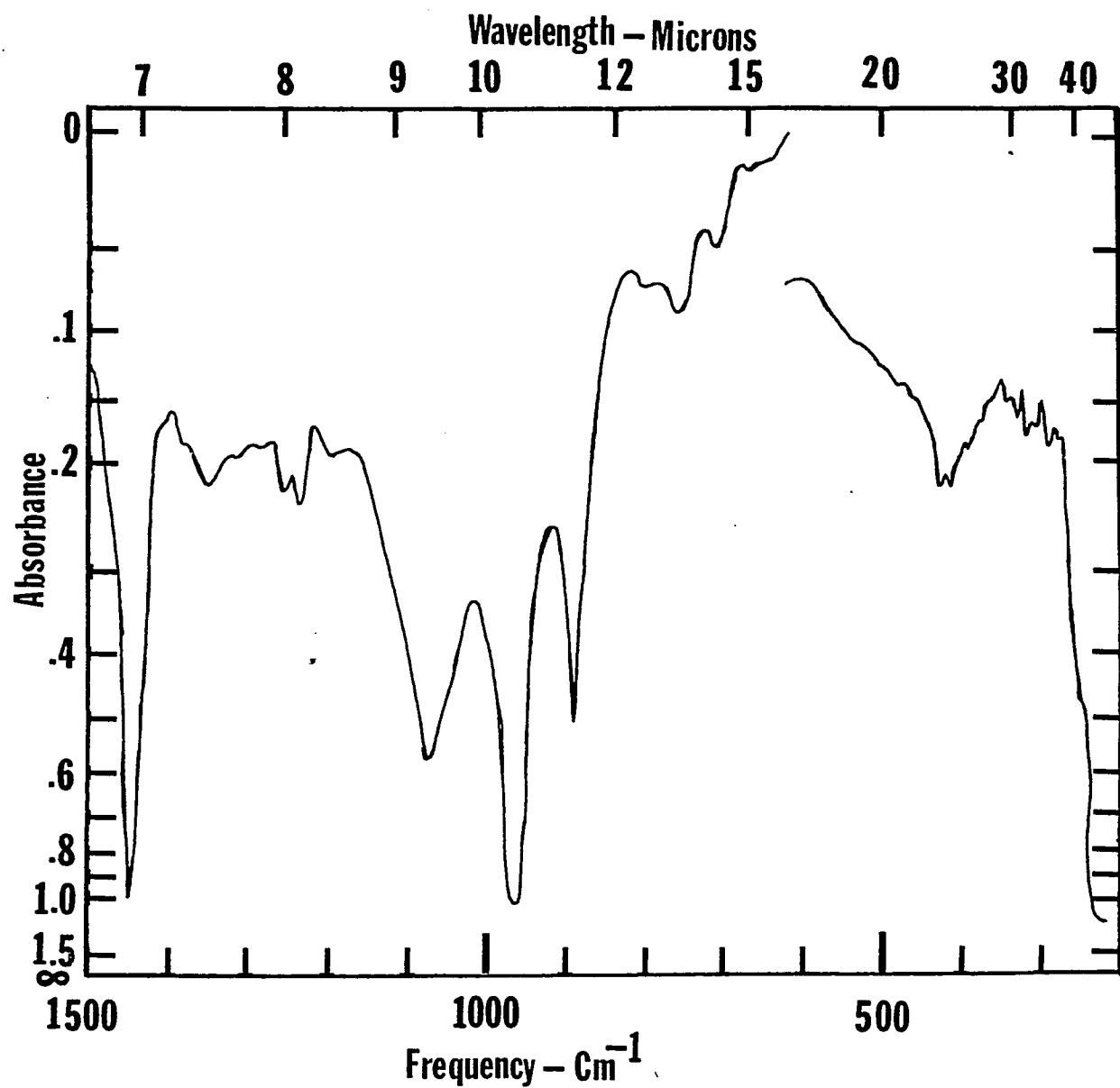


Fig. 38 IR spectrum of PTBD-K toluene grown crystals after epoxidation at 6°C



77

Fig. 39 IR spectrum of PTBD-K toluene grown crystals after epoxidation at 6°C and annealed at 90°C

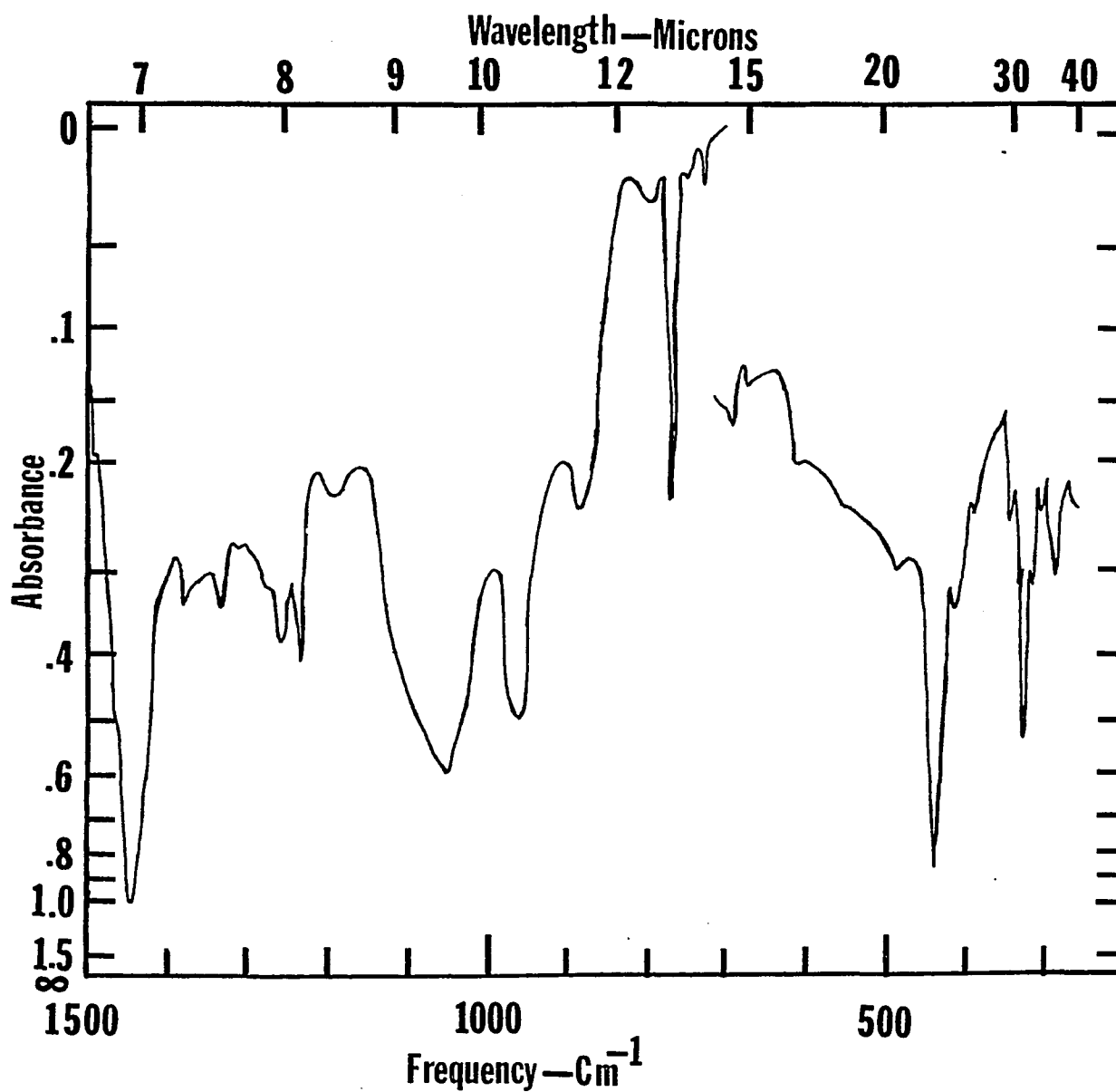


Fig. 40 IR spectrum of PTBD-K toluene grown crystals after epoxidation at 12°C

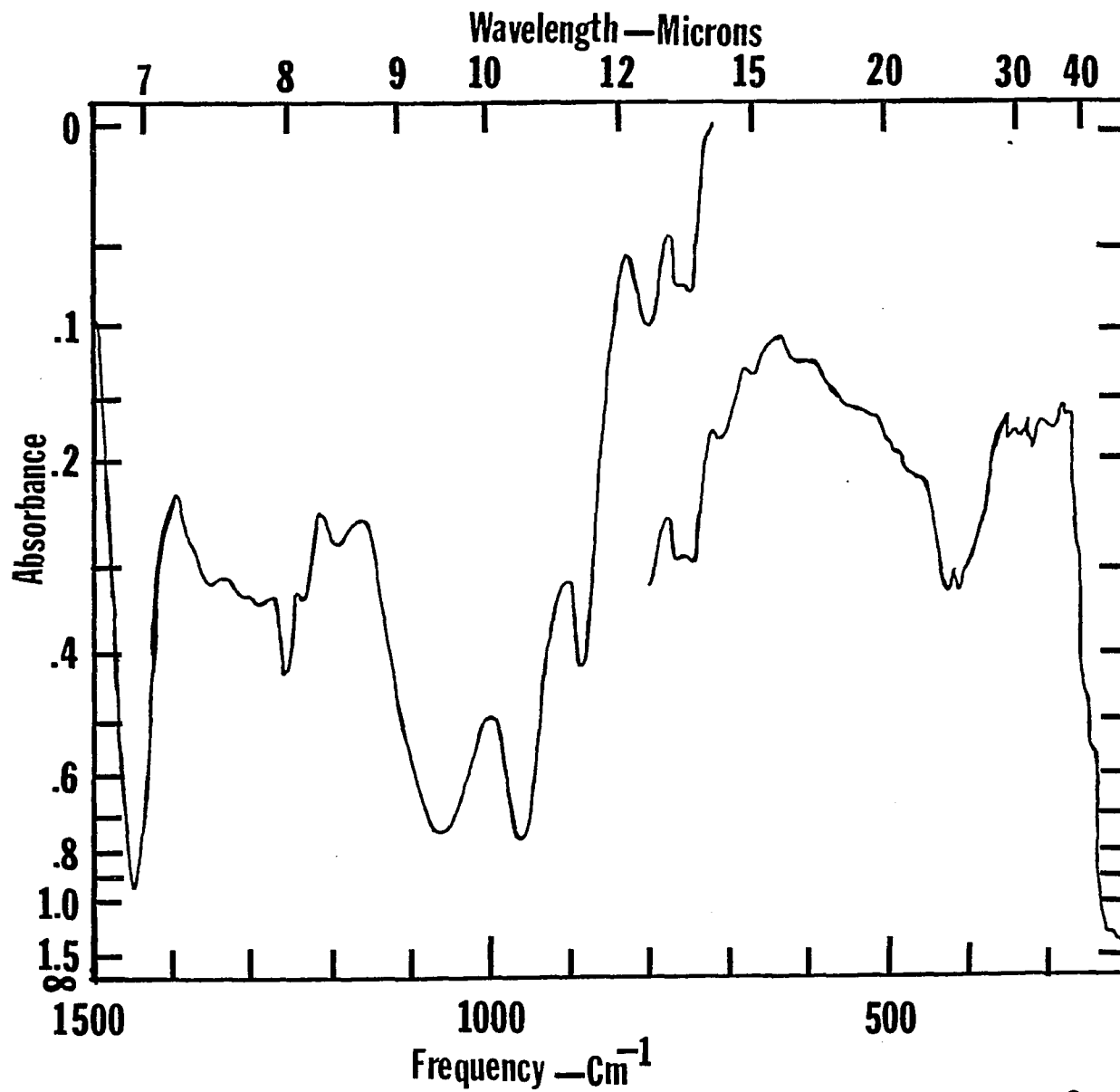


Fig. 41 IR spectrum of PTBD-K toluene grown crystals after epoxidation at 12°C and annealed at 90°C

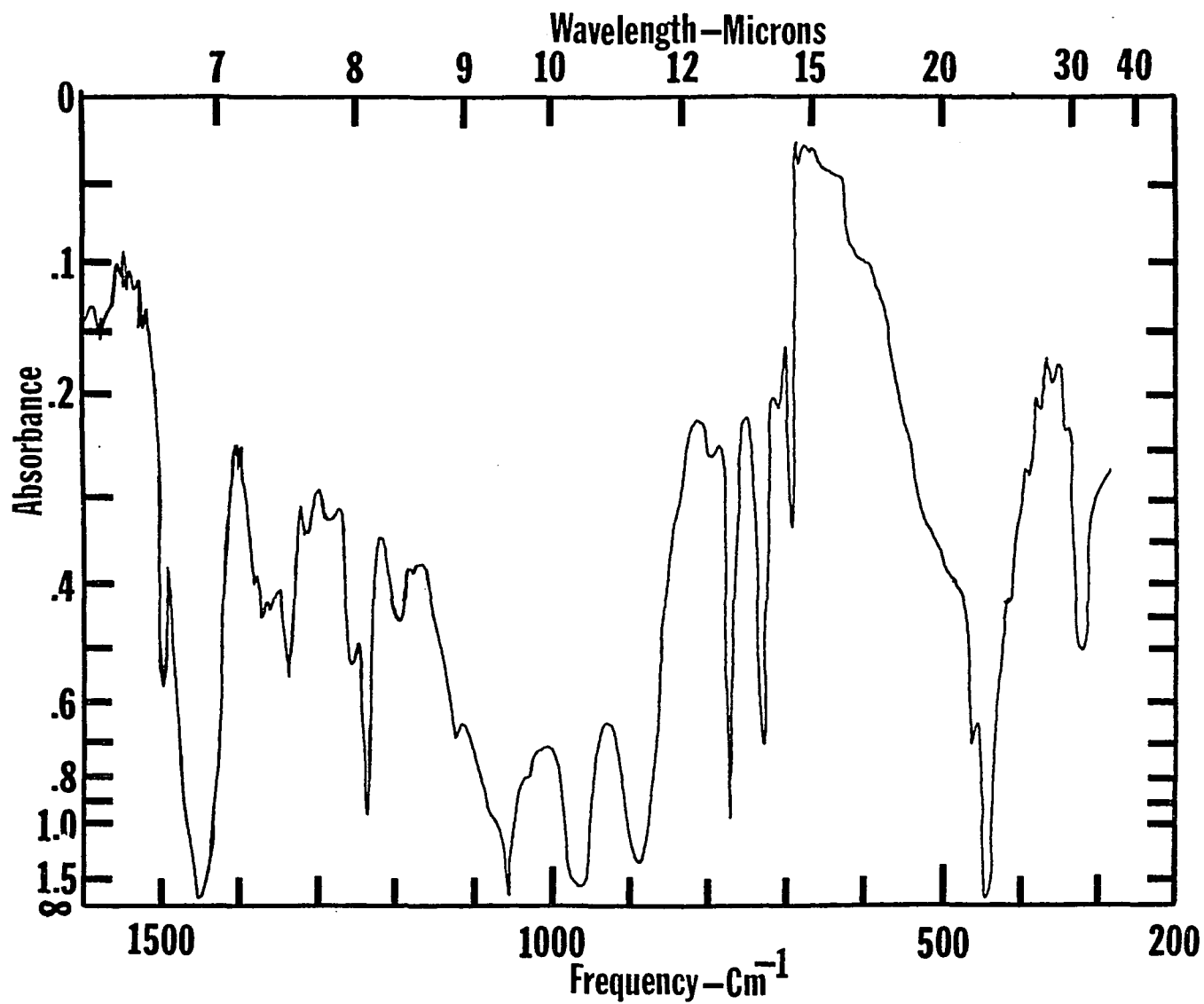


Fig. 42 IR spectrum of PTBD-K toluene grown crystals after epoxidation at 21°C

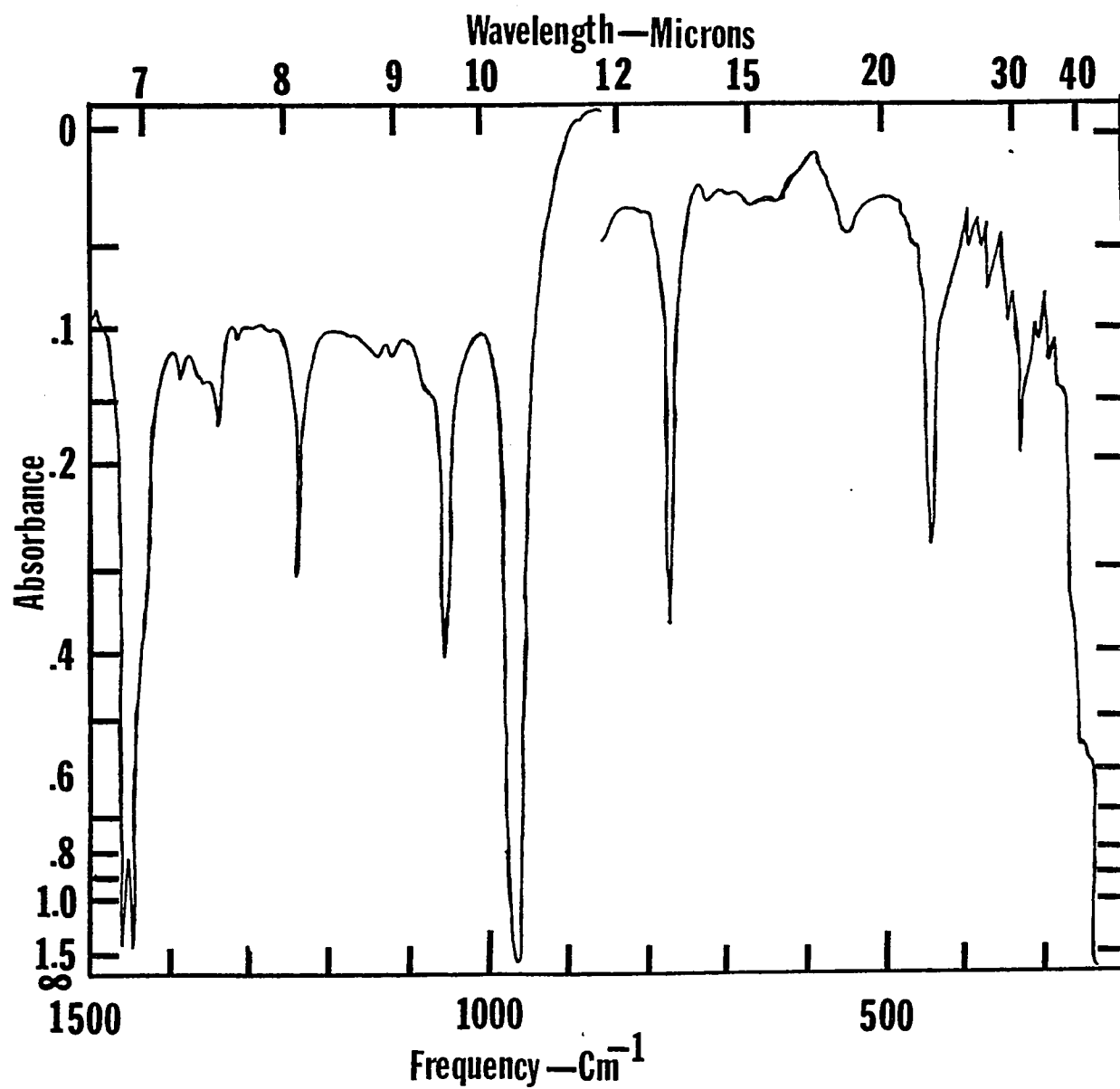


Fig. 43 IR spectrum of PTBD-K toluene grown crystals after bromination at 0°C

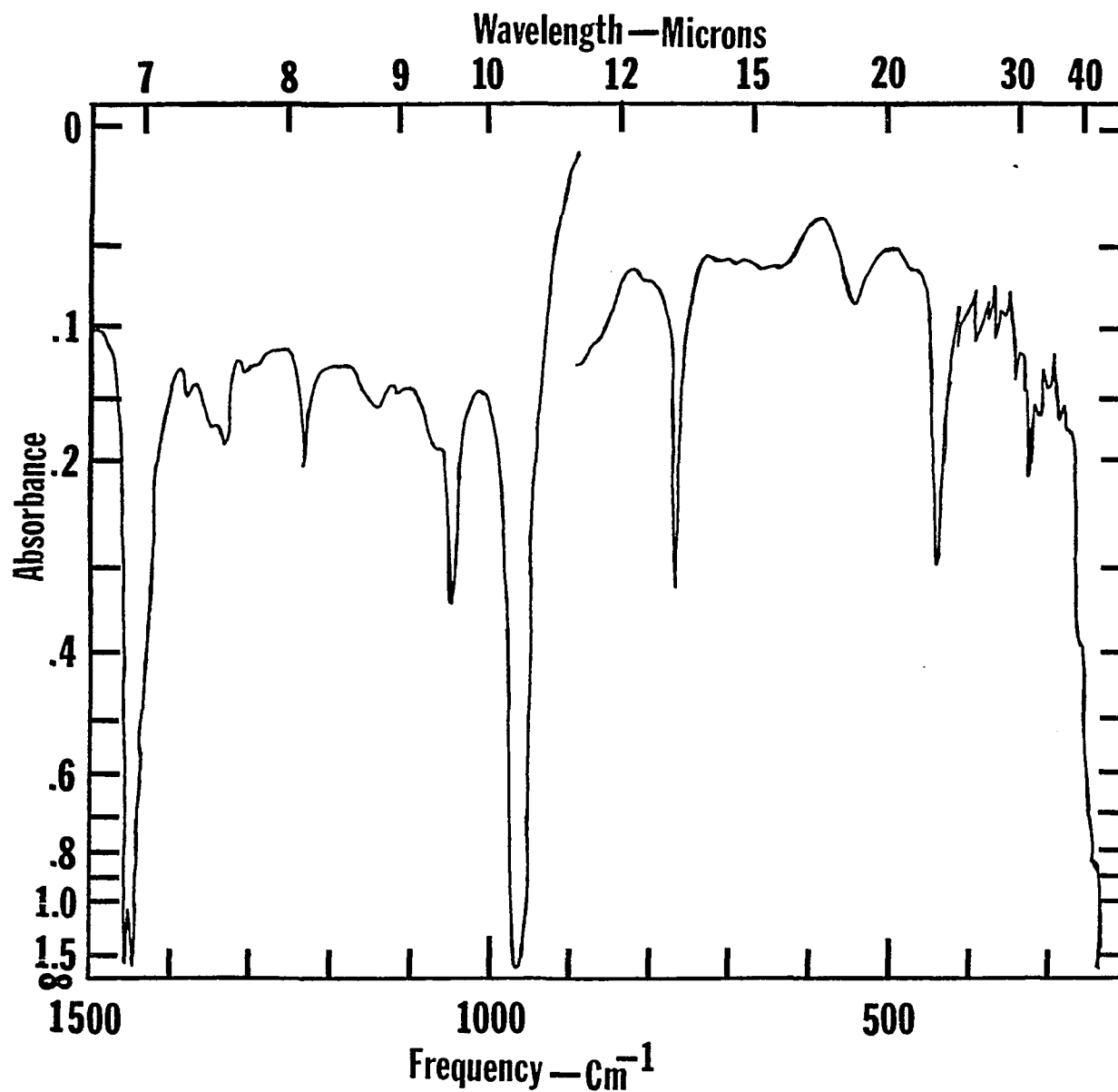


Fig. 44 IR spectrum of PTBD-K toluene grown crystals after bromination at 0°C and annealed at 90°C

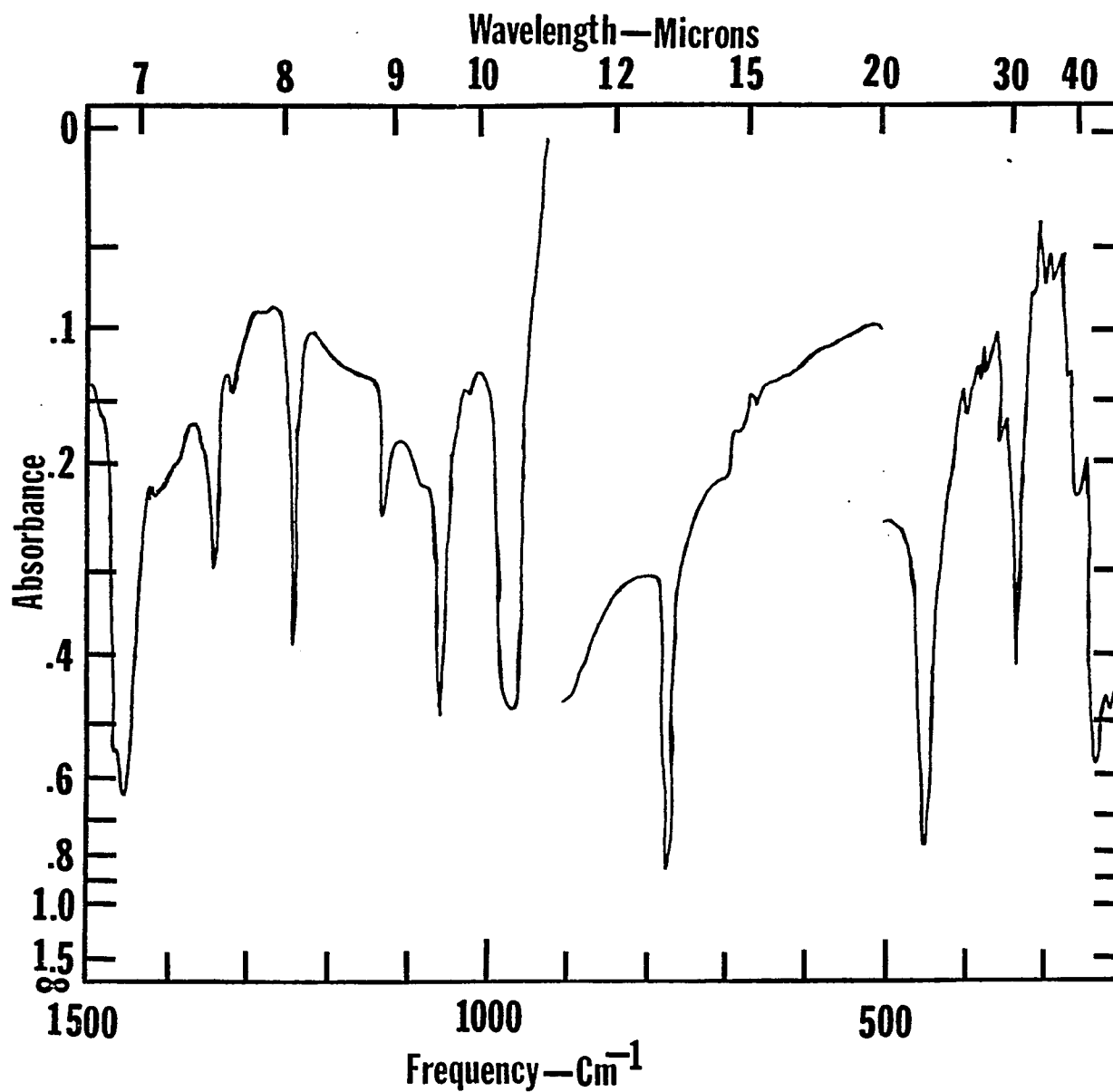


Fig. 45 IR spectrum of as-grown PTBD-K heptane grown crystals.

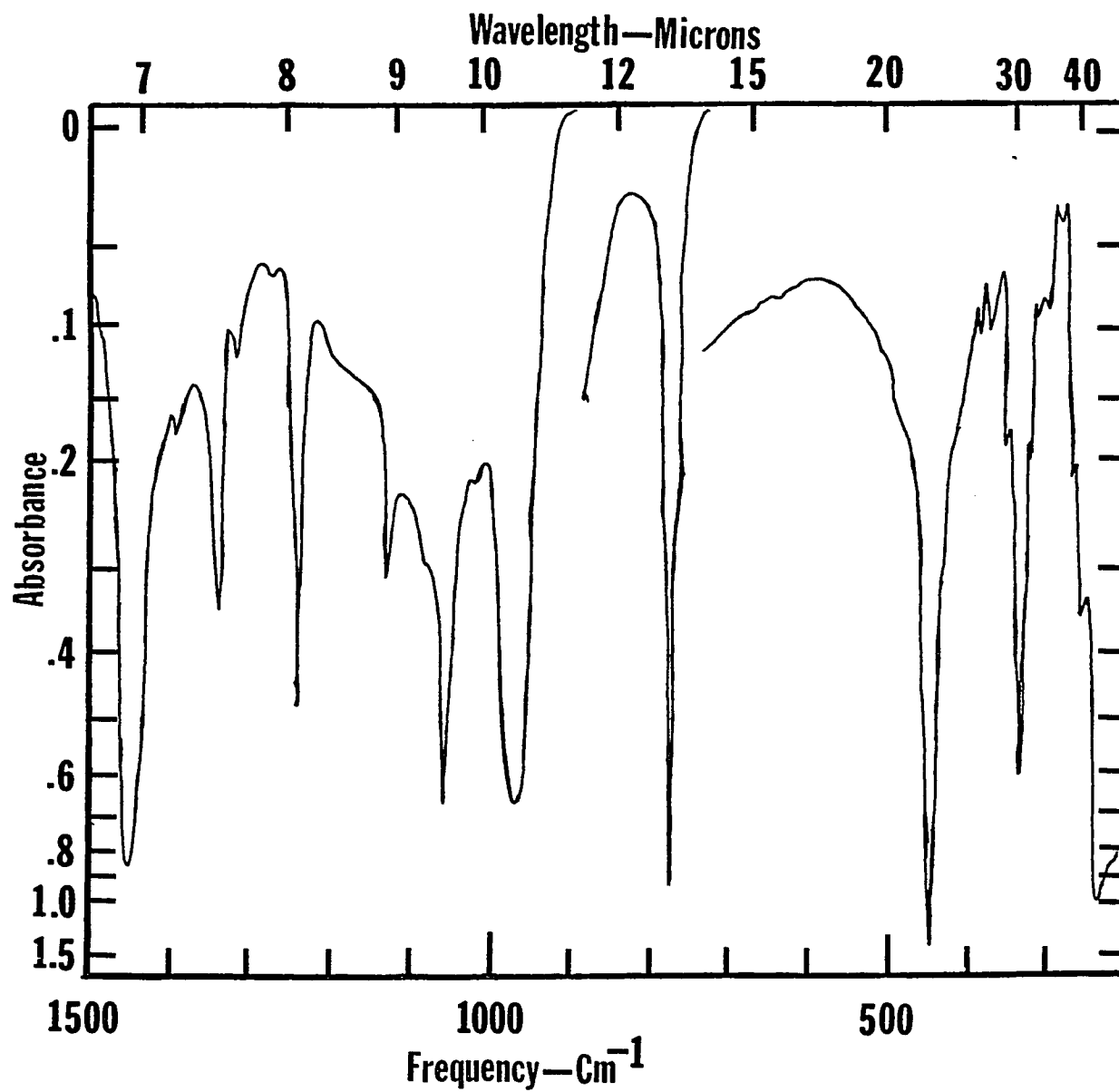


Fig. 46 IR spectrum of PTBD-K heptane grown crystals annealed at 68°C

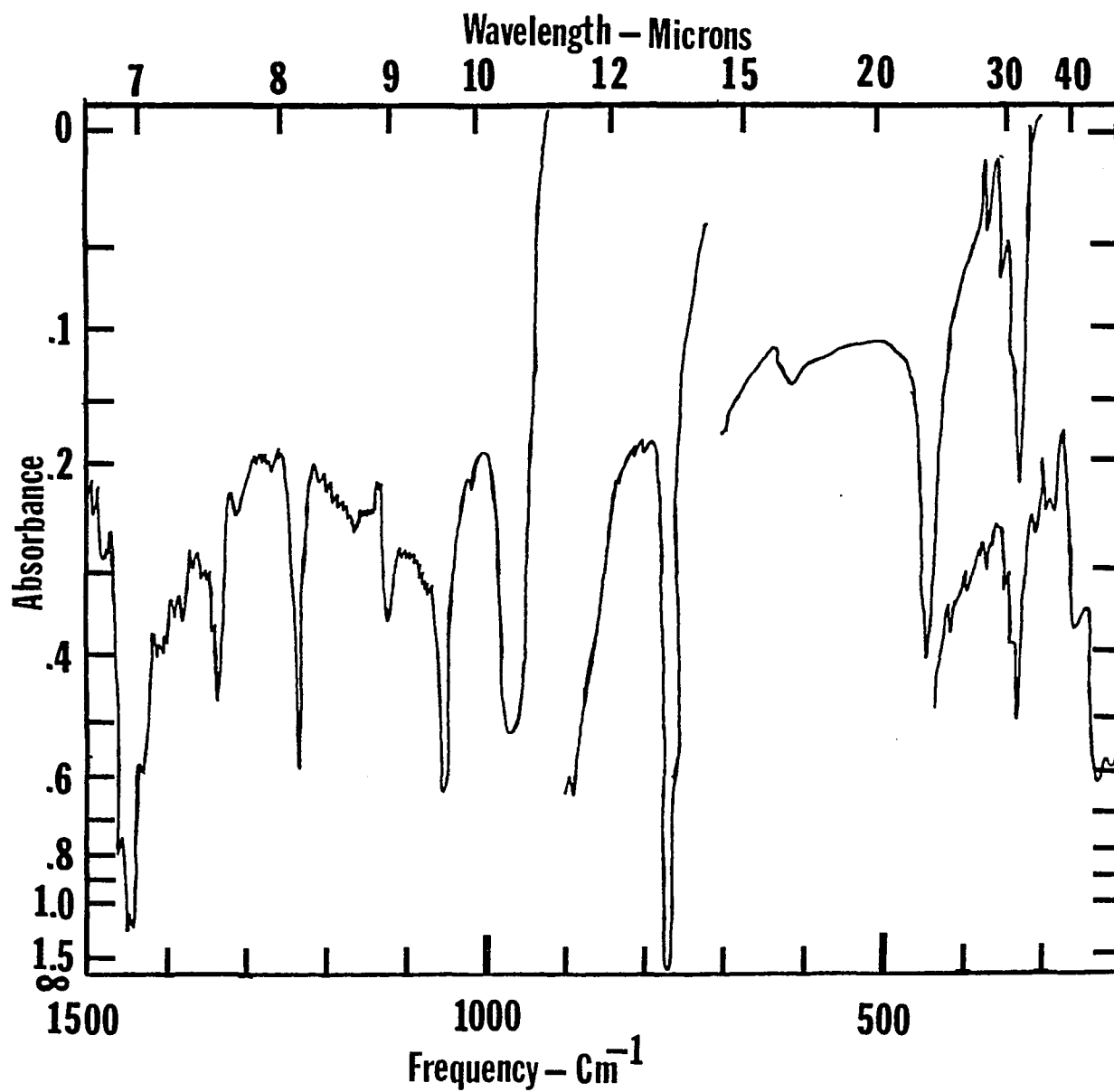


Fig. 47 IR spectrum of PTBD-K heptane grown crystals annealed at 80°C

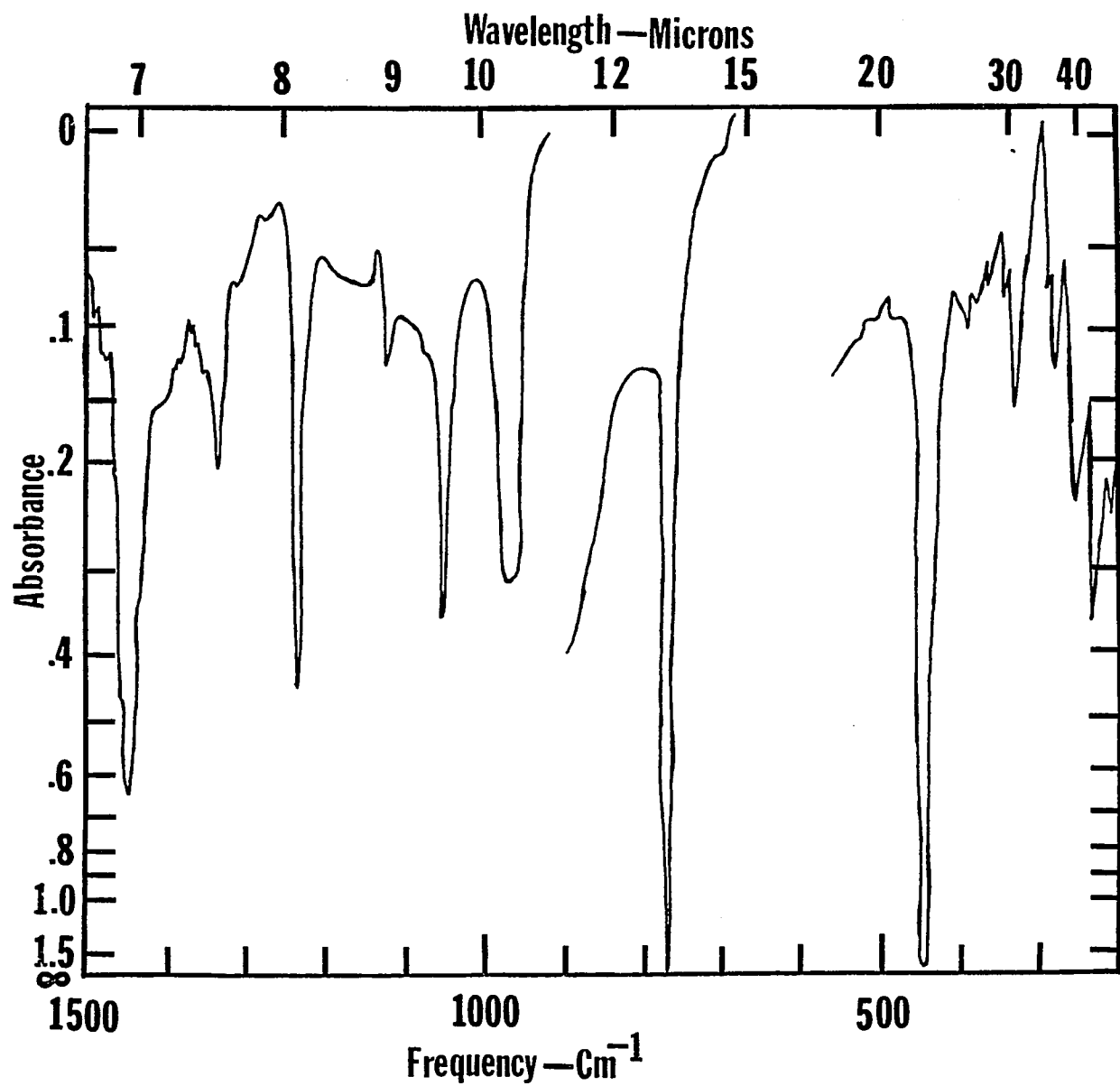


Fig. 48 IR spectrum of PTBD-K heptane grown crystals annealed at 138°C

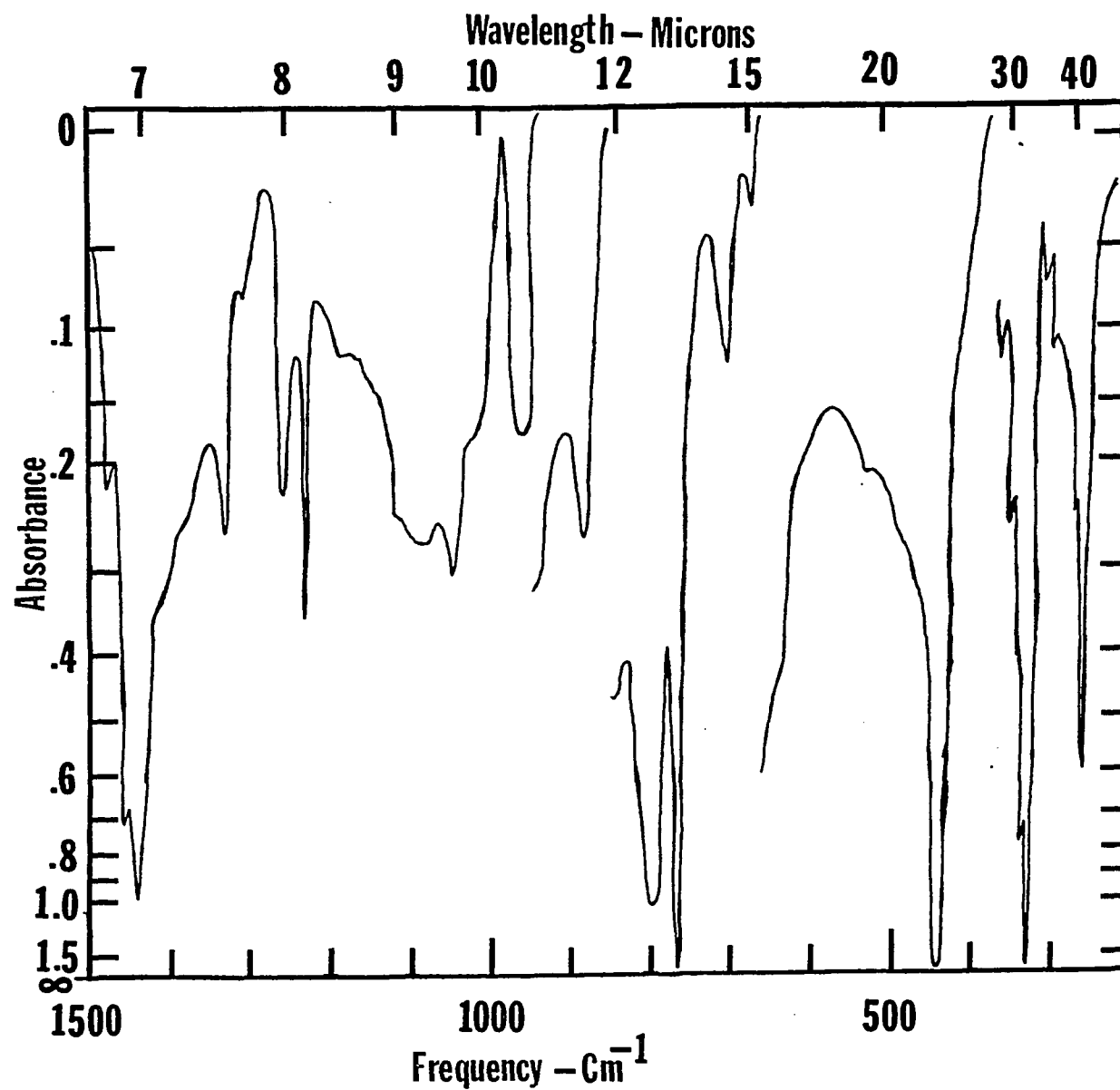


Fig. 49 IR spectrum of PTBD-K heptane grown crystals after epoxidation at 21°C

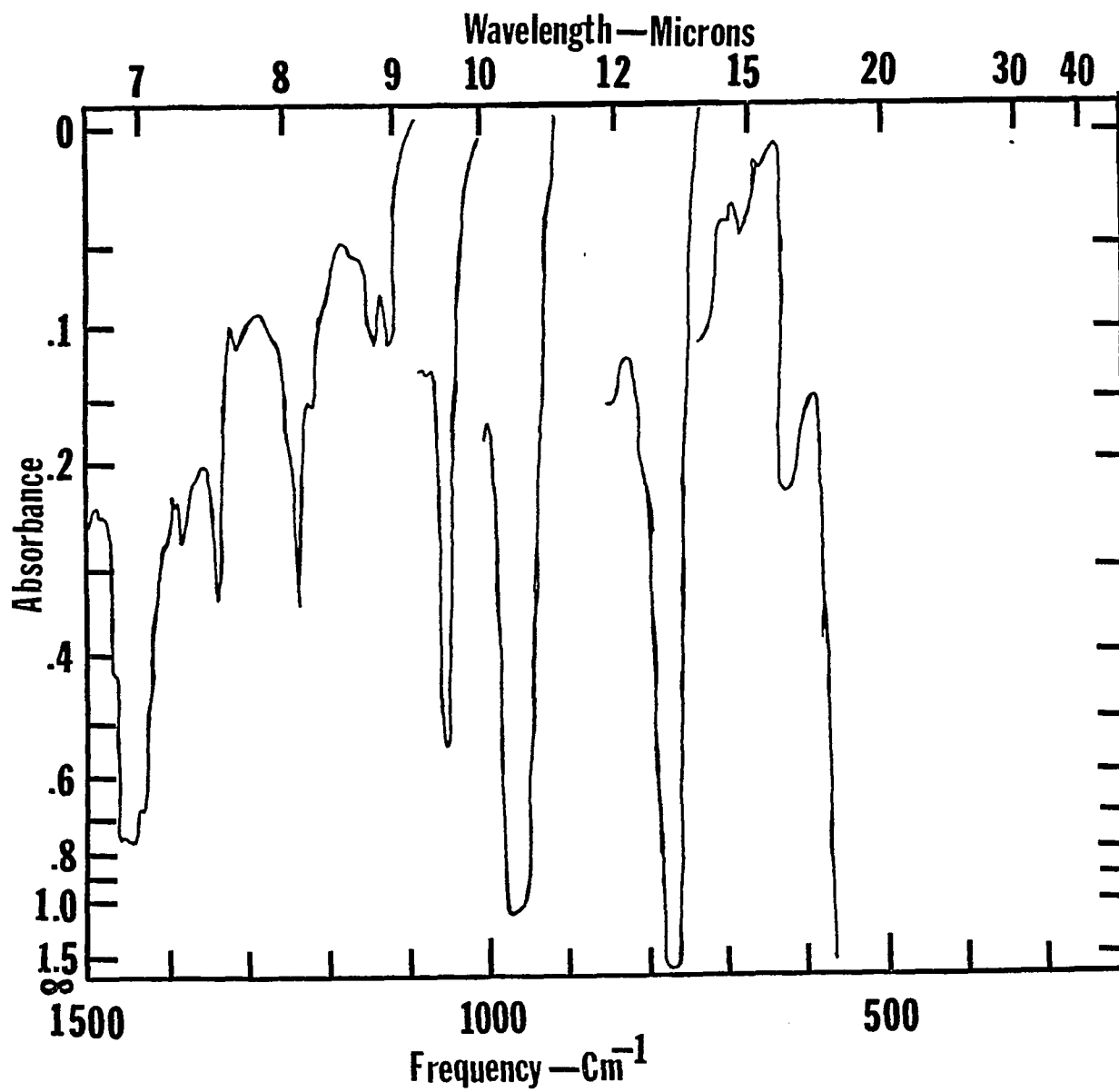


Fig. 50 IR spectrum of PTBD-K heptane grown crystals after bromination at 0°C

TABLE XIII

IR Spectrum of PTBD - K Toluene Grown Crystals

PTBD in As Toluene Grown	Annealed at T°C			Epoxidized at T°C			Epox ^d 6°	Brom ^d 0°C	Brom ^d Ann. 90°
	68°	80°	138°	6°	12°	21°	Ann. 90°	0°C	Ann. 90°
	1785(w)	1785(w)		1780(w)	1790(w)				
1722(s)	1725(w)	1725(w)	1725(w)	1720(w)	1720(m)	1725(w)	1740(w)	1720(B)	
			1665(w)	1710(m)					
	1630(w)	1630(w)	1630(w)		1630(w)		1630(w)		
					1605(m)				
								1500(w)	
				1490(m)	1495(m)			1495(m)	
				1475(w)	1475(w)	1475(w)			
	1458(s)	1458(s)	1458(s)	1458(s)	1458(s)	1458(s)	1458(s)	1458(s)	1458(s)
	1449(s)	1449(s)	1449(s)	1449(s)	1449(s)	1449(s)	1449(s)	1449(s)	1449(s)
		1438(m)	1438(m)	1438(m)					
1409(B)		1400(w)							
	1385(w)		1385(w)	1370(B)	1370(B)	1370(B)		1385(w)	1385(w)
1355(s)	1350(w)	1350(w)	1350(w)	1350(w)			1350(w)		1350(w)
	1335(m)	1335(m)	1335(m)	1335(m)	1335(m)	1335(m)	1335(m)	1335(m)	1335(m)
	1312(w)	1312(w)	1312(w)	1312(w)	1312(w)	1312(w)	1312(w)	1312(w)	1312(w)
	1275(w)	1270(w)	1270(w)	1270(w)	1280(w)	1285(B)			
				1255(w)	1255(m)	1255(m)	1255(w)		
	1235(m)	1235(m)	1235(m)	1235(m)	1235(m)	1235(m)	1235(w)	1235(m)	1235(m)
1212(m)									
	1193(w)			1193(w)	1190(w)	1193(w)	1190(w)		
								1150(B)	1150(B)

TABLE XIII (cont.)

PTBD in As Toluene Grown	Annealed at T°C			Epoxidized at T°C			Epox ^d 6°	Brom ^d	Brom ^d 0°C
	68°	80°	138°	6°	12°	21°	Ann. 90°	0°C	Ann. 90°C
1120(w)	1120(w)	1120(w)	1120(w)	1120(w)	1120(w)	1120(w)		1120(w)	1120(w)
1080(w)	1075(w)	1075(w)	1075(w)	1075(w)	1075(w)	1070(w)	1070(w)	1070(w)	1075(w)
1050(w)	1053(s)	1053(s)	1053(m)	1053(s)	1053(s)	1053(s)	1053(s)	1053(s)	1053(s)
								1028(w)	
960(s)	965(s)	965(s)	965(s)	965(s)	965(s)	965(s)	965(s)	965(s)	965(s)
								888(m)	885(m)
								885(m)	888(m)
								795(w)	800(w)
	770(s)	770(s)	770(s)	770(s)	770(s)	770(s)		770(s)	770(s)
								750(w)	750(w)
								760(B)	
								726(w)	726(w)
								710(w)	730(s)
698(w)	698(w)	698(w)	698(w)	700(w)	690(m)	691(s)		690(s)	
								680(m)	
								545(w)	545(w)
								462(s)	460(w)
445(s)	445(s)	445(s)	445(s)	445(s)	432(s)	445(s)	425(w)	445(s)	445(s)
345(w)	345(w)	345(w)	345(w)					415(w)	345(w)
330(s)	330(s)	335(s)	330(s)					325(m)	325(m)
310(w)								310(w)	310(w)
280(w)	255(m)	255(m)	255(m)					290(w)	
225(m)	230(m)	225(s)	225(s)					225(s)	

TABLE XIV

IR Spectrum of PTBD-K Heptane Grown Crystals

PTBD, in Toluene	AS Grown	Annealed at T °C			Epoxidized 21° C	Brominated 0° C
		68°	80°	138°		
1722(s)	1720(vw)	1725(w) 1630(w)	1725(w) 1630(w)	1725(w) 1630(w)	1725(w) 1630(w) 1490(w) 1475(m)	1725(w) 1635(w)
	1458(s) 1450(s)	1480(w) 1450(s)	1480(w) 1451(s) 1438(m) 1420(B)	1480(w) 1458(m) 1450(s) 1438(m)	1458(s) 1450(s) 1442(s)	1449(s)
1409(B)		1385(w)	1380(w)	1380(w) 1400(sh)	1380(w)	1385(w)
1355(m)	1350(w) 1335(m) 1312(w)	1350(w) 1335(m) 1312(w) 1275(w)	1350(w) 1335(m) 1312(w) 1275(w)	1350(w) 1335(m) 1312(w) 1275(w)	1335(m) 1312(w)	1335(m) 1312(w)
	1235(m)	1235(s)	1235(s)	1235(s)	1255(m) 1235(s)	1235(s) 1220(s)
1212(s)			1160(B)	1160(B)	1180(w) 1135(w)	1138(m) 1120(w)
1080(w)	1120(w) 1075(sh)	1125(m) 1075(sh)	1120(m) 1075(w)	1120(w) 1075(sh)	1120(w) 1085(B)	1075(sh)
1050(w)	1053(s)	1055(s)	1050(s)	1050(s)	1050(s) 1015(sh)	1053(s)
960(s)	965(s)	965(s)	965(s)	965(s)	965(s) 885(m) 795(s)	965(s)
	770(s)	770(s)	770(s)	770(s)	770(s) 700(m)	770(s) 585(B) 550(s)
	450(s)	450(s)	445(s)	445(s)	445(s)	445(s) 380(w)
	345(w) 330(s)	345(w) 330(s)	345(w) 330(s)	345(w) 330(m)	345(w) 330(s)	345(w) 330(s)
	255(m) 235(m)	260(m) 235(s)	255(m) 235(s)	255(m) 235(s)	255(m)	280(w)

In the analysis of infrared spectrum by Krimm, the infrared absorption peak at 1350 cm^{-1} is assigned to the amorphous component and the 1335 cm^{-1} is a crystalline peak for PTBD single crystals. If it is assumed that the absorption at 1350 cm^{-1} is proportion to the total amorphous content of the crystals, the percent amorphous content of the crystals can be calculated from the absorbance ratios. The results are summarized in Table XV.

TABLE XV

The Amorphous Content of PTBD-K Crystals from IR Measurements.

Treatment	PTBD-K Heptane Grown Crystals	PTBD-K Toluene Grown Crystals
As grown	21 %	35 %
Annealed at 68°C	14 %	18 %
Annealed at 80°C	15 %	18 %
Annealed at 138°C	30 %	30 %
Epoxidized at 6°C	-	a
Epoxidized at 12°C	-	a
Epoxidized at 21°C	0 %	a
Epoxidized at 6°C & Annealed at 90°C	-	42 %
Brominated at 0°C	0 %	30 %
Brominated & Annealed at 90°C	-	40 %

a) can not be determined due to interfering from the peak at 1365 cm^{-1} .

The amorphous content of heptane grown PTBD-K crystals is smaller than toluene grown PTBD-K crystals, but after annealing the amorphous content becomes the same within experimental errors as shown earlier⁵⁰. After epoxidation and bromination the amorphous peak seems to have disappeared, but the amorphous content increases when the epoxidized crystals and brominated crystals were annealed at 90°C for 24 hours.

DISCUSSION

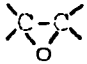
In earlier studies^{51,53,54} it was concluded that the amount of amorphous material in PTBD crystals, suspended in a liquid medium, available for reaction and / or penetration by low molecular weight substances depends on the crystal preparation conditions. This investigation supports that conclusion and give more accurate values for the amount of penetration taking place during the epoxidation reaction between MCPBA and the available double bonds in PTBD crystals.

A comparison of values of the amorphous content in PTBD crystals obtained by five methods is given above in Table XII. Two of these methods, DSC and IR measure the total amorphous regions in the lamellae available for reaction and / or penetration from a liquid phase. For toluene grown PTBD-K crystals, 40 \pm 10% amorphous content was reported by the DSC method, and 50 % by the IR method. The DSC value has a low precision as shown, and the IR value is inaccurate due to overlapping and to the low intensities of the two peaks used. In contrast to these values the epoxidation results from this study show a maximum amorphous content of 29 %; due to fluctuation of the measurements, this value might be lower by 2-3 %. Therefore it appears that there are amorphous regions not reached by penetrants within the toluene grown PTBD-K crystals as stated earlier^{51,54}, although due to the various uncertainties the question is still an open one.

The crystallization temperatures of heptane and toluene grown PTBD-K crystals are 63.5° and 23°C respectively. The lower amorphous content of PTBD-K heptane grown crystals is

believed⁵³ to be a consequence of growth at a temperature which is twelve degrees below the crystal-crystal transition temperature reported for dry crystals, whereas the toluene grown PTBD-K crystals are precipitated fifty three degrees below this transition temperature. At the higher crystallization temperature used, a considerable amount of torsional motion is possible for parts of the polymer chains, so that they have the opportunity to arrange into ordered crystallites. For toluene grown PTBD-K crystals, the same amount of freedom of movement is not available because the crystallization temperature is much lower, resulting in a higher amorphous content.

It was found in the present study that the number of double bonds available for epoxidation depends on the reaction temperature. The increase in available double bonds with reaction temperature observed could be due to 1) penetration of additional amorphous regions 2) reaction of double bonds in the crystalline portions 3) reaction with additional solubilized polymer or 4) a combination thereof. Since upon use of any of the three surface penetration methods on PTBD crystals, a limiting value for the amount of penetration and / or reaction is always reached with time at constant temperature, the second explanation above is not considered likely. Further-more, the IR spectra of brominated and epoxidized crystal mats show that large portions of the sample retain the PTBD crystal structure original present; and annealing of the reacted crystals leads to an increase in the amount

of crystal disorder, as shown by the increase in the 1350 cm^{-1} peak relative to the 1335 cm^{-1} , apparently due to the inability of the crystal lattice to include the  or $\begin{matrix} \text{Br} \\ | \\ -\text{CH}-\text{CH}- \\ | \\ \text{Br} \end{matrix}$ groups.

In order to obtain information about the solubility of PTBD crystals at the reaction temperature, 74.5 mg. of PTBD-U heptane grown crystals were suspended in toluene for 9 days, and toluene was separated from the crystals. It was found that there is no polymer residue in the filtrate. It is concluded that PTBD-U heptane grown crystals are not appreciably soluble in toluene at 21°C ; this should also be true for PTBD-K crystals for which the molecular weight is approximately seven fold higher.

It is concluded from the above discussion that most and possibly all of the increase in total double bonds reacted with epoxidation temperature for toluene grown PTBD-K crystals is due to increased penetration of amorphous parts made available by expansion of the fold region of the crystals. The amorphous content from bromination at 0°C and penetration by CS_2 at -20°C and lower (broad line NMR method) shows that in addition to the reaction temperature, the size of the penetrant is important. Both Br_2 and CS_2 are smaller sized molecules than MCPBA and therefore can penetrate deeper into the amorphous regions at any particular temperature.

For PTBD-K heptane grown crystals on the other hand, all the various measures of amorphous content give about the same results independent of the methods and temperatures used (see Table XII). This is an indication that both the fold region and the crystal interior are higher ordered.

The maximum available double bonds of PTBD-U heptane grown crystals is 2-3 fold larger than that for crystals grown from the same solvent using PTBD-K; the amount found by epoxidation increases in the temperature range 6-12°C and stays approximately constant thereafter up to about 21°C. A small change (2-3 %) is probably due to fluctuation in the measurements especially at high reaction temperature. A greater amorphous content for PTBD-U than for PTBD-K crystals were found earlier by Stellman and Woodward⁵³ and is due to the approximately seven fold lower molecular weight for PTBD-U. It is expected that the lower molecular weight sample should contain more chain ends (cilia) and therefore these should result in more disordered material in the fold region. Rank and Krimm⁴⁹ showed that on oxidation of polyethylene single crystals with ozone, the absorbance at 910 cm^{-1} which is due to the vinyl end group, falls rapidly to a constant low value. This suggests strongly that the end groups are largely excluded from the interior of the crystals. Chemical assay on PTBD crystals by Stellman and Woodward⁵³ also led to the same conclusion.

The increase in the amount of amorphous material available for epoxidation as the temperature is increased for PTBD-U heptane grown crystals as compared to PTBD-K heptane grown crystals within the same temperature range suggests that PTBD-U heptane grown crystals also have some disordered folds.

Ng et. al.⁵¹ reported direct evidence for the existence of an irregular fold region by following the behavior of the NMR narrow line with time upon addition of CS_2 to the dry

material at a low temperature. Solvation of a large portion of the disordered region of PTBD-K toluene grown crystals took place immediately as indicated by the sudden increase in I_N/I_B ratio; then further solvation was effected at a slower rate as was seen by the slow increase with time for the ratio of I_N/I_B . The second stage was not found for PTBD-K heptane grown crystals. This also leads to the conclusion that the fold region in the heptane grown PTBD-K crystals is significantly more regular than in toluene grown PTBD-K crystals.

Three different types of folds have been proposed for polymer single crystals:

- 1) The irregular adjacent re-entry (loose fold)¹⁹
- 2) The regular adjacent re-entry (tight folds)^{22,23}
- 3) The switchboard or non-adjacent re-entry folds^{25,26}.

Takayanaki et. al.⁶³ proposed a crystal lamella model for PTBD crystals grown from benzene solvent; the model is a two phase structure which contains irregular adjacent re-entry fold making up the amorphous layer and a crystalline core as shown in Fig. 51.

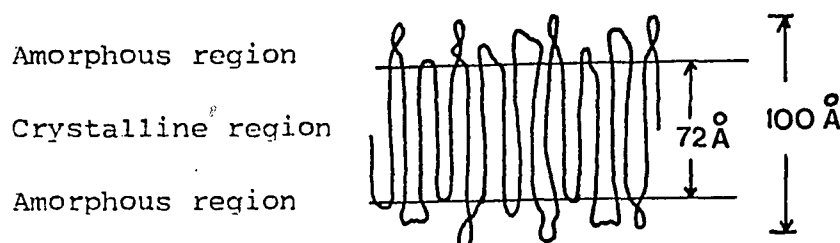


Fig. 51 Two component microcrystalline model for PTBD crystals.

Bank and Krimm⁴⁹ showed that the study of the infrared spectra of mixed crystals of polyethylene and perdeutero polyethylene provides information on the structural characteristics of the fold geometry in crystalline polyethylene. This is possible because different patterns of folding place different restrictions on the arrangement of the chain stems, with the result that different spectra are predicted by normal coordinate analyses for pure polymers⁸⁶ and mixed crystal systems⁸⁷. The experimental studies of the mixed crystal polymers show that folding in the (100) plane predominates in solution grown crystals. This result implies that adjacent re-entry is favored; adjacent re-entry is more strongly indicated by lattice frequency studies^{34,35} with which the above results are therefore completely consistent

Recently Keller et. al.⁸⁰ suggested a model of crystal lamella based on the adjacent re-entry fold which includes hidden folds, this is illustrated in Fig. 52.

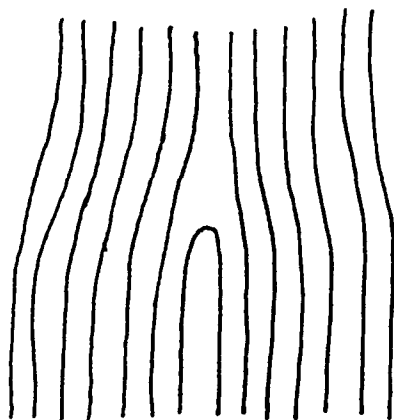


Fig. 52 Crystal defect due to fold buried deep inside the Crystal.

In deciding on the appropriateness of a model it is instructive to calculate the average number of monomer units per fold from the fold region amorphous content. The average number of monomer units per fold can be calculated from the following equation.

$$\frac{(A \times F) + C}{N} = B \dots\dots\dots(7)$$

A = average number of monomer units per fold

N = degree of polymerization (DP)

= number of monomer units per chain

F = number of folds per chain

= $\frac{(DP) \times \text{repeat distance}}{\text{crystal thickness}} - 2$

C = average number of monomer units in both cilia

B = fraction of double bonds available for epoxidation

The crystal structure of PTBD has been reported⁵⁹ as monoclinic with a chain repeat distance of 4.83 Å. "C" is calculated by assuming that the average length of a cilia is one-half the thickness of the crystal⁴⁷.

Using eq. (7), the average number of monomer units per fold for heptane and toluene grown PTBD-K crystals are found to be 2.4 and 5.6 respectively, and 4.0 for PTBD-U heptane grown crystals.

Woodward and coworkers⁵³ concluded that the average number of of monomer units necessary for the tightest re-entrant fold should be between 1.5 and 2. Oyama et.al.⁸⁵ showed that eight bonds were necessary for the shortest regular

(100) fold of polyethylene single crystals. The distance between adjacent chain of a fold is 4.60 Å for PTBD. Oyama et. al.⁸⁵ concluded that the shortest fold possible for PTBD contains three repeating units.

Comparison of these values with the value calculated from eq. (7) leads to the conclusion that PTBD-K heptane grown crystals principally contain regular re-entrant folds. For PTBD-K toluene grown crystals the average number of monomer units per fold is twice that for PTBD-K heptane grown crystals, this indicates a possibility of irregular re-entrant folds. In order to have non-adjacent re-entry folds there would have to be several regular re-entry folds present for compensation. The rate data and the temperature effect for PTBD-K toluene grown crystals do not support the presence of non-adjacent re-entry folds. It can be concluded that PTBD-K toluene grown crystals have irregular adjacent re-entry folds. The temperature effect as discussed above indicates that there are some buried folds. The discrepancy in the result from epoxidation and from IR measurement also indicate a possibility of more defects in the crystalline region. These defects can be a combination of the following 1) deep folds 2) chain ends inside the crystal 3) a kink chain defect and 4) a mosaic block. (see Fig. 53). This study could not distinguish the above defects.

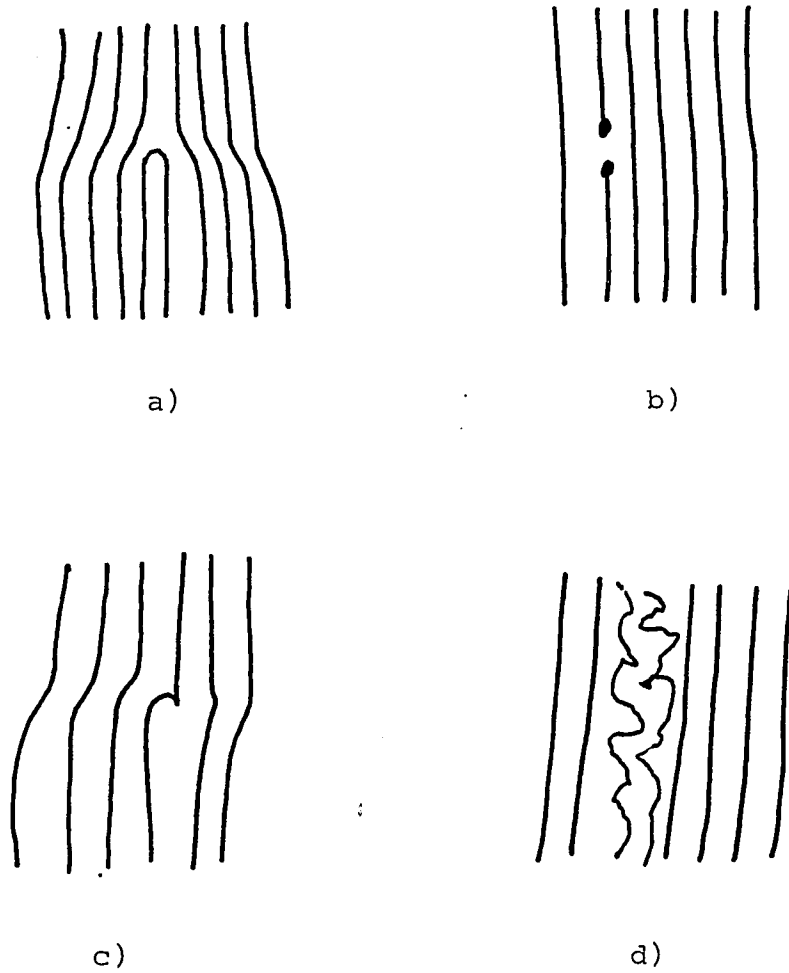
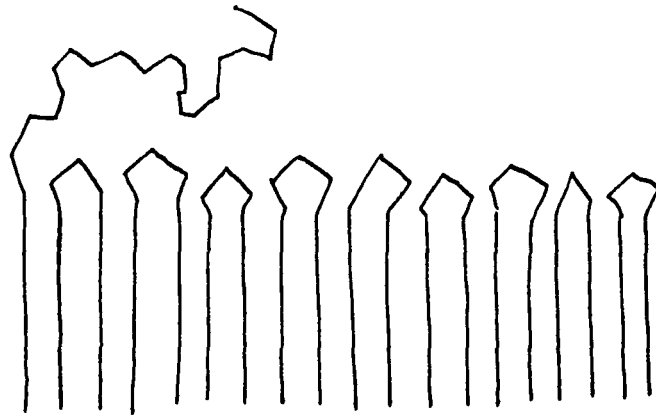


Fig. 53 Different kinds of defects in the crystalline region, a) deep fold b) chain end inside the crystal, c) kink chain defect, d) mosaic block.

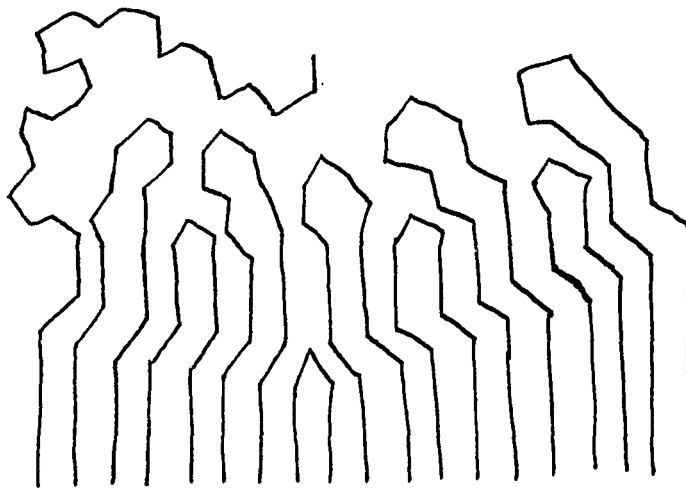
It was concluded above that PTBD-U heptane grown crystals have mainly regular folds in addition to a large number of chain ends not included in the crystalline portions. To summarize the above, models of the fold region for the three types of crystals studied are drawn in Fig. 54.

We turn now to the effects of annealing PTBD crystals, as prepared and after reaction, on the amorphous component. The amorphous component of PTBD-K heptane grown crystals as calculated from the IR absorbance ratio is smaller than that for toluene grown PTBD-K crystals, but after annealing it becomes the same within experimental errors, as shown earlier⁵⁰. The amorphous content decreases when the annealing temperature is near to the crystal-crystal transition temperature and increases as the annealing temperature is raised to a value near the melting temperature. It appears that for crystals with uneven fold regions, heating just above the transition temperature and subsequent cooling leads to a more ordered internal structure and more regular folding.

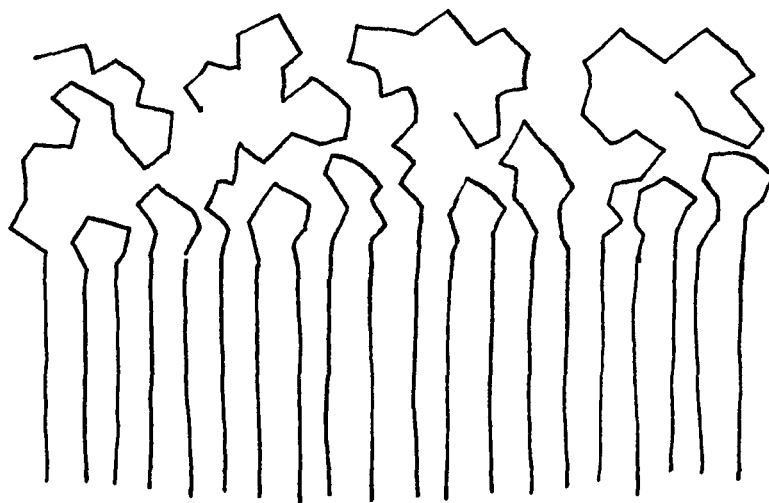
After epoxidation and bromination the amorphous peak at 1350 cm^{-1} seems to disappear, because an introduction of epoxide groups or bromine atoms changes the polymer chain chemically in the fold region. When the epoxidized crystals and brominated crystals are annealed at 90°C for 24 hours, the amorphous content increases. The thickening of crystals after annealing would result in a pulling of the chains into the crystal lattice which would introduce defects due to the inability of epoxidized and brominated units to fit into the crystal lattice.



**PTBD-K
Heptane
Grown
Crystals**



**PTBD-K
Toluene
Grown
Crystals**



**PTBD-U
Heptane
Grown
Crystals**

FIG. 54

Different models of the fold region for PTBD-K crystals from various preparations.

In the next section below a discussion of the kinetics of the epoxidation reaction of various diene polymers and related substances will be given and those results compared with the results of this study.

A reaction between diene polymers and peracids (peracetic, perbenzoic, perphthalic) forms the basis of one of the analytical methods for determining the degree of unsaturation in polymers^{61-62;72}. The reaction is a convenient means for introducing epoxide groups into the macromolecules without any side reaction if the reaction is done in a non-polar solvent and at very low reaction temperature⁷³. This reaction is used for the modification of elastomers with a view to increasing their elastic modulus and compatibility with other polymers of the polyvinyl chloride and butadiene acrylonitrile types and for improvement of the film forming characteristic of diene oligomers⁷⁴. The kinetics of the epoxidation of peracid with polybutadiene rubber in solution has been shown to be first order with respect to both peracid and double bond concentration⁷⁵. It was found in the present study that at least the first 50 % of the reaction of PTBD single crystals suspended in toluene with MCPBA could be represented by a second order rate equation. The rate increased as a function of temperature and followed the Arrhenius equation. The experimental results were processed by the least squares method, and the correlation coefficients were near unity. The agreement of the temperature dependence of the rate constants with the Arrhenius equation is evidence of the constancy of the mechanism in the investigated temperature

range. The negative activation entropies ΔS^\ddagger confirmed a transition complex formation between the peracid and the double bonds of the polymer which had a smaller number of degrees of freedom than the double bond unit and the peracid molecule. Poluektov et. al.⁷⁶ studied the epoxidation kinetics of isoprene, piperylene, and butadiene polymers and copolymers with styrene, with peracetic acid. It was concluded that the rate of diene polymer epoxidation is much slower in an aqueous medium than in chloroform. This is believed to be due to the formation of intermolecular hydrogen bonds between peracetic acid and water, as well as the destruction of the reactive five membered ring present in the peracetic acid molecules and the fracture of the intermolecular hydrogen bonding.

Dogadkin et. al.⁷⁷ showed that there are two stages in the epoxidation of squalene with o-monoperphthalic acid. They concluded that the first stage is evidently due to reaction of o-monoperphthalic acid with the more reactive terminal double bonds of squalene, which with the coiled conformation of the squalene molecules are more accessible than the inner double bonds. The second (slow) stage corresponds to reaction of o-monoperphthalic acid with the inner double bonds. This is consistent with the data given by Van Duuren and Schmitt⁷⁸ on the epoxidation of squalene with peracetic acid. There is a strong indication of such behavior from the results for PTBD-U crystals (see Fig. 14-17). Although the data seems to be scattered due to the low concentrations, it appears that two stages of reaction are occurring. It is reasonable

to advance the explanation that the fast stage is due to the reaction of MCPBA with the double bonds on the chain ends (cilia) and the slow stage corresponds to the reaction with the double bonds in the fold region. For the PTBD-U crystals grown from heptane, it is seen that the decrease in rate constant takes place at a value of % double bonds reacted of 15-20 %. This is approximately the percent of double bonds in the chain ends for this preparation. Therefore, it is possible that the double bonds in the chain ends are more reactive than the double bonds in tight folds.

An interesting result of the present work is that the second order rate constant for the epoxidation of double bonds in the fold region of PTBD crystals is dependent on 1) the crystal preparation condition and 2) the molecular weight. The double bonds in the tightest folds have the lowest rate constant (PTBD-K heptane grown crystals); the preparation believed to contain about an equal amount of double bonds in chain ends and in relatively tight folds show the next largest rate constant (PTBD-U heptane grown crystals) and the preparation with about double the number of monomer units per fold expected in a tightly fold has the largest rate constant (PTBD-K toluene grown crystals). This can be interpreted in term of the dependence of the reactivity of the double bonds in the PTBD chain on chain flexibility. The order of the greater reactivity is expected to be :

chain ends > "loose" folds > "tight" folds

To obtain a rate constant for the reaction of the double bonds in the chain ends, one can use the results for PTBD-U heptane grown crystals corrected for the presence of the relatively unreactive double bonds in the regular folds.

CONCLUSION

The following conclusions can be drawn from this investigation:

1) The fraction of amorphous material on PTBD-single crystals available for epoxidation by MCPBA is found for certain preparations to depend on the reaction temperature.

2) The kinetics of epoxidation of PTBD single crystals in toluène suspension by MCPBA was shown to follow the second order rate equation for at least 50 % of reaction, ie. the rate is proportional to the double bond concentration and to the peracid concentration.

3) The rate constant for the epoxidation of PTBD crystals is markedly dependent on the crystal preparation conditions and on the polymer molecular weight.

4) Results to date suggest that chain folding in PTBD crystals is re-entrant and under the right crystallization conditions can be predominantly regular.

REFERENCES

- 1) K.H. Starks , J. Am. Chem. Soc. , 60 1753 (1938)
- 2) R. Jaccodine, Nature , 176 301 (1955).
- 3) P.H. Till , J. Polym. Sci., 24 301 (1957).
- 4) A. Keller , Phil. Mag., 8(2) 1171 (1957).
- 5) E.W. Fischer , Z. Naturforsch, 12a 753 (1957).
- 6) P.H: Geil, " Polymer Single Crystals " Interscience, New York. (1963).
- 7) B.G. Ranby, F.F. Morehead and N.M. Walter, J. Polym. Sci., 34 349 (1960).
- 8) P.H. Geil, N.K.J. Symons, R.G. Scott, J. Appl. Phys., 30 1516 (1959).
- 9) D.A. Blackadder, J. Macromol. Sci., Rev. Macromol. Chem., C1 297 (1967).
- 10) P.H. Geil, J. Polym. Sci. , 44 449 (1960).
- 11) E.W. Fischer , Z. Naturforsch., 14a 584 (1959).
- 12) A. Peterlin , J. Appl. Phys., 31 1934 (1960).
- 13) A. Peterlin, E.W. Fischer, Chr. Reinhold, J. Chem. Phys., 37 1403 (1962).
- 14) A. Peterlin, E.W. Fischer, Z. Physik, 159 272 (1960).
- 15) T.P. Lin, Unpublished calculations.
- 16) F.P. Price, J. Chem. Phys., 31 1679 (1959).
- 17) F.P. Price, J. Polym. Sci., 42 49 (1960).
- 18) J. I. Lauritzen Jr., J.D. Hoffmann, J. Chem. Phys., 31 1680 (1959).
- 19) A. Keller , Kolloid. Z. 197 98 (1964).

- 20) V.P. Holland, P.H. Lindenmeyer, J. Appl. Phys., 36
3049 (1965).
- 21) J.D. Hoffmann , Soc. Plastic Eng., 4 315 (1964).
- 22) P.H. Geil , J. Polym. Sci. , 47 65 (1960).
- 23) J.D. Hoffmann, J.I. Lauritzen, E. Passaglia, G.S. Ross,
L.J. Frolin, J.J. Weeks, Kolloid. Z. , 231 564 (1969).
- 24) E.W. Fischer, R. Lorenz, Kolloid. Z. 189 97 (1963).
- 25) E.W. Fischer, G. Schmidt, Angew. Chem., 74 551 (1962).
- 56) J.B. Jackson, P.J. Flory, R. Chiang, Tran. Faraday Soc.
59 1906 (1963).
- 27) P.J. Flory , J. Am. Chem. Soc., 84 2857 (1962).
- 28) R.J. Roe and H.E. Bair, Macromolecule, 3 454 (1970).
- 29) A. Keller, E. Martucelli, D.J. Priest and Y. Udagawa,
J. Polym. Sci. A2 10 1807 (1971).
- 30) R.J. Roe , J. Chem. Phys., 53 3026 (1970).
- 31) R.G. Brown , J. Appl. Phys., 34 2382 (1963).
- 32) J.C. Koenig, D.E. Witenhafer, Macromol. Chem., 99 193
(1966).
- 33) J.C. Koenig. and M.J. Hannon, J. Macromol. Sci., Phys.,
B1 119 (1967).
- 34) M.I. Bank and S. Krimm, J. Appl. Phys., 39 4951 (1968)
- 35) S. Krimm and M.I. Bank, Preprints of paper presented at
Int. Symp. on Macromolecular Chemistry, Toronto, Canada,
A6 18 (1968).
- 36) T. Kawai, T. Goto, and H. Maeda, Kolloid. Z. 223 117 (1968).
- 37) J.C. Koenig and M.C. Agboatwalla, J. Macromol. Sci.,
Phys., B2 391 (1968).

- 38) Y. Udagawa and A. Keller, J. Polym. Sci., A2 9 437 (1971).
- 39) A. Peterlin and G. Meinel, J. Polym. Sci., B3 1059 (1965).
- 40) D.J. Blundell, A. Keller and I.M. Ward, J. Polym. Sci.,
B4 781 (1966).
- 41) T. Williams, D.J. Blundell, and A. Keller, J. Polym. Sci.,
A2 6 1613 (1968).
- 42) T. Sakurai, T. Ito, H. Iwasaki, Y. Watanabe and M. Fukuhara,
Rep. Int. of Phys. Chem. res., 43 62 (1967).
- 43) A. Keller and Y. Udagawa, J. Polym. Sci., A2 1793 (1971).
- 44) F.H. Winslow, M.Y. Hellman, W. Matreyek and R. Salovey,
J. Polym. Sci., B5 89 (1967).
- 45) D.M. Sadler, T. Williams, A. Keller, and I.M. Ward, J.
Polym. Sci., A2 7 1819 (1969).
- 46) D.J. Priest, J. Polym. Sci., A2 9 1777 (1971).
- 47) A. Keller, and D.J. Priest, J. Macromol. Sci., B2 479 (1968).
- 48) A. Keller, and D.J. Priest, J. Polym. Sci., B8 13 (1970).
- 49) S. Krimm and M.I. Bank, J. Polym. Sci., A2 7 1785 (1969).
- 50) C. Hendrix, D.A. Whiting, and A.E. Woodward, Macromolecule,
4 571 (1971).
- 51) S.B. Ng, J.M. Stellman and A.E. Woodward, J. Macromol. Sci.,
Phys., B7(3) 539 (1973).
- 52) J.M. Stellman and A.E. Woodward, J. Polym. Sci., B7 755 (1969).
- 53) J.M. Stellman and A.E. Woodward, J. Polym. Sci., A2 59 (1971).
- 54) S.B. Ng and A.E. Woodward, J. Macromol. Sci., Phys.,
10 627 (1974).
- 55) T. Nagamura and A.E. Woodward, J. Polym. Sci., A2 (14) 275 (1976).

- 56) H. Evans and A.E. Woodward, *Macromolecule* 9 88 (1976).
- 57) S. Takamura, T. Tatsumi and M. Takayanaki, *Reports on Progress in Polymer Physics in Japan*, 10 333 (1967).
- 58) G. Natta and P. Corradini, *Nuovo. Cimento.*, 15 Sup. 1 9 (1960).
- 59) S. Iwayanaki, I. Sakurai and T. Sakurai, *J. Macromol. Sci., Phys.*, B2 (2) 163 (1968).
- 60) J.M. Stellman, A.E. Woodward, and S.D. Stellman, *Macromolecule*, 6 330 (1973).
- 61) I.M. Kolthoff, T.S. Lee and M.A. Mairs, *J. Polym. Sci.* 2 199 (1947).
- 62) I.M. Kolthoff and T.S. Lee, *J. Polym. Sci.*, 2 226 (1947).
- 63) T. Tatsumi, T. Fukushima, K. Imada and M. Takayanaki, *J. Macromol. Sci., Phys.*, B1 (3) 459 (1967).
- 64) G. Natta, P. Corradini, *Porri. Rend. Acad. Nazl. Lincei* 20 728 (1956).
- 65) G. Moraglio, G. Polizzotti and F. Danusso, *Eur. Polym. J.*, 1 183 (1965).
- 66) J.J. White, A.U. Hasan and W.C. Sears, *Bull. Ga. Acad. Sci.*, 29 136 (1971).
- 67) T. Oyama, K. Shiokawa, and Y. Murata, *Polymer J.*, 6 549 (1974).
- 68) A. Marchetti and E. Martucelli, *J. Polym. Sci., Phys.*, 14 151 (1976).
- 69) A. Marchetti and E. Martucelli, *J. Polym. Sci., Phys.*, 14 323 (1976).
- 70) J.M. Stellman, PhD Thesis, The City University of New York, (1972).
- 71) F. Jackson, L. Mandelkern, *Macromolecule*, 1 547 (1968).

- 72) B.A. Dogadkin, A.V. Dobromyslova, F.S. Tolstukhima and N.G. Samsonova, *Kolloidn. Zh.*, 19 188 (1957).
- 73) C.E. Wheelock, *Ind. Eng. Chem.*, 50 299 (1950).
- 74) V.N. Gorbunov, S.S. Rydvanova and G.I. Zalkind, *Plastmassy*. № 8 7 (1964).
- 75) C. Pinazzi, J.C. Sautif and J.C. Brosse, *Bull. Soc. Chim. de France* #5 1652 (1973).
- 76) P.T. Poluektov, T.B. Gonsovskaya, F.G. Ponomarev and Yu. K. Gusev, *Vysokomol. Soyed.*, A15 (3) 606 (1973).
- 77) B.A. Dogadkin, I.A. Tutorskii and I.D. Khodzhaeva, *Kolloidn. Zh.*, 32 #3 315 (1970).
- 78) B.L. Duuren and F.L. Schmitt, *J. Org. Chem.*, 25 1761 (1960).
- 79) S. Krimm and M.I. Bank, *J. Polym. Sci.*, A2 (7) 1785 (1969).
- 80) A. Keller, E. Martucelli, D.J. Priest and Y. Udagawa, *J. Polym. Sci.*, A2 (10) 1807 (1971).
- 81) S. Krimm, *J. Polym. Sci., Phys.*, 14(3) 521 (1976).
- 82) D.J. Blundell, A. Keller, I.M. Ward and I.J. Grant, *J. Polym. Sci.*, B4 781 (1966).
- 83) K. Suehiro and M. Takayanaki, *J. Macromol. Sci.*, B4(1) 39 (1970).
- 84) R. Endo, *Nippon Gomu. Kyokaishi*, 34 527 (1961).
- 85) T. Oyama, K. Shiokawa and T. Ishimaru, *J. Macromol. Sci., Phys.*, B8 247 (1973).
- 86) M. Tasumi and S. Krimm, *J. Chem. Phys.* 46 755 (1967).
- 87) M. Tasumi and S. Krimm, *J. Polym. Sci.*, A-2 6 995 (1968).